RECLAMATION

Managing Water in the West

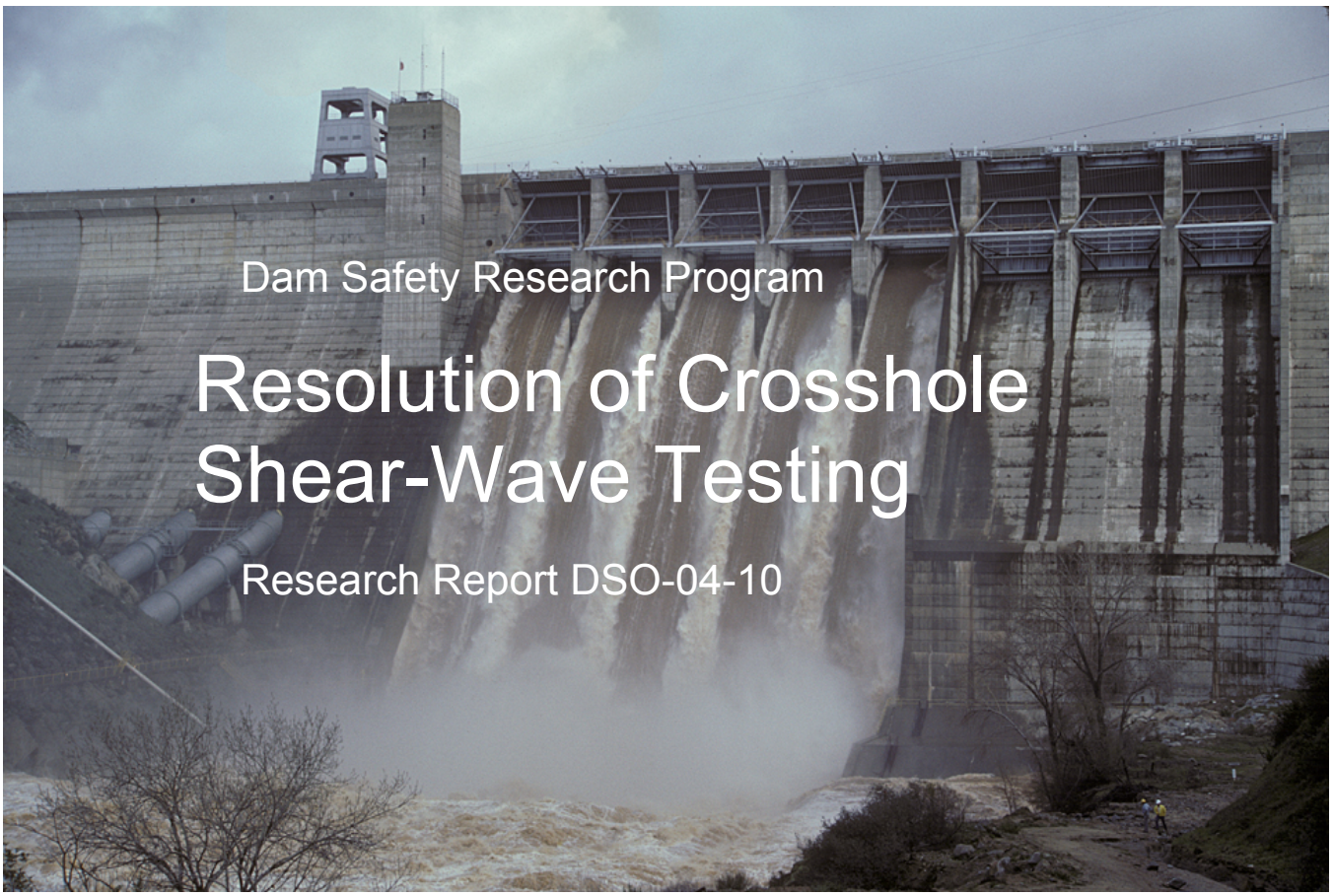

Dam Safety Research Program

Resolution of Crosshole Shear-Wave Testing

Research Report DSO-04-10

U.S. Department of the Interior
Bureau of Reclamation

March 2005

DSO-04-10

Resolution of Crosshole Shear-Wave Testing

By
Lisa Block
Dan O'Connell

U.S. Department of the Interior
Bureau of Reclamation

March 2005

Contents

Tables

Figures

Executive Summary

This project investigates the ability of crosshole shear-wave testing to resolve low-velocity layers of varying thickness. The resolution of crosshole shear-wave testing, as currently implemented by Reclamation, is investigated by generating and analyzing synthetic waveform data for seven shear-wave velocity models. The models include velocity layers of varying thickness and velocity contrast. Three experienced geophysicists from the Bureau of Reclamation, U. S. Geological Survey, and U. S. Army Corps of Engineers independently estimated the shear-wave arrival times on the synthetic waveforms. Velocity-depth profiles were computed from the arrival times using Reclamation's standard crosshole processing procedures.

In this study, shear-wave velocities within layers more than five feet thick were determined with errors of less than 1.5%. Velocities within layers two to five feet thick were determined with errors of less than 6.5%. Because the synthetic waveforms do not contain all of the complexities of field data, errors of velocities computed from field data are likely to be somewhat greater than those computed from these synthetic data. Even so, given the results presented here, we estimate that errors of velocities computed from crosshole field data are less than 5% for layers greater than five feet thick and less than 10% for layers two to five feet thick. Although layers less than two feet thick can be detected with the crosshole method, the accuracy of the method (using Reclamation's current field equipment) greatly deteriorates for such layers. Velocities computed within the 1-ft-thick low-velocity layers included in these models have errors of 29% to 35%.

The thin-bed resolution limit of the crosshole shear-wave method is controlled mainly by the frequency content of the propagated seismic energy. Tests conducted during this investigation indicate that incorporation of ray bending into the data processing procedures has little effect on the resolution of velocities within layers less than two feet thick. The most effective way to improve the resolution of Reclamation's crosshole shear-wave surveys would be to use a higher-frequency borehole shear-wave source.

These tests also demonstrate that computed crosshole velocities are smeared at layer interfaces, with velocities being overestimated in the lower-velocity layer near an interface and velocities underestimated in the adjacent higher-velocity layer. The smearing at layer interfaces is caused by refraction of seismic energy and the finite frequency range of the propagated seismic energy. Because of this smearing near layer interfaces, the most accurate crosshole velocities are those computed near the centers of velocity layers. The exact depths of layer interfaces are better determined from geologic drill logs and geophysical borehole logs rather than from crosshole velocity profiles.

1. Introduction

Crosshole shear-wave (S-wave) testing has been an integral part of earthquake engineering for more than twenty years. The technique is used to evaluate the potential for liquefaction of soil deposits, based upon in-situ shear-wave velocity, and to develop subsurface models for use in ground response calculations.

Questions have recently been raised regarding the ability of the crosshole shear-wave technique to resolve thin low-velocity layers within a complicated soil profile. Resolution of arbitrarily thin layers requires very high frequencies (i.e. short wavelengths). Practical considerations place limits on the frequencies that can be produced by the downhole seismic source. In addition, attenuation limits the distance over which high frequencies can be propagated while maintaining usable signal-to-noise characteristics. Individual interpretation of the resulting complicated waveforms adds an additional uncertainty to the results.

The goal of this research project is to evaluate the limitations imposed upon the resolution of crosshole shear-wave testing by the constraints described above. We want to determine the layer thicknesses that can be resolved using the crosshole seismic data acquisition and processing procedures currently in use at Reclamation. The resolution of Reclamation's crosshole shear-wave testing is investigated by generating and analyzing synthetic waveform data for several models containing various shear-wave velocity structures, including low-velocity layers of varying thickness and velocity contrast.

2. Reclamation's Crosshole Shear-Wave Data Acquisition and Processing Procedures

Crosshole shear-wave surveys are usually performed between three boreholes, referred to as a crosshole triplet. For measuring S-wave velocities in soils, the borehole spacing is typically 10 to 12 feet, with larger spacings being used for deeper boreholes. The source is placed in a borehole at one of the ends of the triplet, and receivers are placed in each of the other two boreholes (figure 2-1). The sources and receivers are maintained at approximately equal elevations during the survey. Data are acquired at numerous depths, usually at an equal depth increment.

A downhole shear-wave hammer is used to generate the seismic energy. This source consists of a central cylinder that is locked inside the borehole casing with hydraulically-powered pads and a sliding arm with reversible impact directions. The downhole hammer source is designed to preferentially generate shear-wave energy in the vertical plane (SV-waves). At each recording depth, two records are acquired, one for each source polarization direction (i.e., one "down hit" and one

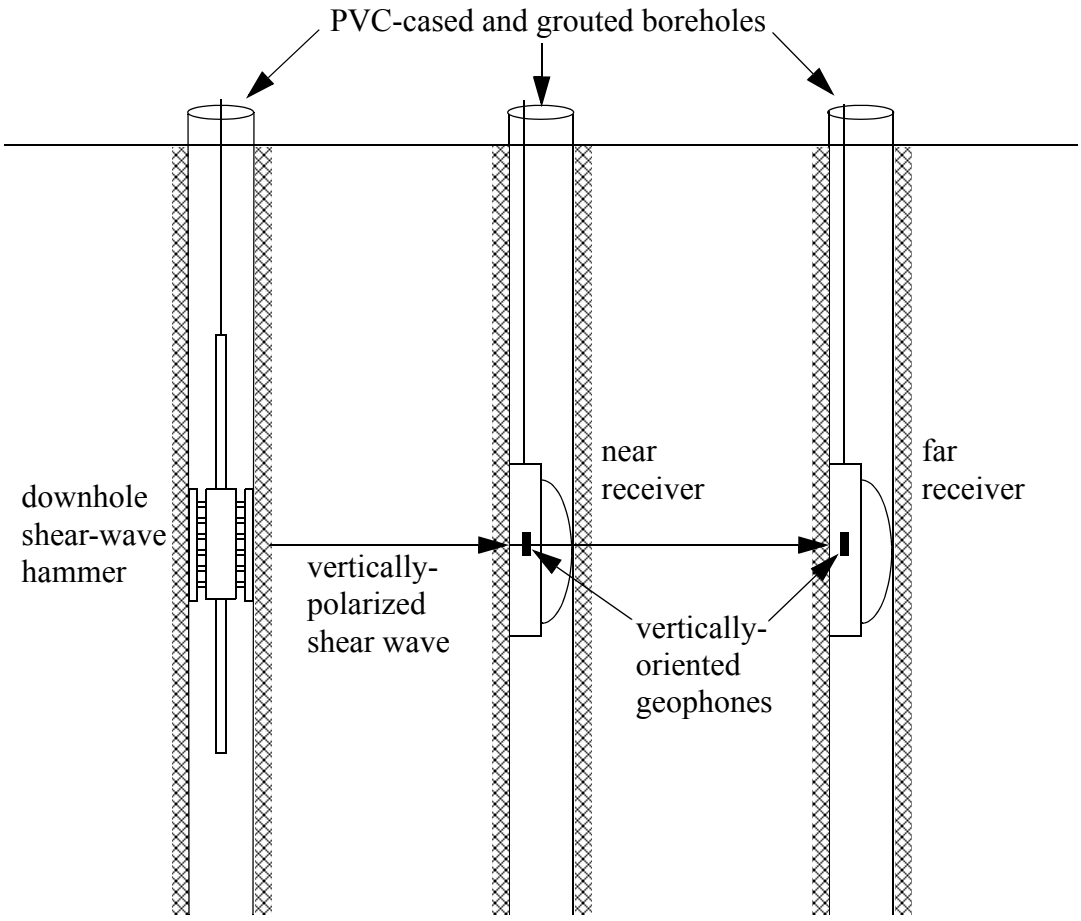

Figure 2-1: Crosshole shear-wave data acquisition geometry.

"up hit"). A vertically oriented geophone is used in each receiver borehole to record the S-wave data.

Reclamation's current data processing procedure is fairly simple. We estimate travel times for the horizontally-propagating direct S wave from the geophone waveforms recorded in the near and far receiver boreholes. Crosshole distances are computed from borehole directional surveys and relative distances and azimuths between boreholes measured in the field. We then compute velocities from the travel times and crosshole distances assuming straight (horizontal) ray paths. Three velocity-depth profiles are generated. Two direct S-wave velocity curves are computed using the S-wave travel times from the source to the near and far receivers. One interval S-wave velocity curve is computed using the differences in S-wave arrival times at the near and far receivers. Discrepancies in velocities computed from the near- and far-receiver data are used to judge whether some arrival times are strongly biased by refracted energy (near layer boundaries). If a discrepancy occurs, the velocity data point that is believed to be the most strongly biased by refracted energy is eliminated.

The reason that we use straight (horizontal) ray paths rather than curved paths in our computations is that we believe that we can usually estimate the arrival times of the direct, large-amplitude, horizontally-traveling S waves more consistently than we can estimate the times of the first-arriving, generally lower-amplitude, refracted S waves. The difficulty in determining arrival times of refracted shear waves is increased by interference from P-wave energy, as well as likely converted phases, on our field records (and our limitation of only recording a single geophone component).

3. Velocity Models and Synthetic Waveforms

Seven crosshole models were developed containing a wide range of velocity structures. The models were designed to test resolution using a variety of layer thicknesses and velocity contrasts, as well as to simulate field-measured velocity structures. All models contain horizontally-layered velocity structures. Layer thicknesses, densities, P-wave and S-wave velocities, and P-wave and S-wave attenuation factors were defined for each model. The model parameters are presented in Appendix A.

Synthetic crosshole vertical-component seismograms were calculated for each of the seven velocity models using an efficient frequency-wavenumber integration method (Hisada, 1994; Hisada, 1995). A vertically-polarized shear point source was used to approximate the source properties of the crosshole shear-wave hammer. For presentation purposes, waveforms were provided for both "up" and "down" hits of source, but one record is simply the inverse of the other. Waveforms were computed at a 1-foot depth increment for source-receiver depths ranging from 5 to 95 feet. (For model 7, which contains two 1-ft-thick low-velocity layers, additional waveforms were computed at the centers of these thin layers, in order to determine the thin-bed resolution limit of the crosshole method under optimum conditions.) At each depth, waveforms were computed for a near receiver located 10 feet from the source and for a far receiver located 20 feet from the source, to duplicate typical crosshole shear-wave data acquisition geometry. (Note that for the deepest source/receiver depths in model 5, located in relatively high-velocity simulated bedrock, only the far-receiver waveforms are used in the following analysis. The near-receiver waveforms are strongly affected by near-source affects relating to the waveform computation method used. These near-receiver waveforms are not representative of field data and were therefore eliminated from the analysis.) Additional details of the waveform computation procedure are provided in Appendix B. Appendix C contains plots of the waveforms generated for each model.

By varying the model attenuation factors and post-processing filter parameters, we attempted to match both the frequency content and general characteristics (appearance) of typical crosshole field data. (We tried to compute attenuation factors from field data but were unsuccessful because of variability in geophone receiver response and coupling within the boreholes.) The frequency range of the data was matched fairly well. The maximum frequency is about 500 Hz, corresponding to wavelengths of 1 to 3 feet for typical soil shear-wave velocities (500 to 1500 ft/s). The peak frequency is about 200 Hz, corresponding to wavelengths of 2.5 to 7.5 ft. Frequency spectra

of a representative sample of the synthetic data are compared to spectra of typical field data in Appendix D. Some other characteristics of the field data could not be matched as well. The nature of the synthetic waveforms differs from typical field data in two ways. First, the synthetic data lack the P-wave energy and converted phases that are often seen in field data. This may be due to several simplifying assumptions made when computing the synthetic waveforms. The model source representation may be too simplistic; we were not able to perform field tests with our shear-wave hammer to construct a more realistic source representation. Perfect single-component vertically-oriented geophone receivers are assumed in the modeling. In reality, single-component geophones have some sensitivity to off-axis energy. Also, boreholes normally have some non-negligible deviation so the geophone axes are not perfectly vertical (nor is the source axis). Also, the boreholes may contribute to the presence of converted phases in field data; boreholes were not incorporated into the modeling. The second major difference between the synthetic and field data is that the S-wave arrivals on the synthetic waveforms are more emergent than we typically see in crosshole field data. In typical crosshole field data, we usually have a distinct inflection point just before the large S-wave arrival. On the synthetic waveforms, the S-wave energy emerges gradually from a flat noise-free "zero line". The overly-emergent nature of the synthetic S-wave arrivals is likely due, at least in part, to the simplifying assumption of constant attenuation factors in the modeling (that is, Qp and Qs do not vary with frequency). This assumption is a limitation of the waveform computation algorithm used. The lack of other phases preceding the S-wave arrival in the synthetic data, as discussed above, may also contribute to its apparent overly-emergent nature. That is, some emergent low-amplitude S-wave energy may be masked in field data by the presence of other phases whereas these other phases are not present in the synthetic data. Despite these discrepancies in characteristics between the synthetic and typical field data, we believe that the modeling and subsequent waveform analyses provide a reliable first-order indication of the resolution limitations of the crosshole shear-wave method.

4. Analysis

Three geophysicists from the Bureau of Reclamation (BOR), U. S. Geological Survey (USGS), and U. S. Army Corps of Engineers (COE) independently estimated the direct shear-wave arrival times on the near- and far-receiver synthetic waveforms for models 1 to 6 (with no knowledge of the model parameters). For model 7, which was added late during the course of the research, only two geophysicists (from BOR and USGS) were able to complete the picking. All geophysicists have experience processing field shear-wave seismic data (either crosshole or surface refraction data). Velocity-depth profiles were computed from the arrival times using Reclamation's standard crosshole processing procedures. The resulting velocity profiles are compared to the correct velocity models in figures 4-1 to 4-7. With a few exceptions, the results from the three independent data analyses are fairly consistent with each other. The overly emergent nature of the synthetic waveforms, as discussed above (section 3), is responsible for some of the overall velocity differences among interpretations (especially within thick layers). The important conclusion from comparison of these different analyses of the synthetic data is that several different experienced geophysicists can resolve the velocity layers comparably well. All geophysicists identify all velocity layers. In all interpretations, the interfaces between velocity layers are consistently

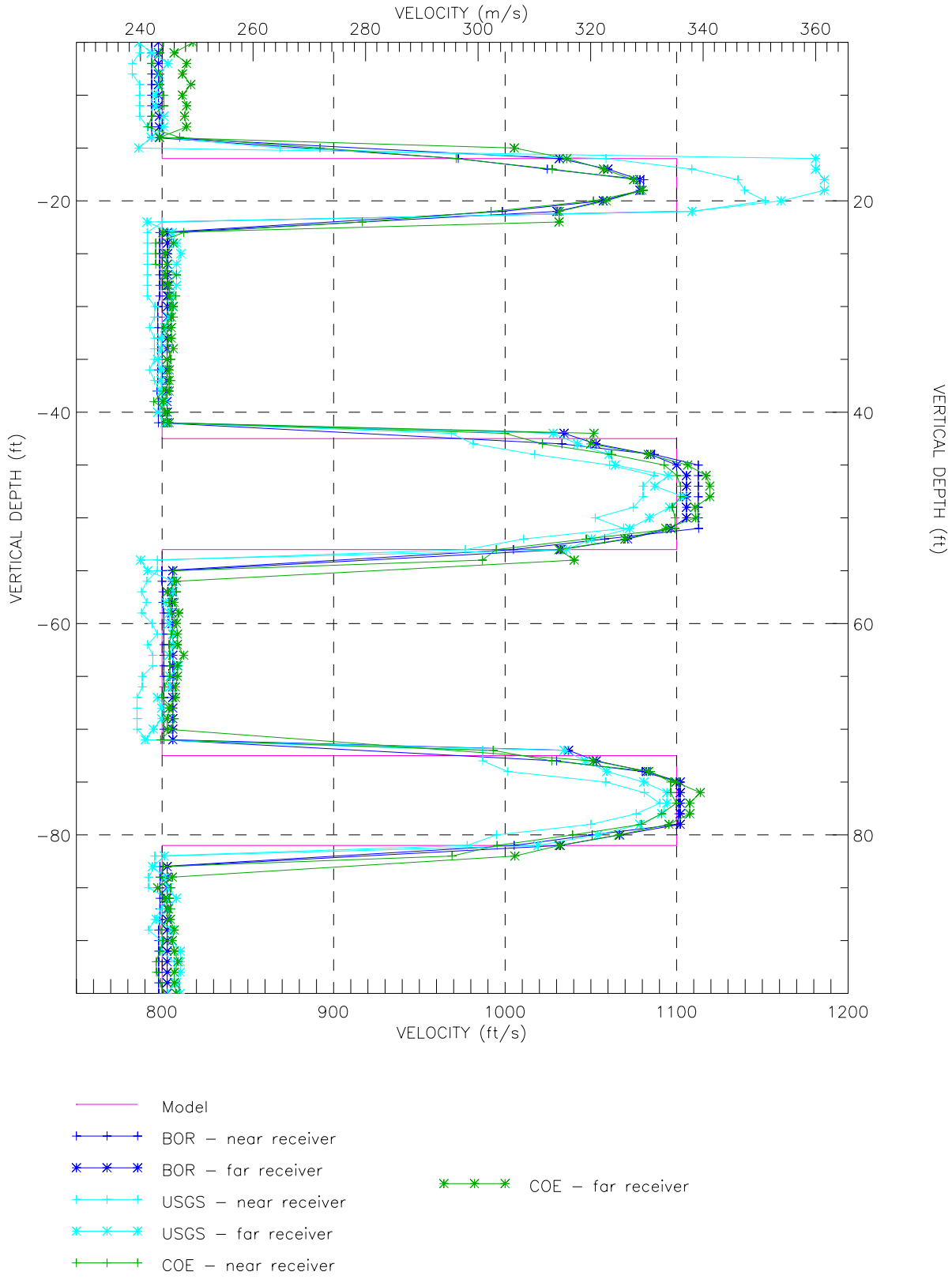

Figure 4-1: Comparison of computed and correct velocity-depth profiles for model 1.

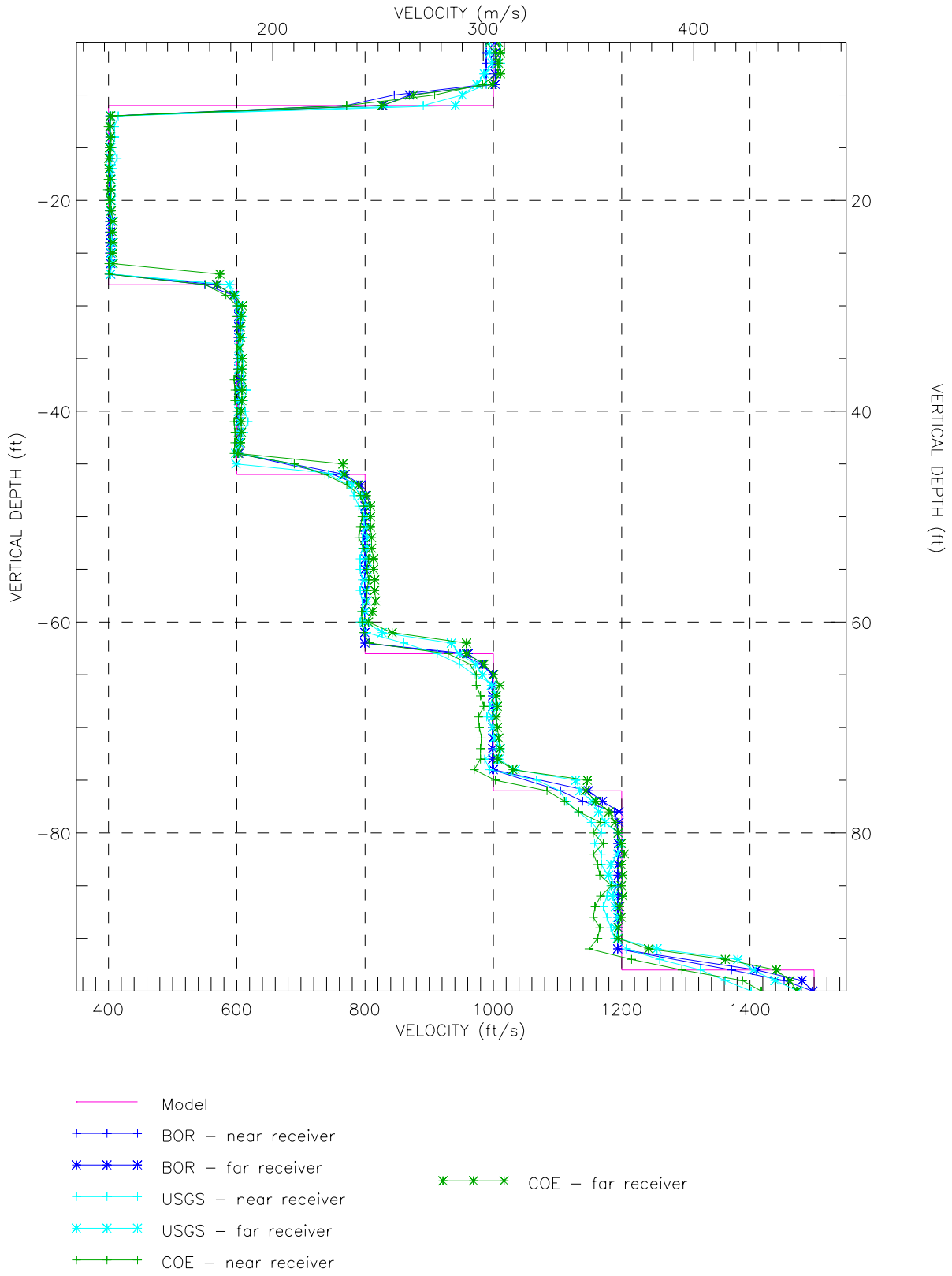

Figure 4-2: Comparison of computed and correct velocity-depth profiles for model 2.

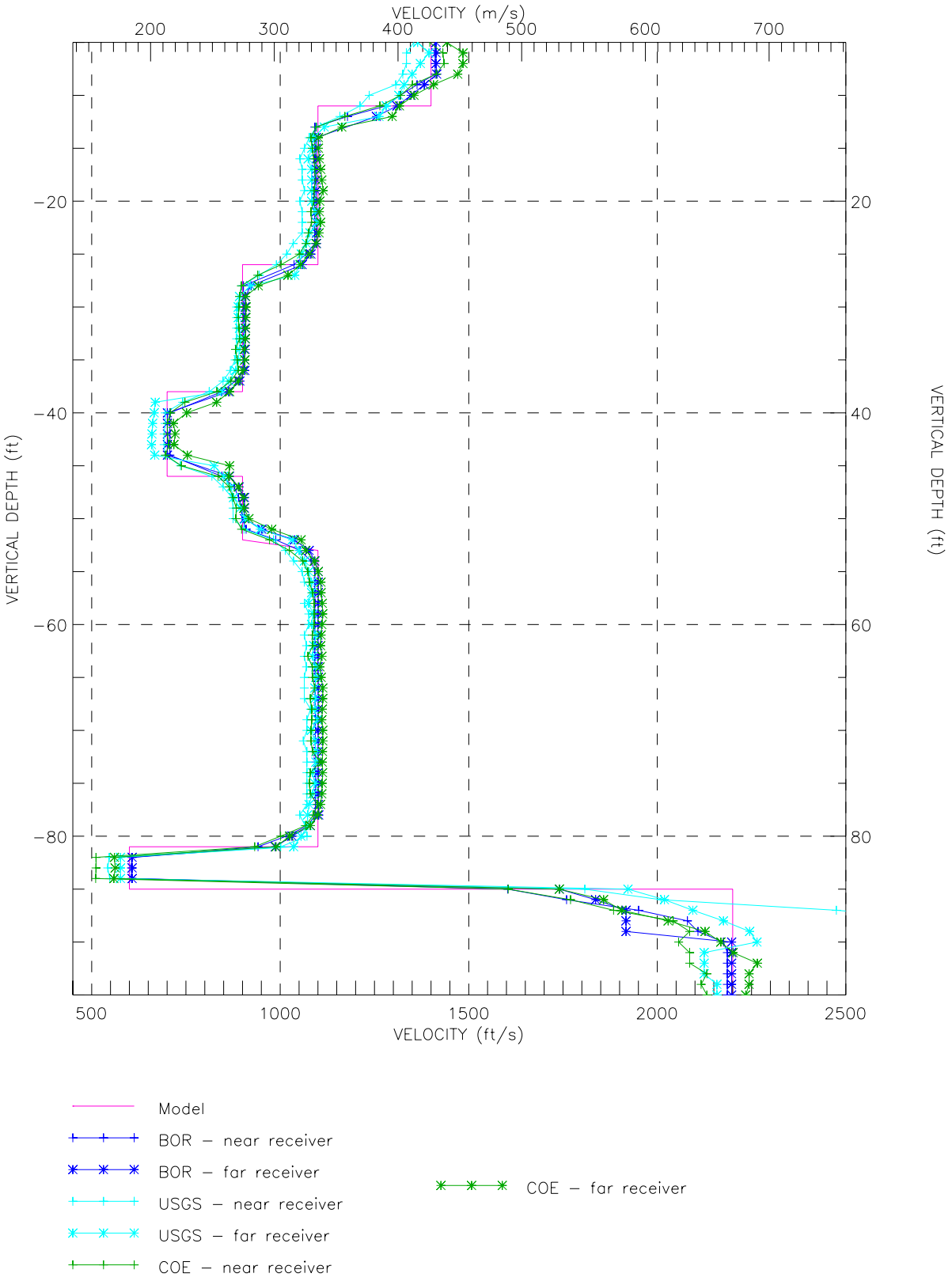

Figure 4-3: Comparison of computed and correct velocity-depth profiles for model 3.

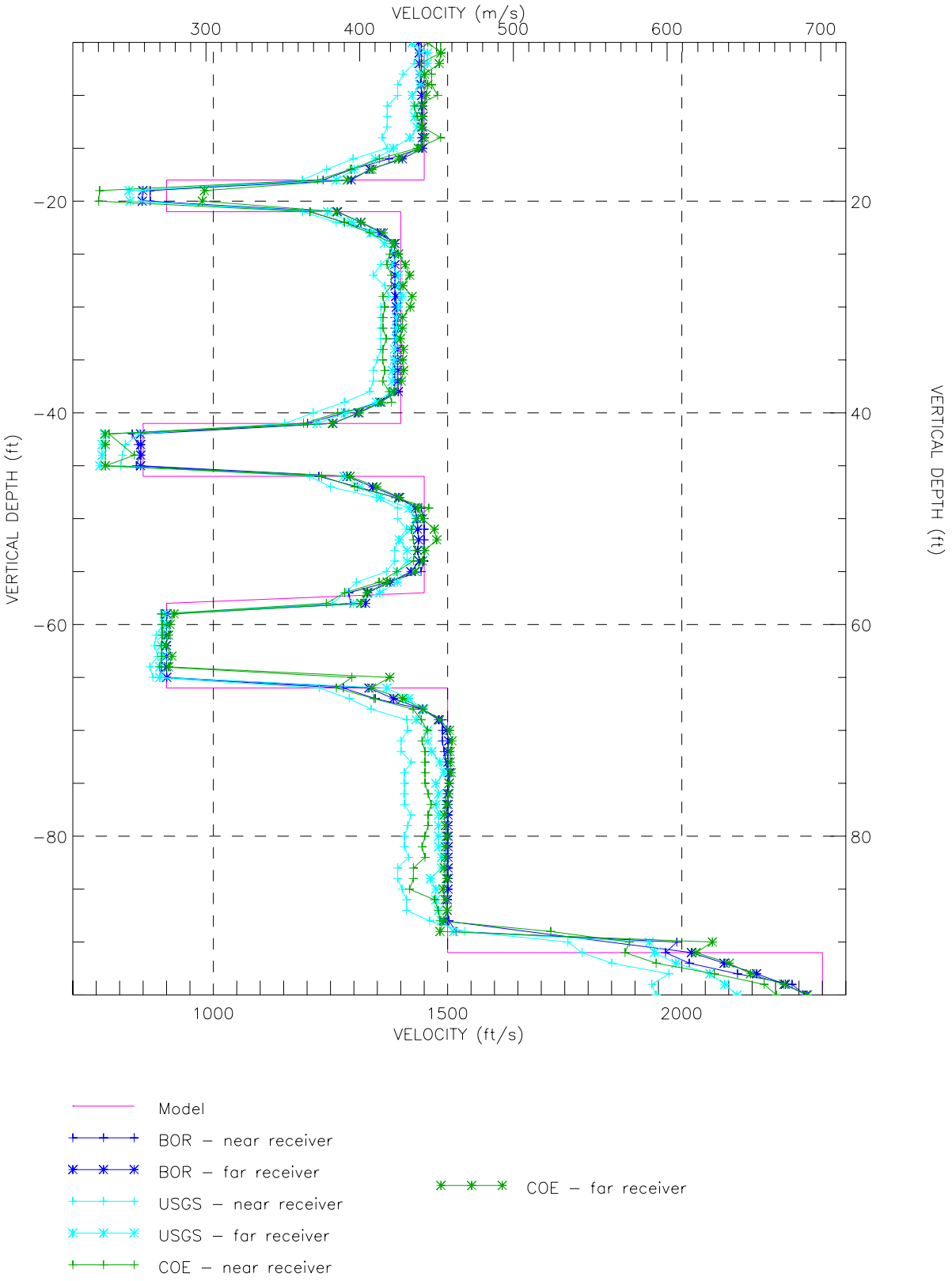

Figure 4-4: Comparison of computed and correct velocity-depth profiles for model 4.

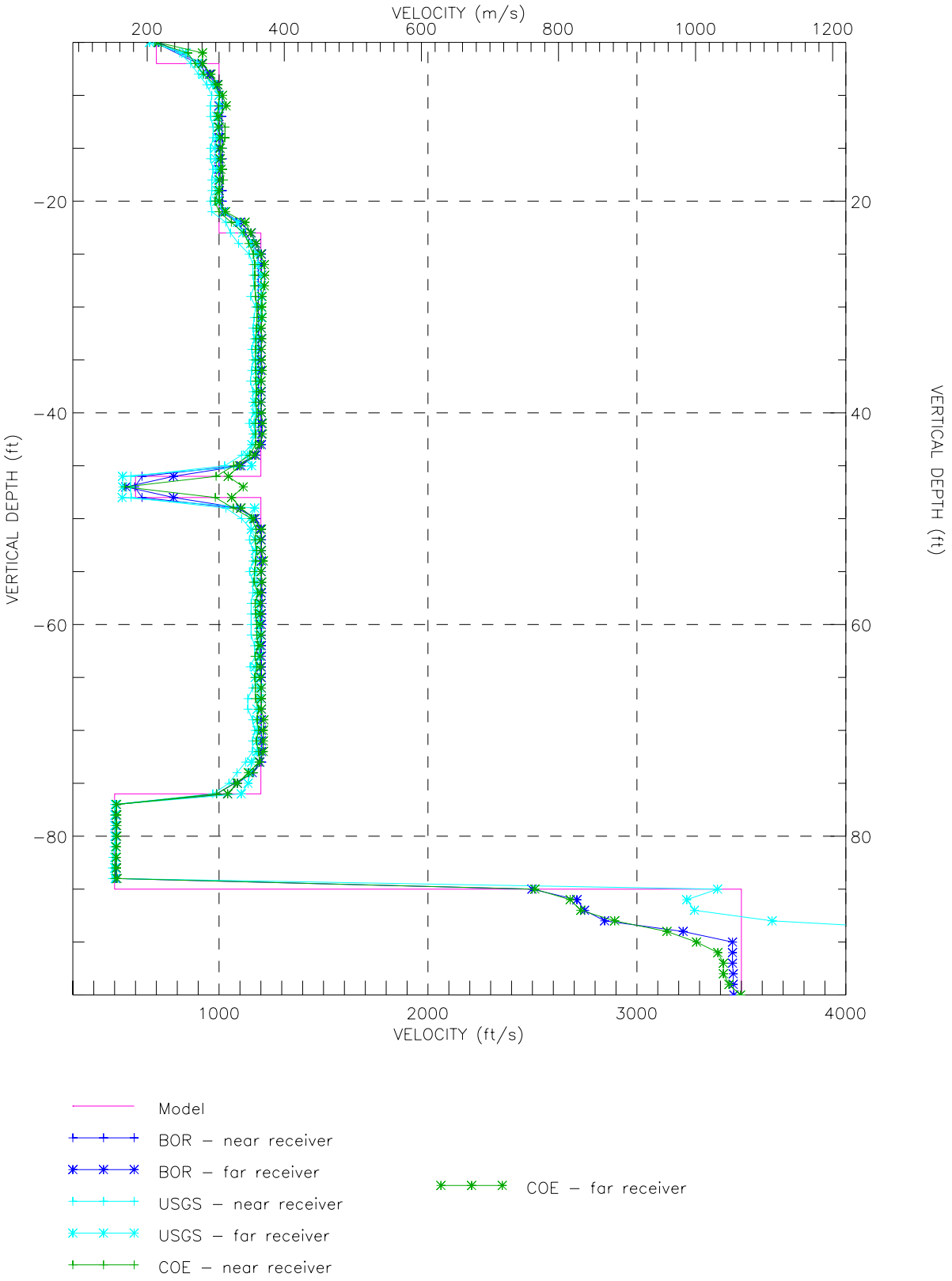

Figure 4-5: Comparison of computed and correct velocity-depth profiles for model 5.

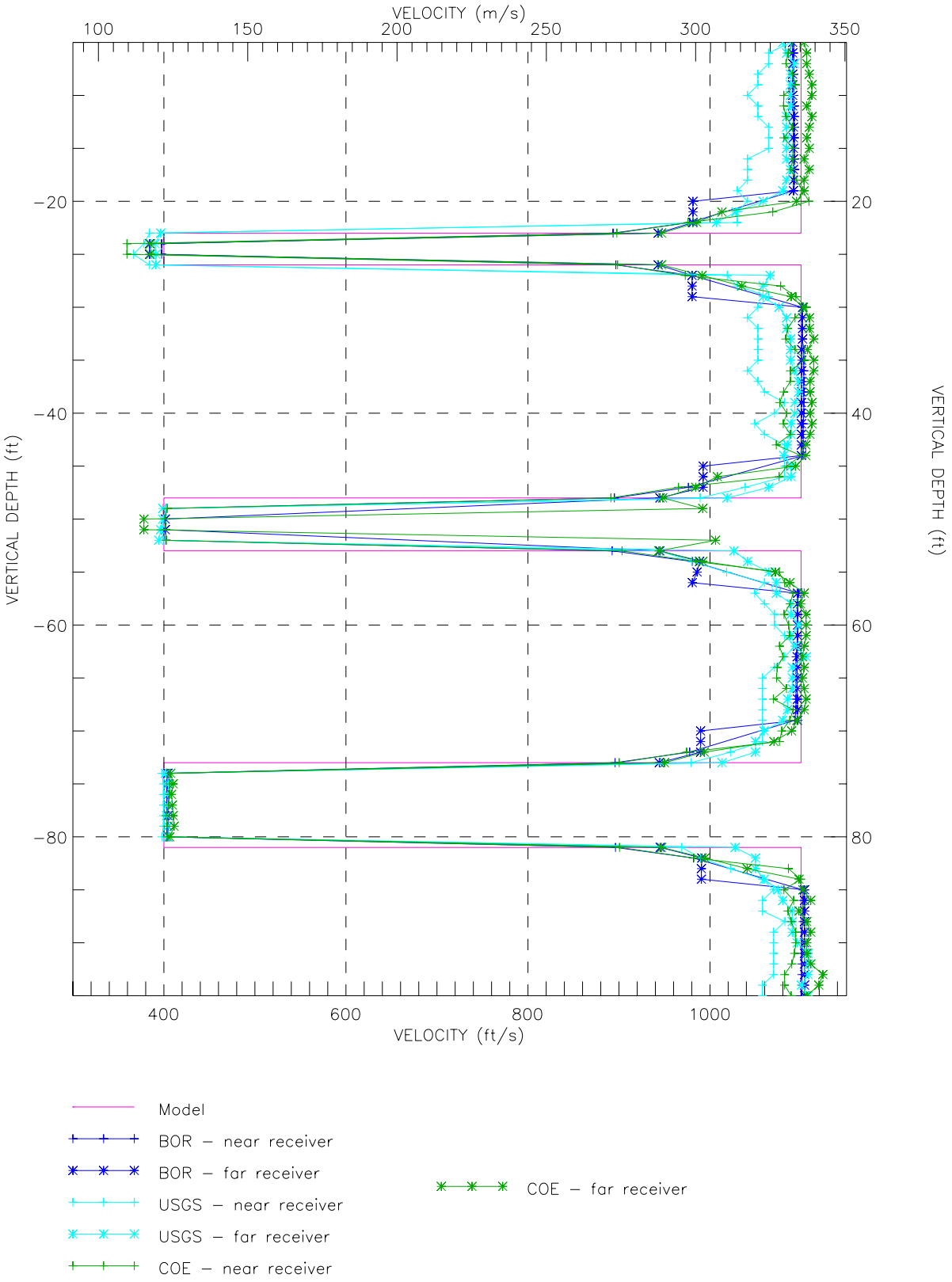

Figure 4-6: Comparison of computed and correct velocity-depth profiles for model 6.

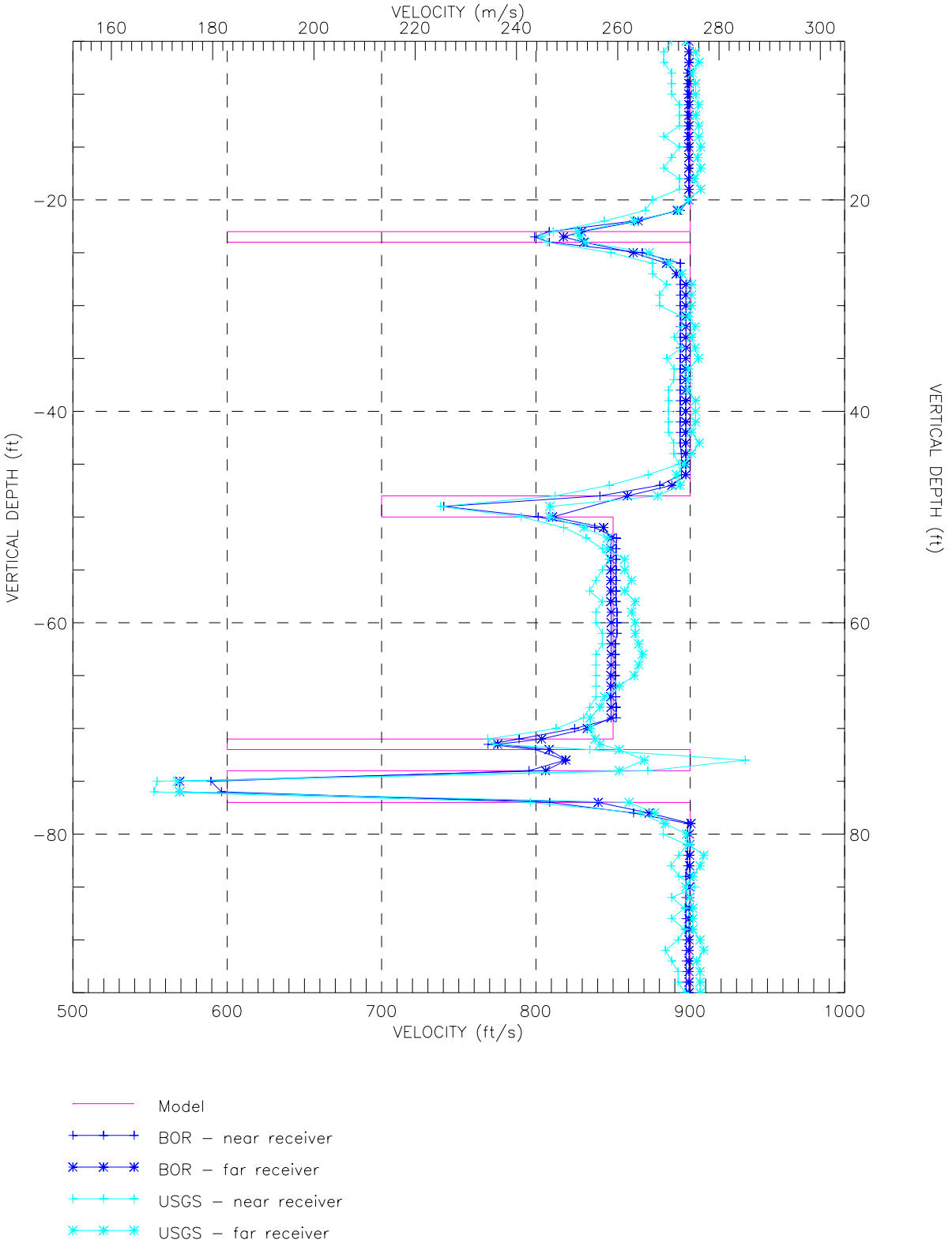

Figure 4-7: Comparison of computed and correct velocity-depth profiles for model 7.

smeared, with velocities being overestimated in the lower-velocity layer near an interface and velocities underestimated in the higher-velocity layer.

The smearing at layer interfaces is caused by refraction of seismic energy along velocity interfaces and the finite frequency range of the propagated seismic energy. Refraction of the seismic energy at the layer interfaces can cause the velocities in the lower-velocity layer to be overestimated when the refracted energy interferes with the onset of the later-arriving direct arrival (and hence arrival times may be picked too early). Because of the finite frequency range of the seismic energy, the energy travels within a zone surrounding the source-to-receiver ray path (the fresnel zone). Data recorded at a single depth are influenced not only by the velocities of materials at that depth but also by the velocities of materials above and below that depth. Velocities in the higher-velocity layer near an interface may be underestimated when large-amplitude shear-wave energy transmitted through the nearby lower-velocity layer interferes with lower-amplitude energy traveling within the higher-velocity layer (resulting in a late arrival time pick).

Median velocity profiles were computed from the six individual near-receiver and far-receiver velocity profiles. Profiles of the percent error were then computed, based on the median calculated velocities and the correct model velocities. The median computed velocity profiles are compared to the model velocities in figures 4-8 to 4-14. The corresponding percent errors are also plotted in these figures. (All velocities, including the model velocities, individual computed near- and far-receiver velocities, and median computed velocities, and the corresponding percent errors are tabulated in Appendix E.) With the exception of velocities near layer interfaces and within thin velocity layers, the absolute errors of the median computed velocities are less than 1.5%. The median computed velocities within thin layers generally have absolute errors greater than 1.5%, because of the same waveform complications that cause velocity smearing across layer interfaces discussed above (refraction and finite frequency effects).

The median velocity errors measured in the centers of layers nine feet or less in thickness are plotted as a function of layer thickness in figure 4-15. The median velocity errors are less than 1.5% for layers more than five feet thick. For layers five feet thick or less, the velocity errors increase with decreasing layer thickness. The trend is gradual for layers two to five feet thick. The 5-ft-thick layers have median velocity errors of less than 3.5%. Layers three to four feet thick have velocity errors between 3.8% and 5.8%. The 2-ft-thick layers have velocity errors between 5.8% and 6.1%. The velocity errors increase dramatically for layers less than two feet thick. The two 1-ft-thick layers in these models have median velocity errors of 29% and 35%. Although most of the thin layers included in these models have low velocities relative to the surrounding materials, the high-velocity layers that are included show the same trend of increasing error with decreasing layer thickness as the low-velocity layers. The median computed velocities and corresponding percent velocity errors at the centers of velocity layers five feet or less in thickness are tabulated in Table 4-1.

MODEL 1

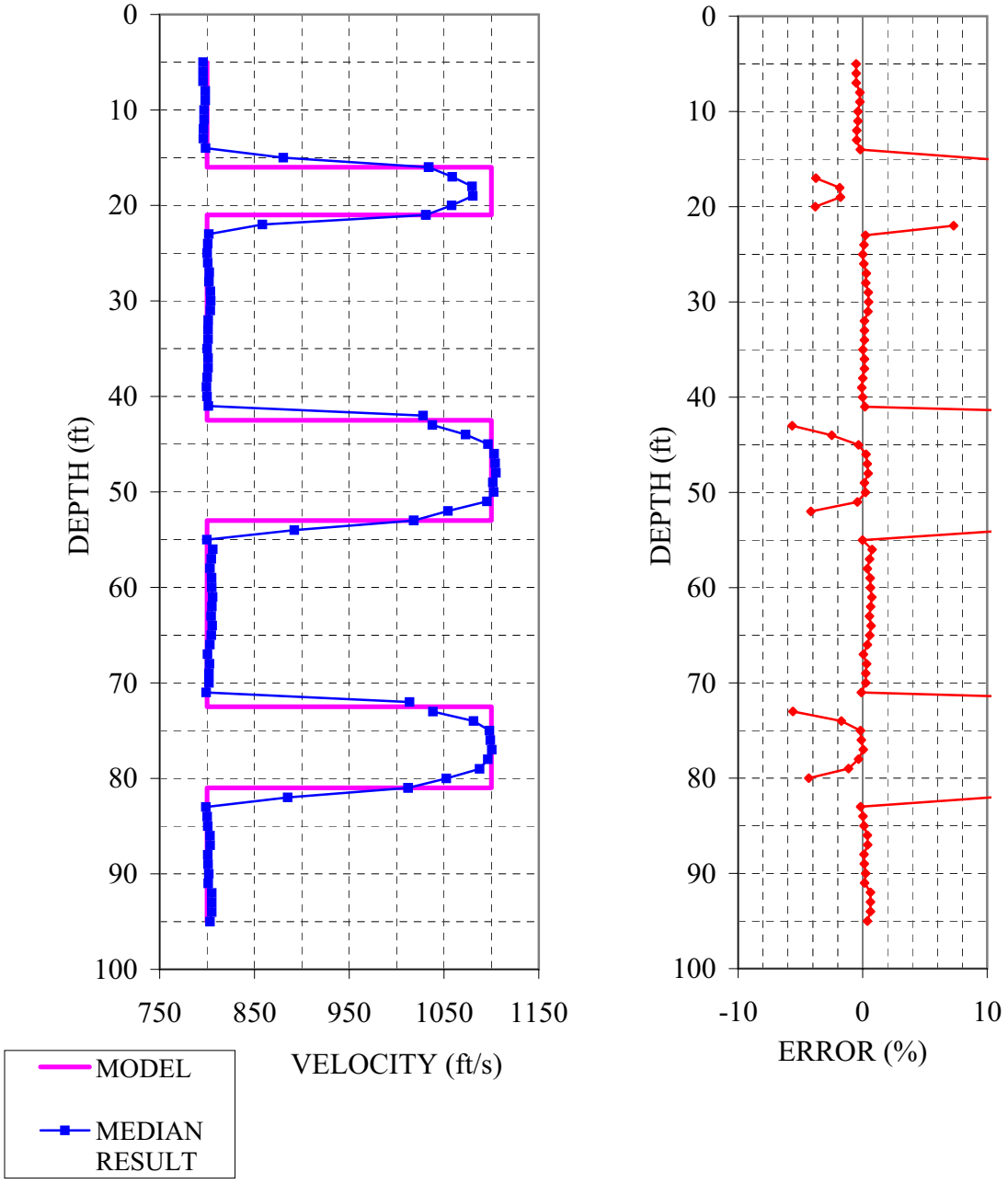

Figure 4-8: Comparison of median computed and correct velocity-depth profiles for model 1 and corresponding percent errors.

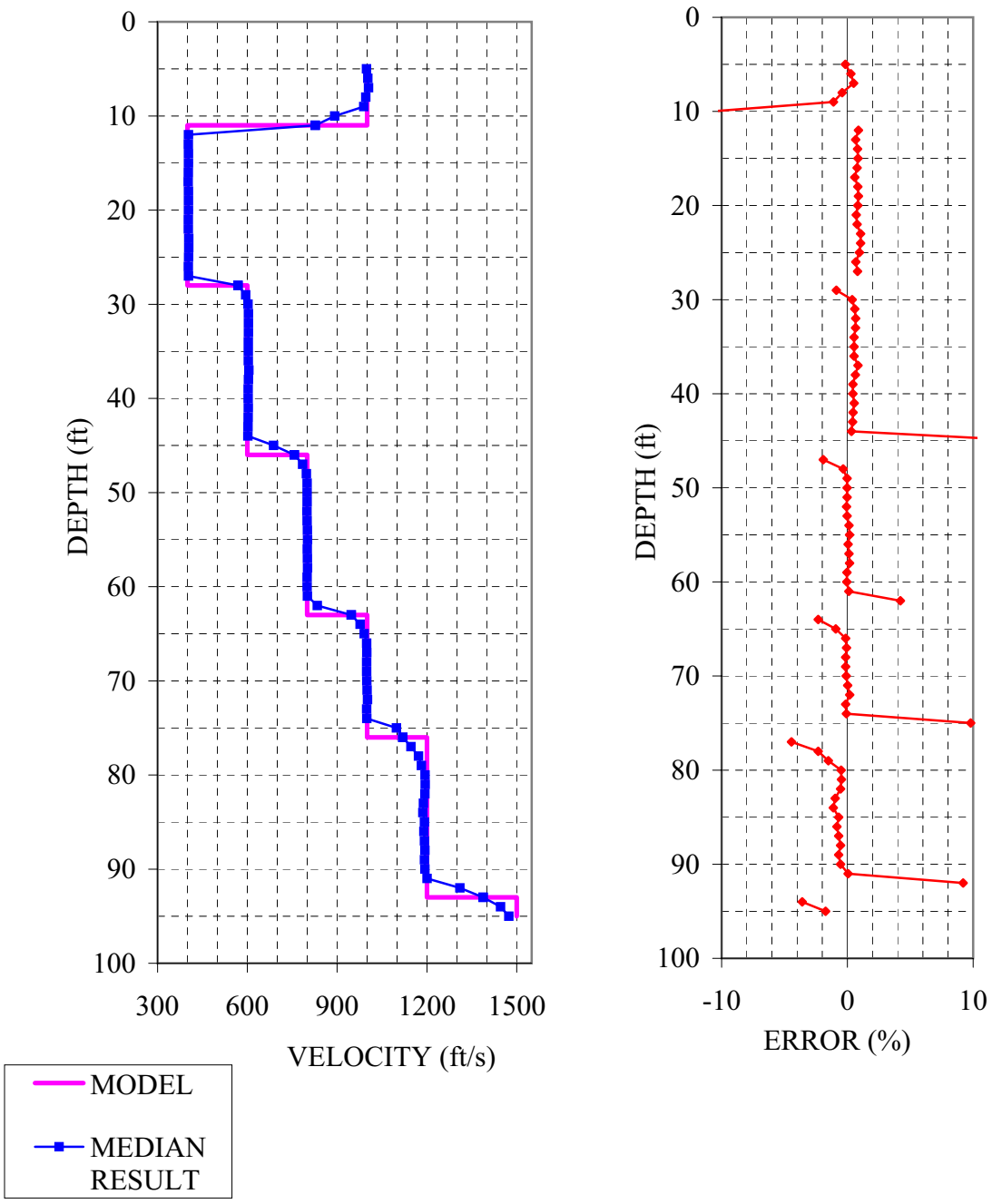

Figure 4-9: Comparison of median computed and correct velocity-depth profiles for model 2 and corresponding percent errors.

MODEL 3

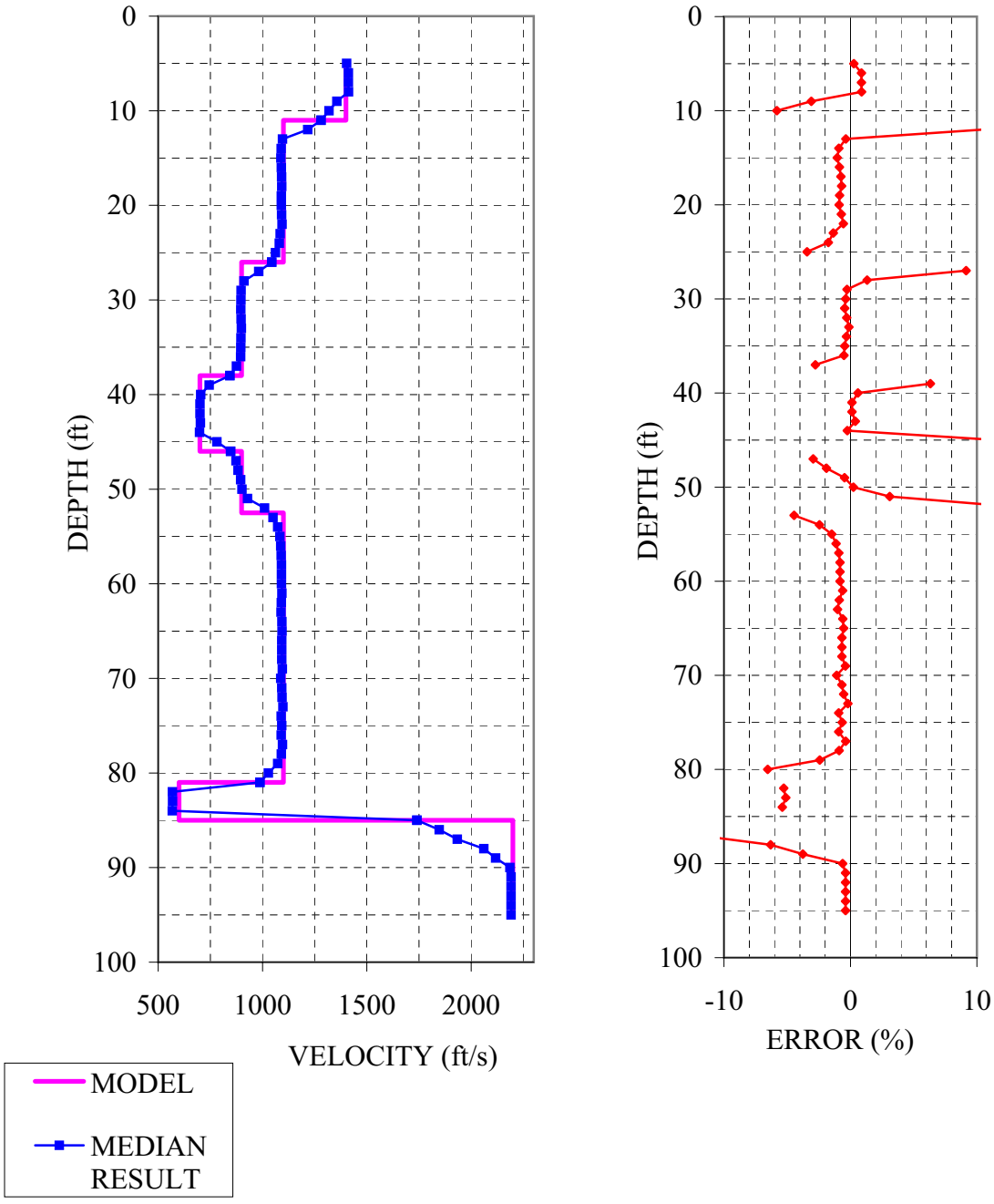

Figure 4-10: Comparison of median computed and correct velocity-depth profiles for model 3 and corresponding percent errors.

MODEL 4

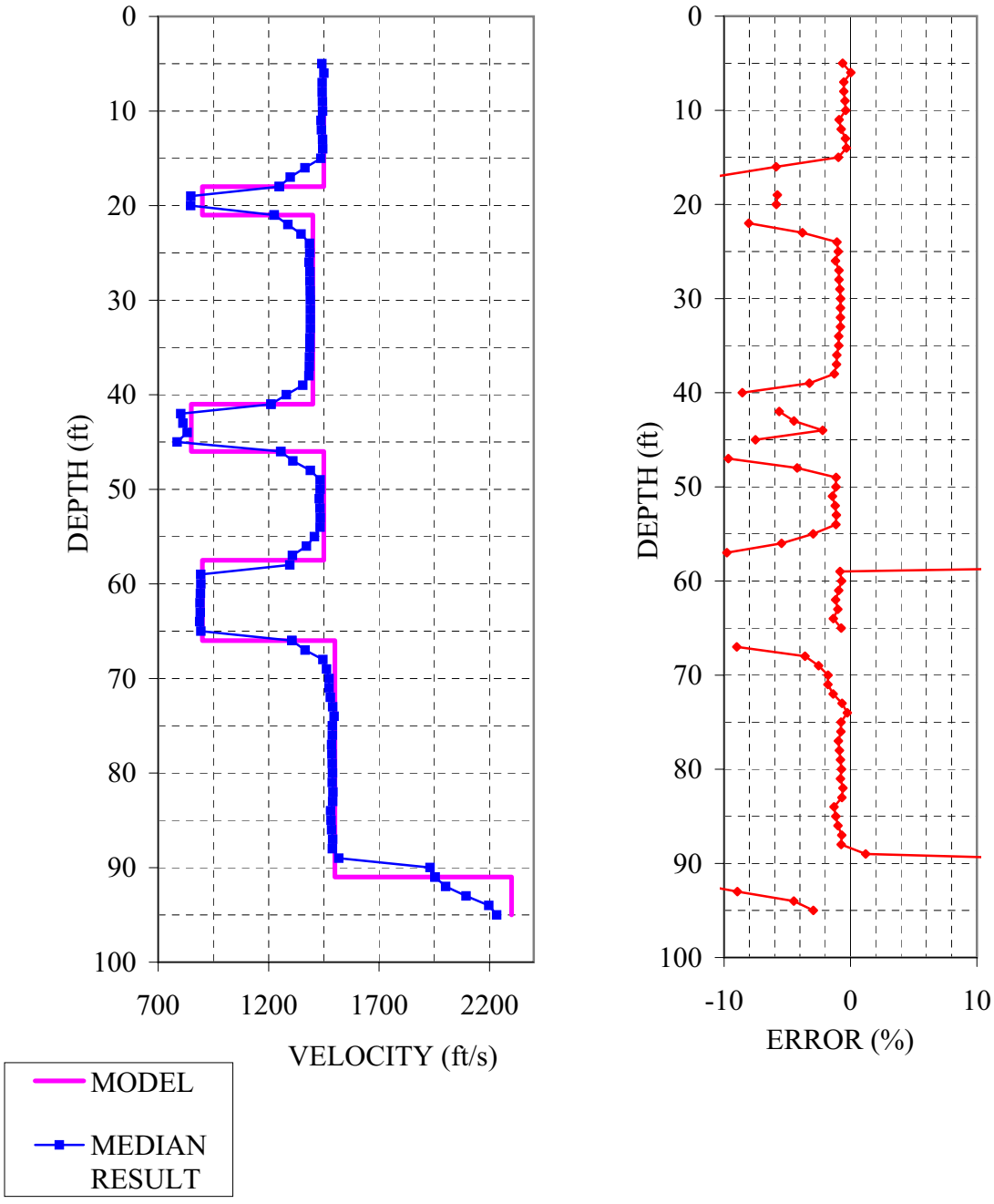

Figure 4-11: Comparison of median computed and correct velocity-depth profiles for model 4 and corresponding percent errors.

MODEL 5

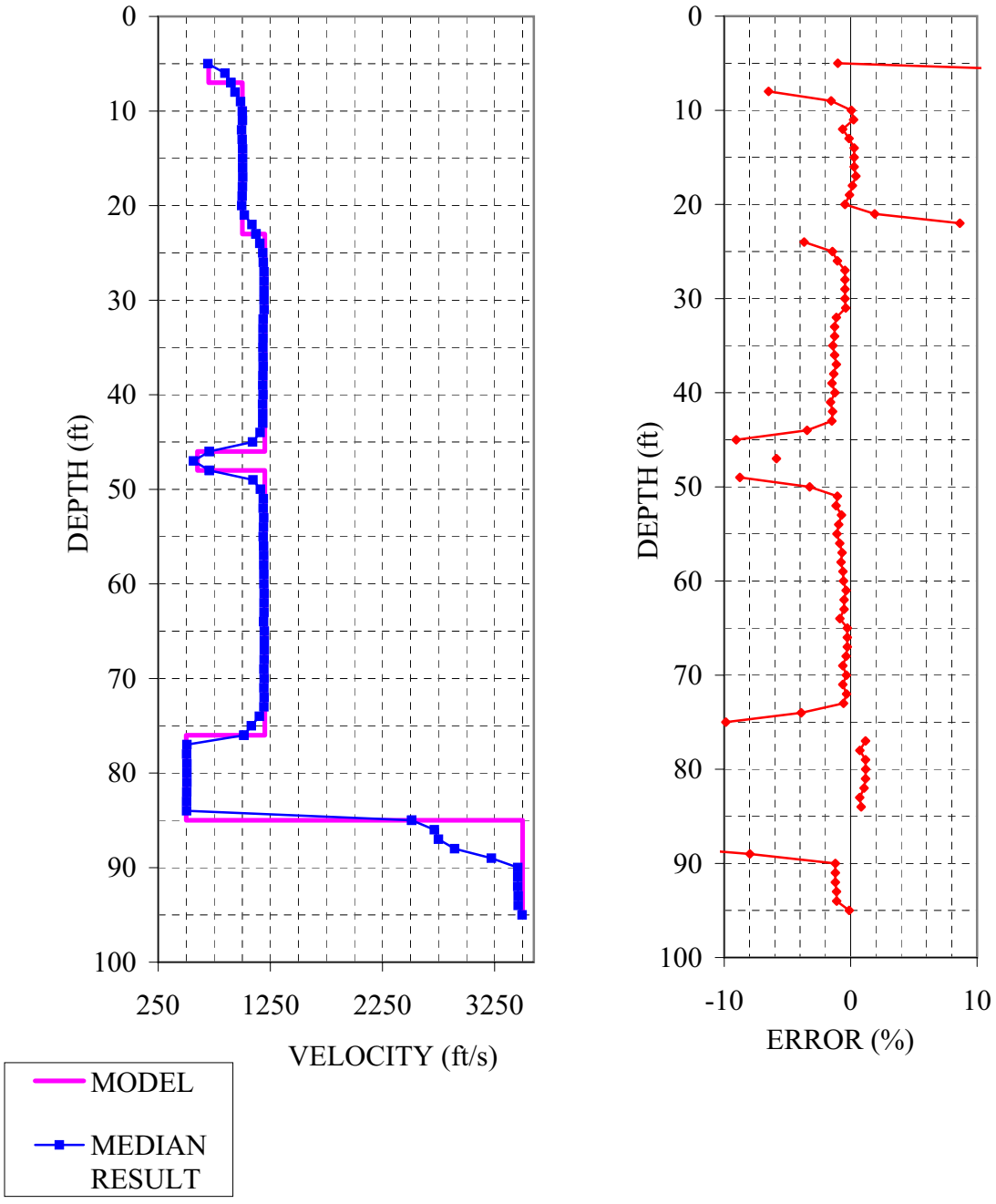

Figure 4-12: Comparison of median computed and correct velocity-depth profiles for model 5 and corresponding percent errors.

MODEL 6

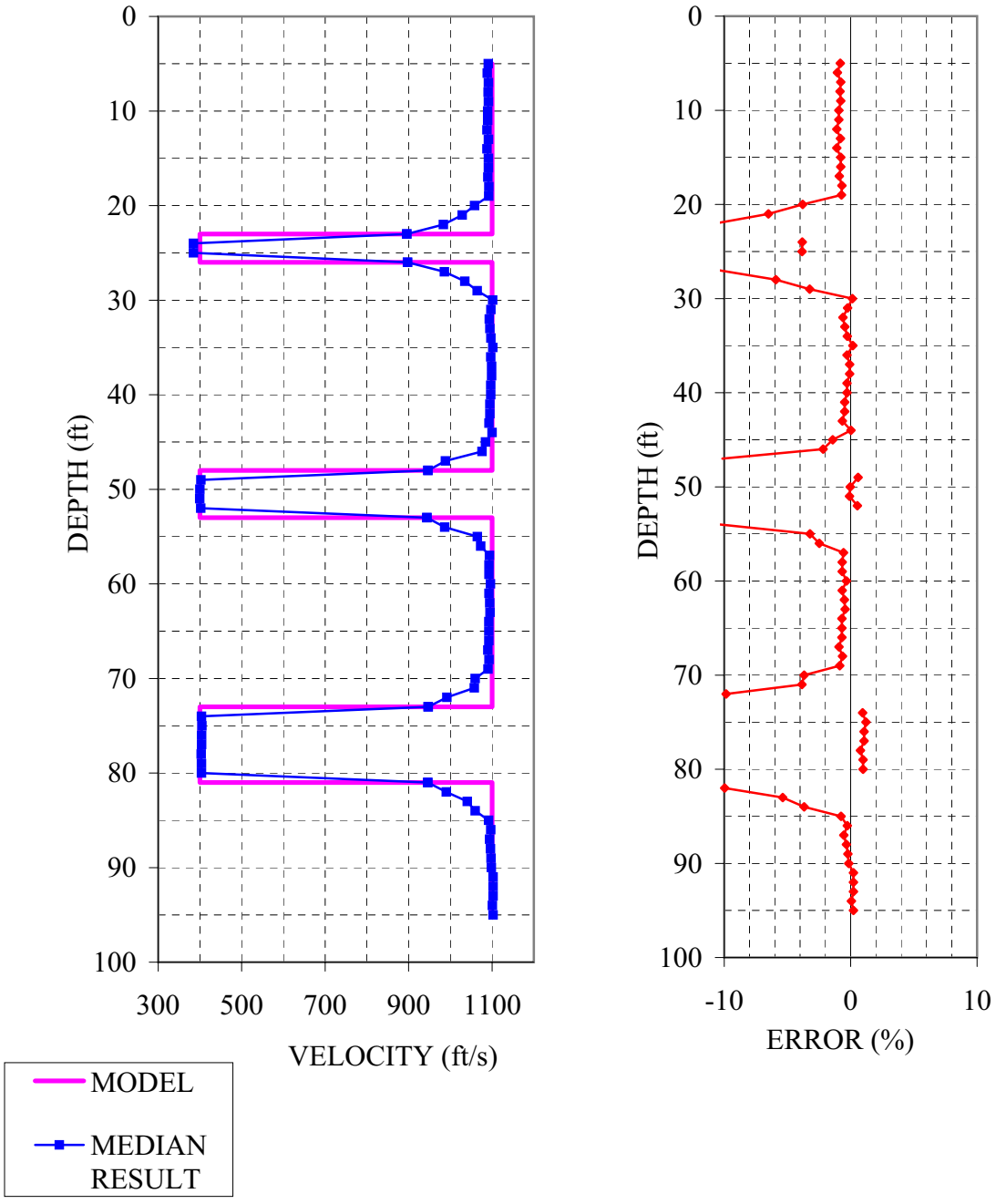

Figure 4-13: Comparison of median computed and correct velocity-depth profiles for model 6 and corresponding percent errors.

MODEL 7

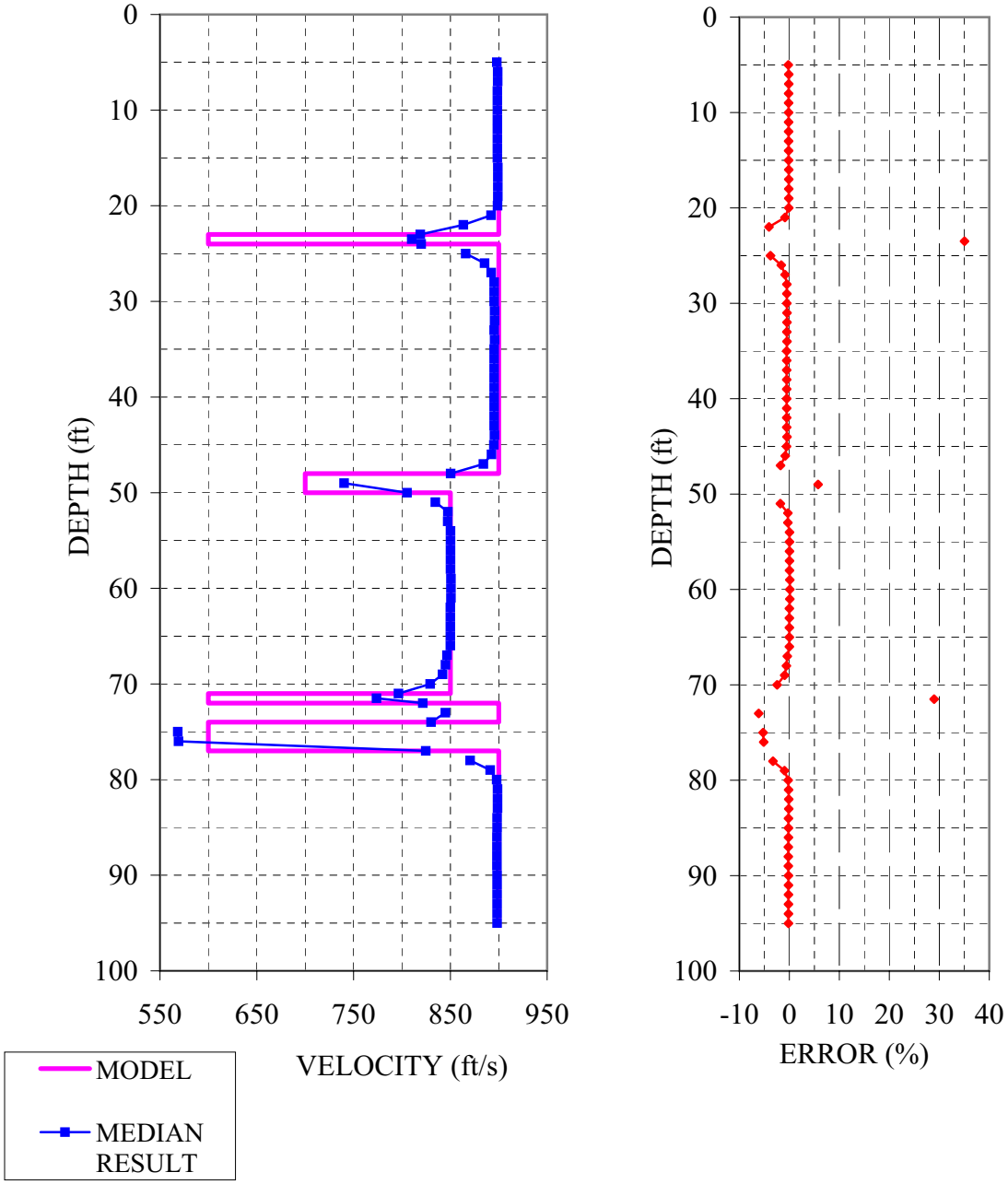

Figure 4-14: Comparison of median computed and correct velocity-depth profiles for model 7 and corresponding percent errors.

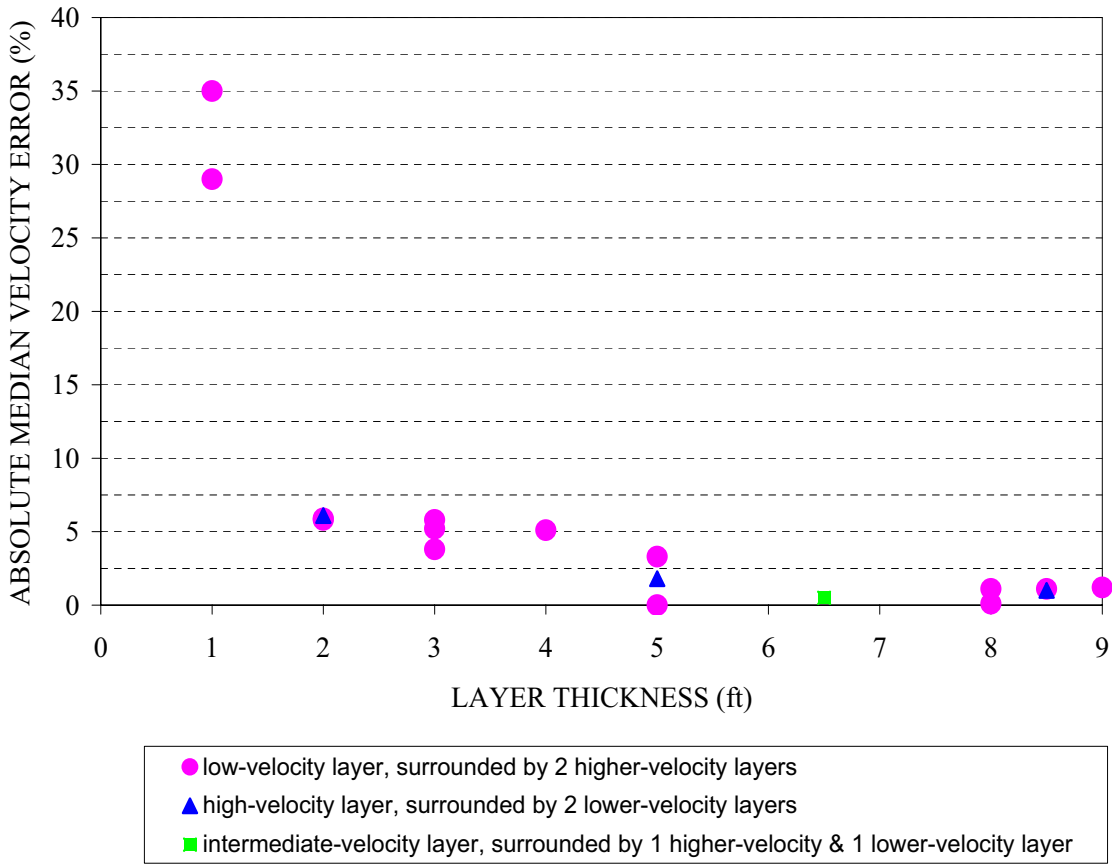

Figure 4-15: Absolute errors of median computed layer velocities (measured at the centers of the layers) plotted as a function of layer thickness.

5. Discussion

The results presented above are based on Reclamation's current data processing procedures. These procedures include determining arrival times for the direct horizontally-propagating shear waves and then computing velocities assuming straight horizontal ray paths. There is some debate about whether resolution could be improved by using ray bending in the velocity computations. Ray bending can account for refraction of seismic energy at layer interfaces. Incorporating ray bending into the velocity computations, therefore, should reduce the smearing of higher velocities into adjacent lower-velocity layers at interfaces and possibly reduce the errors of computed velocities within thin low-velocity layers. Ray bending processing cannot reduce the smearing of lower velocities into adjacent higher-velocity layers nor eliminate all velocity errors

MODEL NO. & DEPTH RANGE OF LAYER (ft)	LAYER THICK-NESS (ft)	LAYER S-WAVE VELOCITY (ft/s)	ADJACENT LAYER VELOCITIES (ft/s) AND VELOCITY RATIOS	MEDIAN COMPUTED S-WAVE VELOCITY IN CENTER OF LAYER (ft/s)	ERROR OF MEDIAN COMPUTED CENTER VELOCITY (%)
1: 16-21	5	1100	800 above & below (0.7 : 1)	1080	-1.8
3: 81-85	4	600	1100 above (1.8 : 1) 2200 below (3.7 : 1)	569	-5.1
4: 18-21	3	900	1450 above (1.6 : 1) 1400 below (1.6 : 1)	848	-5.8
4: 41-46	5	850	1400 above (1.6 : 1) 1450 below (1.6 : 1)	822	-3.3
5: 46-48	2	600	1200 above & below (2 : 1)	565	-5.9
6: 23-26	3	400	1100 above & below (2.75 : 1)	385	-3.8
6: 48-53	5	400	1100 above & below (2.75 : 1)	400	0.0
7: 23-24	1	600	900 above & below (1.5 : 1)	810	35.0
7: 48-50	2	700	900 above (1.3 : 1) 850 below (1.2 : 1)	740	5.8
7: 71-72	1	600	850 above (1.4 : 1) 900 below (1.5 : 1)	774	29.0
7: 72-74	2	900	600 above & below (0.7 : 1)	845	-6.1
7: 74-77	3	600	900 above & below (1.5 : 1)	569	-5.2

Table 4-1: Median computed velocities and corresponding errors in the centers of thin layers (5 feet or less in thickness).

within thin layers, however, because it does not account for the finite frequency range of the seismic data. Resolution limits due solely to the finite frequency range of the data would still exist.

In order to incorporate ray bending into the crosshole data processing, we would need to determine arrival times of the earliest-arriving shear waves, i.e., the refracted shear waves. Computer code that incorporates ray bending into the velocity computations is readily available, but we have been reluctant to use it for crosshole data processing because we do not believe that we can systematically determine the arrival times of refracted shear waves from typical field data. The difficulty of determining arrival times of refracted shear waves is due to several factors, including the relatively low amplitude of refracted arrivals compared to direct arrivals, interference from P-wave energy and possibly converted phases, and the vertical orientation of the geophones which is optimal for recording the horizontally-propagating direct shear waves but not the more vertically-propagating refracted shear waves. For these reasons, we have assumed that we can determine the arrival times of the direct shear waves more systemically than we can determine the arrival times of the refracted shear waves. To investigate our relative ability to determine arrival times of direct and refracted shear waves, we plotted the arrival times of the direct and refracted shear waves on synthetic waveforms from some of the models. These arrival times were computed with a ray bending algorithm using the correct velocity models. Examples from models 3, 4, and 7 are presented in figure 5-1. The vertical black tick marks represent arrival times of refracted waves, while the magenta tick marks represent the times of later-arriving direct waves. If a waveform displays only one tick mark, that indicates that the direct and refracted arrival times coincide. In general, the refracted seismic energy is of low amplitude and relatively low frequency. Even on these noise-free, simplistic synthetic waveforms, the higher-amplitude, higher-frequency direct energy is usually more distinct than the refracted energy. The contrast between the two arrivals is even stronger on field data, where P-wave arrivals tend to obscure the low-amplitude refracted shear waves. The exception is on waveforms that are within low-velocity layers and within one to two feet of an interface with a higher-velocity layer, in which case the refracted arrival has higher amplitude than the direct wave and is more distinct. For example, see the waveforms in figure 5-1b at 58 and 65 feet depth (which are within one foot of an interface with a higher-velocity layer), those in figure 5-1c at 89 and 90 feet depth (which are within two feet of a simulated bedrock interface), and the waveforms in figure 5-1d at 71.5 feet depth (which are within a 1-ft-thick low-velocity layer).

To determine whether incorporating ray bending into the data processing (for those cases in which the refracted shear-wave energy is more likely to be identified than the direct energy) can improve the resolution of thin low-velocity layers, the BOR arrival times from the near geophone data from model 7 were reprocessed in the following manner. Using the direct and refracted shear-wave arrival times calculated from the correct velocity model as a guide, we identified, for each depth, whether the arrival time pick is closer to the correct direct or refracted arrival time. For those depths at which the arrival time pick is closer to the refracted arrival time than the direct arrival time, we used ray bending to process the data. For the near geophone data in model 7, these data are within the two 1-ft-thick low-velocity layers (at 23.5 and 71.5 feet depth) and within the 2-ft-thick low-velocity layer (at 49 feet depth). At all other depths, where the arrival time pick is closer to the direct arrival time than the refracted arrival time, straight rays were used to process the data. A layered velocity model was computed from all data simultaneously using an iterative inversion method (a one-dimensional tomographic matrix inversion with an L1-norm

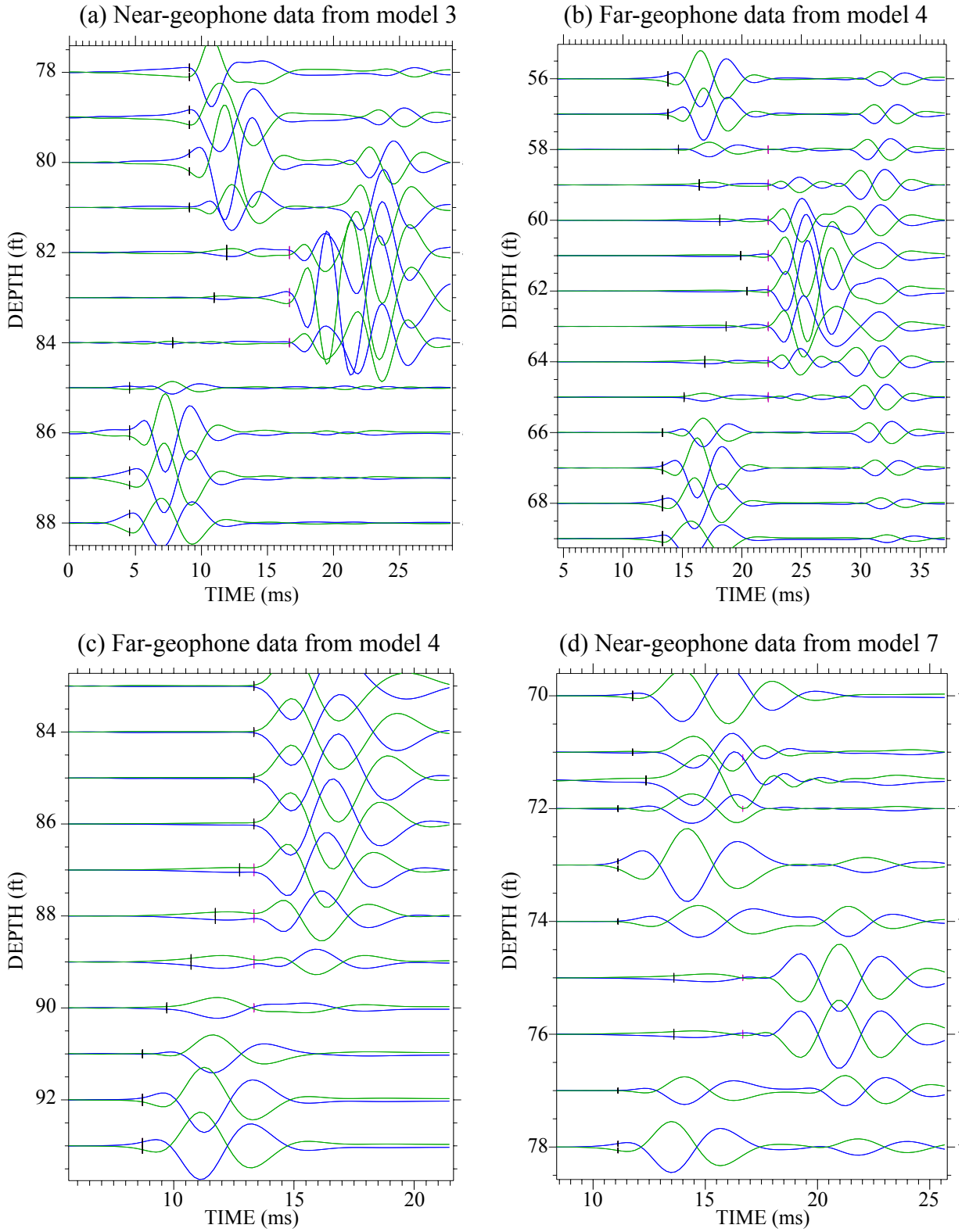

Figure 5-1: Selected synthetic waveforms with arrival times of refracted (black tick marks) and direct (magenta tick marks) shear waves displayed.

minimization). The results from this processing are compared to the correct velocity model, as well as to the results from Reclamation's standard straight-ray processing, in figure 5-2. With the exception of slightly improved resolution of the velocity within the 1-ft-thick low-velocity layer at 71.5 feet depth (the error decreases from 29% to 19.5%), there is negligible difference between the result from the data processing that incorporates ray bending and that from Reclamation's standard straight-ray processing. Including the data from the far geophone does not improve the results. We conclude from this test that the thin-bed resolution limit of crosshole shear-wave surveys is controlled mainly by the finite frequency range of the data; ray bending effects are secondary and relatively small.

The resolution of crosshole shear-wave surveys may potentially be improved by using a processing method that accounts for the finite frequency range of the data, but such a method would be much more difficult to implement than Reclamation's current processing technique. Repetitive forward modeling or waveform inversion techniques could be used to determine P-wave and S-wave velocity models that best match the observed seismic waveforms (rather than just the arrival times). The application of such techniques would require an accurate mathematical representation of the source radiation pattern (pattern of P- and S-wave energy generated by the source), as well as sufficient knowledge of the receiver responses. Field testing would be required to determine this information. Also, the effects of seismic attenuation (which alters the amplitudes and frequencies of recorded waveforms) on field data would have to be investigated and accounted for if necessary. The use of waveform processing techniques would require much more data computation time for each crosshole survey performed, both in terms of computer resources and personnel time, than Reclamation's current processing method. A waveform processing technique, if properly applied, should significantly reduce smearing across layer interfaces. However, it is not known how much it would improve the resolution of S-wave velocities within thin (less than 2-ft-thick) low-velocity layers. Further modeling with synthetic waveforms would be required to determine how sensitive waveform processing techniques would be to the S-wave velocities within thin layers.

The most effective and efficient way to improve the resolution of Reclamation's crosshole shear-wave surveys would be to use a higher-frequency borehole shear-wave source if possible. Borehole seismic sources are available today that were not available when Reclamation began performing crosshole shear-wave surveys more than two decades ago. The strength and frequency range of the shear-wave signals that may be propagated over short distances (10 to 20 feet) through soils by newer sources is not currently known.

6. Conclusions

Tests with synthetic data indicate that the crosshole shear-wave method, as currently implemented by Reclamation, can adequately determine velocities of layers two feet or more in thickness. In these studies, shear-wave velocities within layers more than five feet thick were determined with errors of less than 1.5%. Velocities within layers two to five feet thick were determined with errors of less than 6.5%. Because the synthetic data do not contain all of the complexities of field data, most notably lacking P-wave energy and converted phases, errors of velocities computed

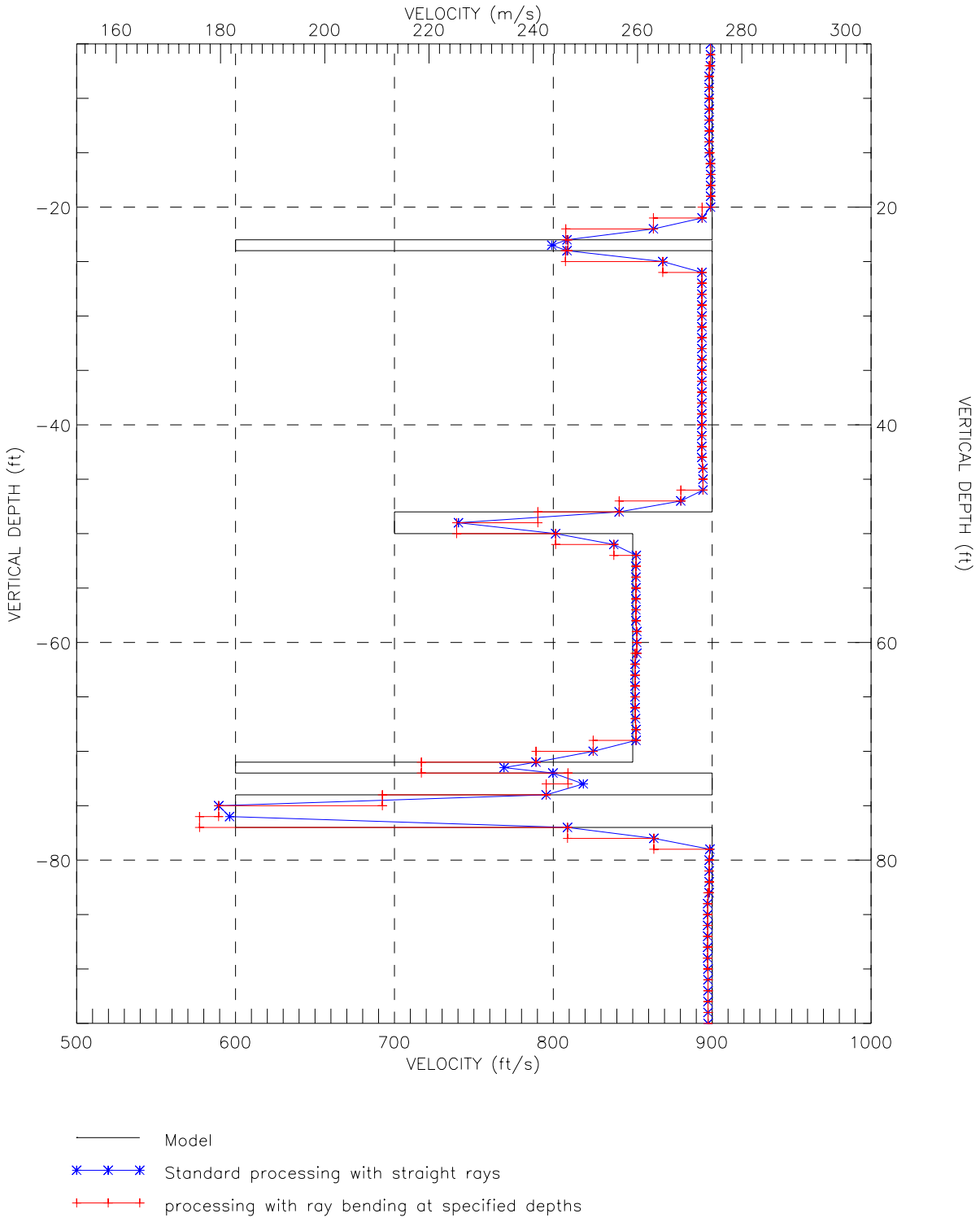

Figure 5-2: Comparison of velocities for model 7 computed with data processing that incorporates ray bending (red line) and velocities computed with Reclamation's standard straight-ray processing (blue line). The correct velocity model is shown for reference.

from field data are likely to be somewhat greater than those computed from these synthetic data. Even so, given the results presented here, we estimate that errors of velocities computed from crosshole field data are less than 5% for layers greater than five feet thick and less than about 10% for layers two to five feet thick. Although layers less than two feet thick can be detected with the crosshole method, the accuracy of the method greatly deteriorates for such layers. Velocities computed within the 1-ft-thick low-velocity layers included in these models have errors of 29% to 35%.

The thin-bed resolution limit of the crosshole shear-wave method is controlled mainly by the frequency content of the propagated seismic energy. Tests indicate that incorporation of ray bending into the data processing procedures has little effect on the resolution of velocities within layers less than two feet thick. Waveform processing would be complex and time-consuming and may not greatly improve thin-bed resolution since the finite frequency range of the data would still effect the accuracy of the results. The most effective and efficient way to improve the resolution of Reclamation's crosshole shear-wave surveys would be to use a higher-frequency borehole shear-wave source.

These tests also demonstrate that computed crosshole velocities are smeared at layer interfaces, with velocities being overestimated in the lower-velocity layer near an interface and velocities underestimated in the adjacent higher-velocity layer. The smearing at layer interfaces is caused by refraction of seismic energy and the finite frequency range of the propagated seismic energy. Because of this smearing near layer interfaces, the most accurate crosshole velocities are those computed near the centers of velocity layers. The exact depths of layer interfaces are better determined from geologic drill logs and geophysical borehole logs rather than from crosshole velocity profiles.

7. Bibliography

Hisada, Y., 1994, An efficient method for computing Green's functions for a layered half-space with sources and receivers at close depths (Part 1), *Bull. Seism. Soc. Am.*, Vol. 84, 1456-1472.

Hisada, Y., 1995, An efficient method for computing Green's functions for a layered half-space with sources and receivers at close depths (Part 2), *Bull. Seism. Soc. Am.*, Vol. 85, 1080-1093.

Acknowledgements

We would like to thank Karl Ellefsen from the U. S. Geological Survey and Jose Llopis from the U. S. Army Corps. of Engineers for contributing to this research effort by providing shear-wave arrival time picks.

APPENDIX A
MODEL PARAMETERS

All models are defined from 0 to 100 feet depth. The models are layered, with no horizontal variations in model paramaters. The tables that follow list the depth range, thickness, density, P-wave and S-wave velocities, and P-wave and S-wave attenuation factors (Qp and Qs) for each layer. The attenuation factors control how much energy is absorbed by the materials as the seismic waves pass through them. Higher Q values indicate lower attenuation (less energy loss), whereas lower Q values indicate higher attenuation (more energy loss).

LIST OF TABLES

Page

DEPTH RANGE (ft)	LAYER THICKNESS (ft)	DENSITY (g/cc)	P-WAVE VELOCITY (ft/s)	Qp	S-WAVE VELOCITY (ft/s)	Qs
0 - 16	16	1.842	1280	55	800	40
16 - 21	5	2.082	2200	65	1100	50
21 - 42.5	21.5	1.922	5400	55	800	40
42.5 - 53	10.5	2.082	5500	65	1100	50
53 - 72.5	19.5	1.922	5200	55	800	40
72.5 - 81	8.5	2.082	5500	65	1100	50
81 - 100	19	1.922	5100	55	800	40

Table A-1: Parameters for model 1.

DEPTH RANGE (ft)	LAYER THICKNESS (ft)	DENSITY (g/cc)	P-WAVE VELOCITY (ft/s)	Qp	S-WAVE VELOCITY (ft/s)	Qs
0 - 11	11	2.002	1800	76	1000	50
11 - 28	17	1.522	1000	55	400	35
28 - 46	18	1.762	5300	57.5	600	40
46 - 63	17	1.842	5400	57.5	800	45
63 - 76	13	1.922	5500	70	1000	50
76 - 93	17	2.824	5500	85	1200	65
93 - 100	7	2.162	5500	95	1500	75

Table A-2: Parameters for model 2.

DEPTH RANGE (ft)	LAYER THICKNESS (ft)	DENSITY (g/cc)	P-WAVE VELOCITY (ft/s)	Qp	S-WAVE VELOCITY (ft/s)	Qs
0 - 11	11	2.082	2500	85	1400	60
11 - 26	15	1.922	5400	75	1100	50
26 - 38	12	1.842	5400	67.5	900	45
38 - 46	8	1.842	5400	57.5	700	35
46 - 52.5	6.5	1.842	5400	68	900	45
52.5 - 81	28.5	1.922	5400	75	1100	50
81 - 85	4	1.602	5100	57	600	35
85 - 100	15	2.243	6700	90	2200	75

Table A-3: Parameters for model 3.

DEPTH RANGE (ft)	LAYER THICKNESS (ft)	DENSITY (g/cc)	P-WAVE VELOCITY (ft/s)	Qp	S-WAVE VELOCITY (ft/s)	Qs
0 - 18	18	2.162	2750	85	1450	65
18 - 21	3	1.842	4900	67.5	900	45
21 - 41	20	2.002	5300	85	1400	60
41 - 46	5	1.842	5100	67.5	850	45
46 - 57.5	11.5	2.082	5300	85	1450	60
57.5 - 66	8.5	1.842	5100	67.5	900	45
66 - 91	25	2.082	5300	95	1500	70
91 - 100	9	2.243	7500	120	2300	90

Table A-4: Parameters for model 4.

DEPTH RANGE (ft)	LAYER THICKNESS (ft)	DENSITY (g/cc)	P-WAVE VELOCITY (ft/s)	Qp	S-WAVE VELOCITY (ft/s)	Qs
0 - 7	7	1.442	1200	58	700	35
7 - 23	16	2.002	1800	75	1000	50
23 - 46	23	2.082	6300	85	1200	60
46 - 48	2	1.89	5300	57	600	35
48 - 76	28	2.162	6400	92	1200	65
76 - 85	9	1.57	6200	57	500	35
85 - 100	15	2.323	7500	100	3500	70

Table A-5: Parameters for model 5.

DEPTH RANGE (ft)	LAYER THICKNESS (ft)	DENSITY (g/cc)	P-WAVE VELOCITY (ft/s)	Qp	S-WAVE VELOCITY (ft/s)	Qs
0 - 23	23	2.082	5400	85	1100	60
23 - 26	3	1.602	5200	58	400	35
26 - 48	22	2.082	5400	85	1100	60
48 - 53	5	1.602	5200	58	400	35
53 - 73	20	2.082	5400	85	1100	60
73 - 81	8	1.602	5200	57.5	400	35
81 - 100	19	2.082	5400	95	1100	60

Table A-6: Parameters for model 6.

DEPTH RANGE (ft)	LAYER THICKNESS (ft)	DENSITY (g/cc)	P-WAVE VELOCITY (ft/s)	Qp	S-WAVE VELOCITY (ft/s)	Qs
0 - 23	23	1.84	5200	70	900	60
23 - 24	1	1.7	5200	58	600	40
24 - 48	24	1.84	5200	70	900	60
48 - 50	2	1.75	5200	58	700	45
50 - 71	21	1.84	5200	70	850	55
71 - 72	1	1.7	5200	57.5	600	40
72 - 74	2	1.84	5200	65	900	60
74 - 77	3	1.7	5200	57.5	600	45
77 - 100	23	1.84	5200	70	900	60

Table A-7: Parameters for model 7.

APPENDIX B
WAVEFORM COMPUTATION METHOD

The synthetic seismograms were calculated using the public-domain computer code "grfault.f" written by Yoshiaki Hisada (Hisada, 1994; Hisada, 1995). This code computes Green's functions for a visco-elastic layered half-space using an efficient frequency-wavenumber method that utilizes both analytical and numerical wavenumber integrations. For this application, integrations were performed for frequencies ranging from approximately 1 to 1000 Hz. A vertical shear dislocation (dipole) source, one centimeter in length and width and having zero rise time and infinite rupture velocity, was used to approximate the radiation pattern generated by the downhole shear-wave hammer. (The program input parameters used in this study are documented in the attached commented input file.)

The output of "grfault.f" is the complex frequency displacements at the receivers for each component. Time-domain waveforms are obtained by inverse FFT. For this application, the time-domain seismograms have a sampling interval of 200 microseconds. The seismograms were post-processed with a seventh-order low-pass Bessel function filter having a 150-Hz corner frequency to match the frequency response of typical crosshole waveforms recorded in the field.

Bibliography

Hisada, Y., 1994, An efficient method for computing Green's functions for a layered half-space with sources and receivers at close depths (Part 1), *Bull. Seism. Soc. Am.*, Vol. 84, 1456-1472.

Hisada, Y., 1995, An efficient method for computing Green's functions for a layered half-space with sources and receivers at close depths (Part 2), *Bull. Seism. Soc. Am.*, Vol. 85, 1080-1093.

COMMENTED INPUT FILE FOR "GRFAULT.F" SPECIFYING THE PARAMETERS USED IN THIS STUDY

```
* OMEGA DATA *
      1      1024   6.13592 : IOM(INITIAL),NOM(FINAL),DOM(Delta Omega)
```

(Integration range of the circular frequency ω $(=2\pi f)$. The initial ω is IOM*DOM (corresponding to $f \approx 1$ Hz in this case) and the final ω is NOM*DOM ($f \approx 1000$ Hz). DOM is the increment of ω.)

```
* MEDIUM DATA *
     8      (NL, the NUMBER OF LAYERS)
 1.842   390.144   55.0   243.840   40.0    4.8768
 2.082   670.560   65.0   335.280   50.0    1.5240
 1.922  1645.920   55.0   243.840   40.0    6.5532
 2.082  1676.400   65.0   335.280   50.0    3.2004
 1.922  1584.960   55.0   243.840   40.0    5.9436
 2.082  1676.400   65.0   335.280   50.0    2.5908
 1.922  1554.480   55.0   243.840   40.0    5.7912
 1.922  1554.480   55.0   243.840   40.0    0.0000
```

(Data for the layered half-space. In this example, the data is for model 1. Each line gives the parameters for one layer in the model. The columns correspond to density (g/cc), P-wave velocity (m/s), P-wave attenuation (Qp), S-wave velocity (m/s), S-wave attenuation (Qs), and thickness (m).)

```
* FAULT DATA *
   1                 : Number
  0.0 (Source 1)       : Time Delay from the origin time
  0.0      0.0        : Location (X and Y: m)
    1.52400  0.0        : Depth(m), Strike(deg)
 90.0     90.0        : Dip(deg), Rake(deg)
 0.01     0.01     0.01 : Length, Width, Dislocation (m)
  0.0   3000.0        : Rise Time (sec), Rupture Velocity (m/s)
   1                 : NVR (If NVR=1 then Vr=infinite)
```

(Location and description of the source. The source is modeled by Haskell's unilateral point source. The seismic moment for the source is given by Dislocation*Length*Width*Rigidity(Density*Vs*Vs). Length is used to consider the source duration (=Length/Rupture Velocity). The X and Y axes correspond to the north and east directions. Note that the last line (NVR set to 1) indicates that an infinite fault rupture velocity is used for this case.)

```
* WAVENUMBER INTEGRATION DATA FOR SIMPSON"S RULE *
   1 : PATTERN 1  OR 2
    41.4528 200      207.264 200 : C1,N1,C2,N2 (C1<C2) for Pattern 1
```

(Data for the wavenumber integration. Simpson's rule is used for the two integration ranges; we divide the total integration range into two parts. The first part consists of the range from zero

(Point A) to a point after passing the Rayleigh and Love poles (Point B), and the second consists of the range from Point B to the upper limit of the range (Point C). Generally, we need a smaller increment for the first range than the second, because of the sharp changes at the poles. (see e.g., Figs. 9 and 10 in Hisada, 1994, BSSA, V.84, p.1466).

There are two patterns from which to choose. Parameters for pattern 1, chosen for these computations, are given on the second line. The wavenumber at Point B is $\omega/C2$ and the wavenumber at Point C is $\omega/C1$ (where C1 and C2 are specified velocities). Therefore, the locations of Point B and C on the wavenumber axis are dynamically changed for each ω. C2 should be smaller than the minimum Vs of the medium (or the lowest phase velocity corresponding to poles). C1 must be small enough to guarantee the convergence of the integrands at the Point C. N1 is the total number of increments for Simpson's rule between zero and Point B, and N2 is that between Point B and Point C.

```
* OBSERVATION POINT DATA *
  1     1.5240 : LAYER NO., DEPTH FROM UPPER BOUNDARY OF THE LAYER (m)
     2 : NUMBER OF OBSERVATION PTS.
    0.0       3.04800  0.0       6.09600 : 2*(X,Y) (Unit :m)
```

(Data for the observation points (receiver locations). The Cartesian coordinate system (x,y,z) is used as seen in Fig.1 in Hisada (1994). The first line is the data for the receiver depth (z). In this example, the receiver is located 1.524 m below the upper boundary of the first layer. Thus, the absolute depth (z) is 1.524 m. In the second line, the total number of receiver locations is given (2). The (x,y) coordinates of the receiver locations are given on line 3 (3.048m (near receiver at y=10 ft) and 6.096 m (far receiver at y=20 ft)).

```
* DATA FOR THE ASYMPTOTIC SOLUTIONS *
        1 : BE USED (=1), OR NOT USED (=0)
```

(Specify whether the asymptotic method by Hisada (1995) is to be used. If the source depth is close to the receiver depth, the asymptotic solutions give quick convergence. Using the asymptotic solutions increases efficiency, in particular, when the source and/or the receiver are close to the free surface or layer boundaries.)

```
* CHANGE OF SIGNS OF IMAGINARY PARTS OF FINAL RESULTS (FOR FFT) *
        1 : CHANGE SIGN (=1), NOT CHANGE SIGN (=0)
```

(Specify whether to change the signs of the imaginary parts of the final results. In this code, we assumed the time-dependent term as $\exp(-i*\omega*t)$. However, some FFT codes, like "grfft.f", require results with $\exp(+i*\omega*t)$. In those cases, you should choose 1.)

```
* output filename for x,y,z complex frequency responses
q1_m1_1d_z05ft_xyz_fresp.dat
```

APPENDIX C
PLOTS OF SYNTHETIC SEISMIC WAVEFORMS

The synthetic crosshole seismic waveforms are plotted below. The waveforms are plotted as a function of depth, with reversed-polarity waveforms overlaid. For each model, the near-receiver and far-receiver data are presented in separate plots. Within each plot, the waveforms are shown with true relative amplitudes. (The amplitudes of the far-receiver data are scaled by a factor of 2.5 compared to the near-receiver data.) The arrival times of the horizontally-propagating direct shear wave, as computed from the model shear-wave velocities, are overlaid on the waveforms (vertical black tick marks). No arrival times are plotted at depths corresponding to layer interfaces.

Note that for the deepest source/receiver depths in model 5, located in relatively high-velocity simulated bedrock, only the far-receiver waveforms are presented. The near-receiver synthetic waveforms are strongly affected by near-source affects relating to the waveform computation method used. These near-receiver waveforms are not representative of field data and were therefore eliminated from the data set.

The waveforms computed within and near the 1-ft-thick layers in model 7 are plotted at magnified scales in Figures C-15 through C-18.

LIST OF FIGURES

Page

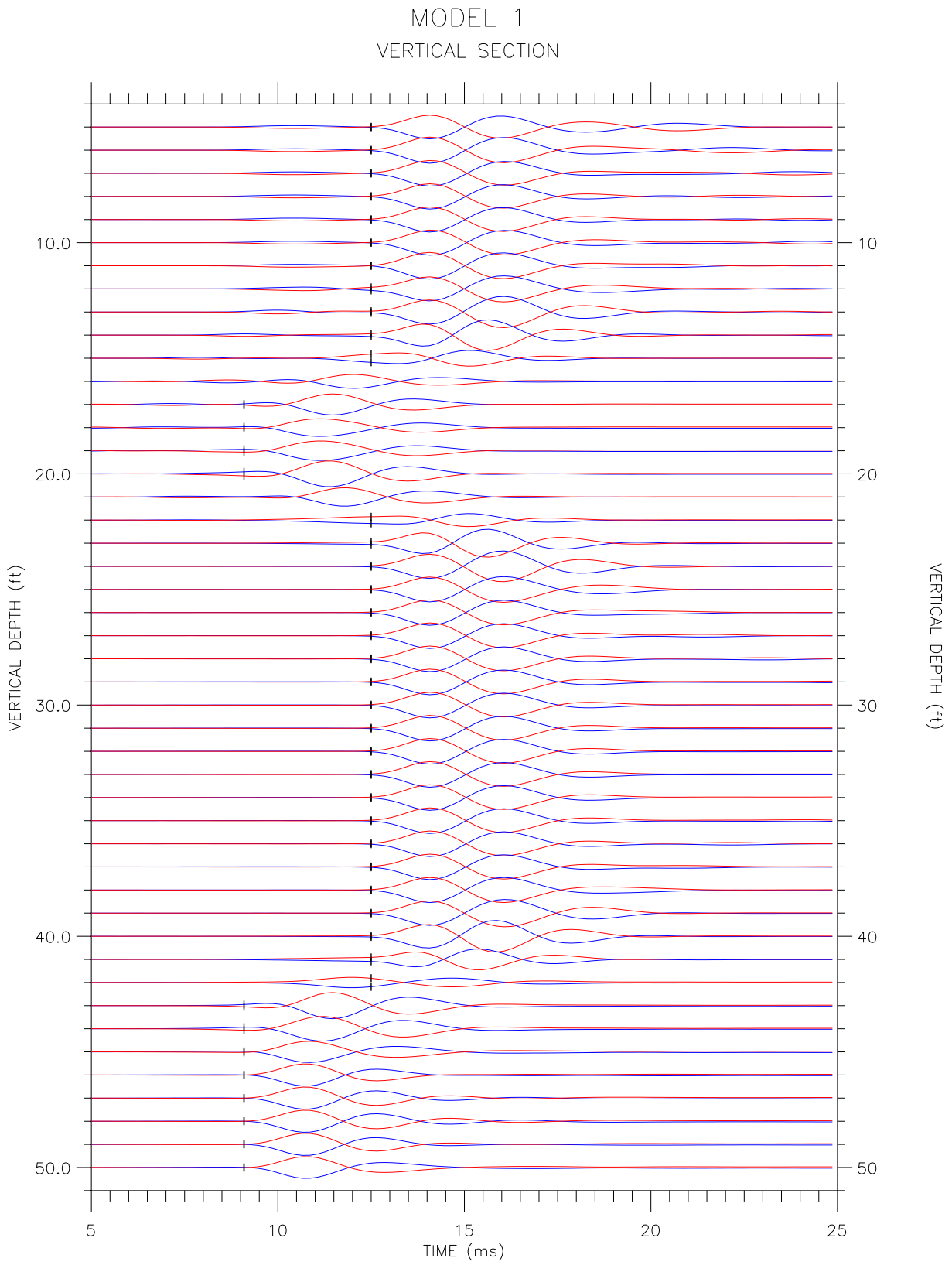

Figure C-1: Synthetic crosshole waveforms for model 1, near receiver.

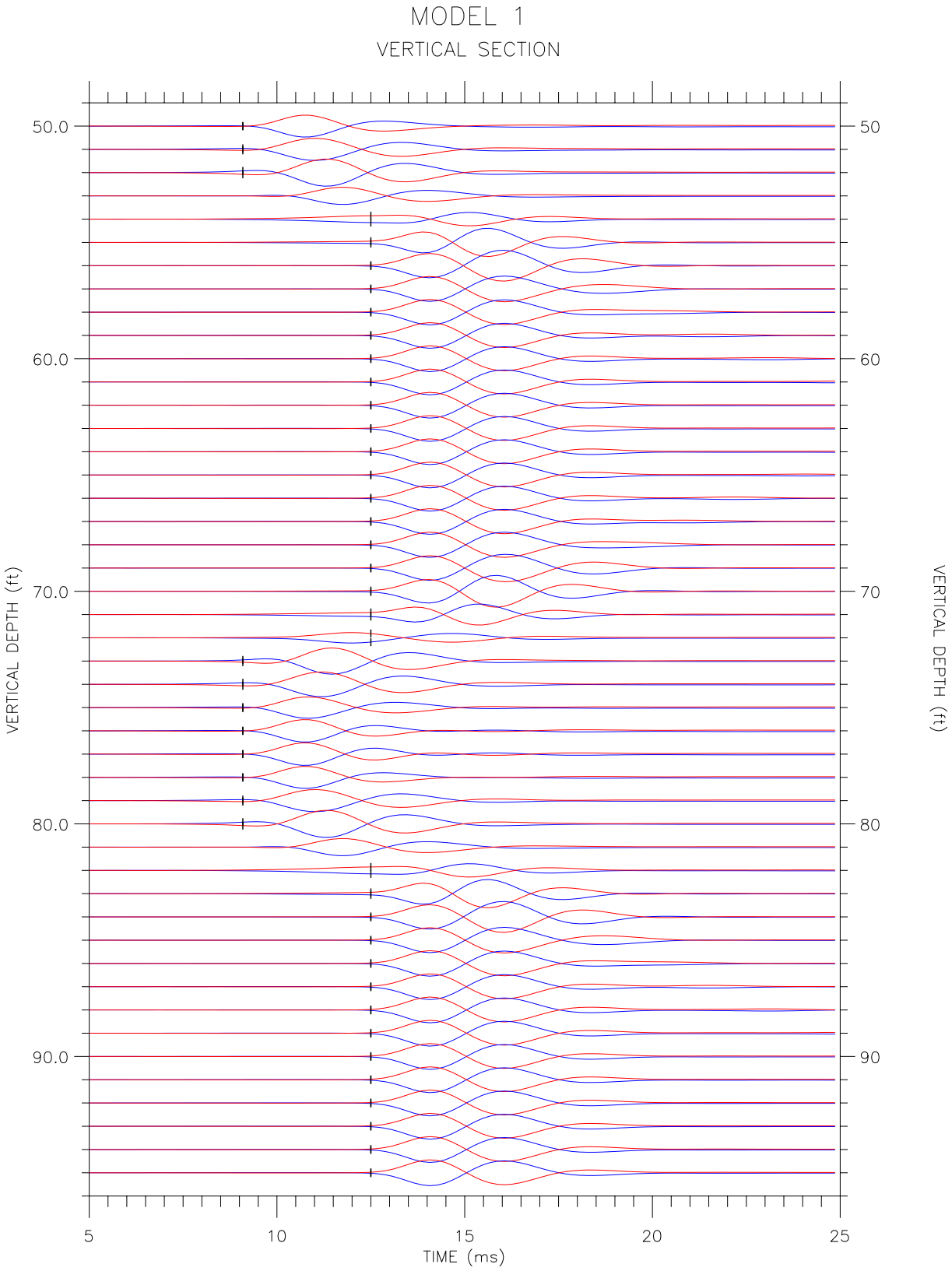

Figure C-1, continued.

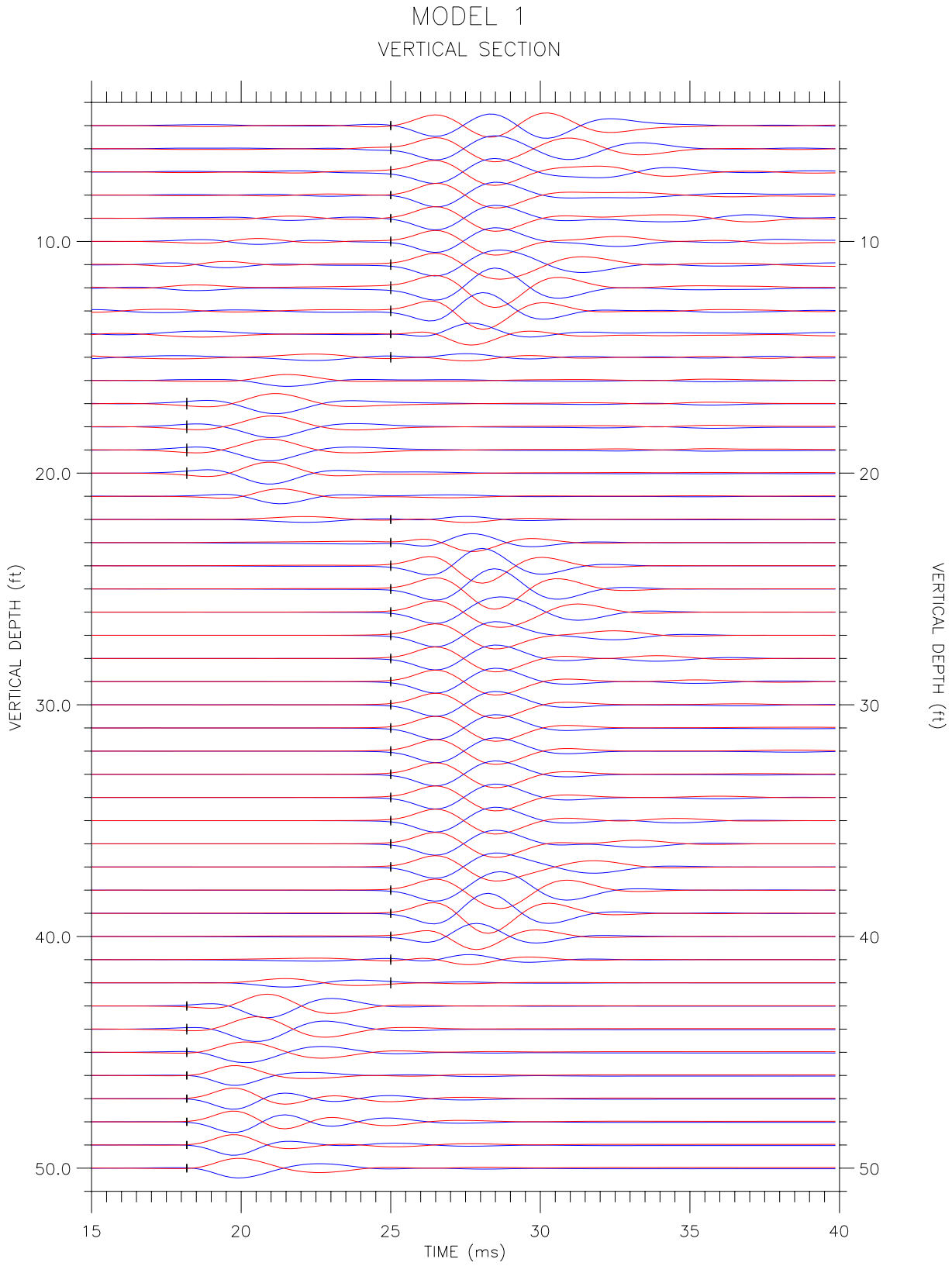

Figure C-2: Synthetic crosshole waveforms for model 1, far receiver.

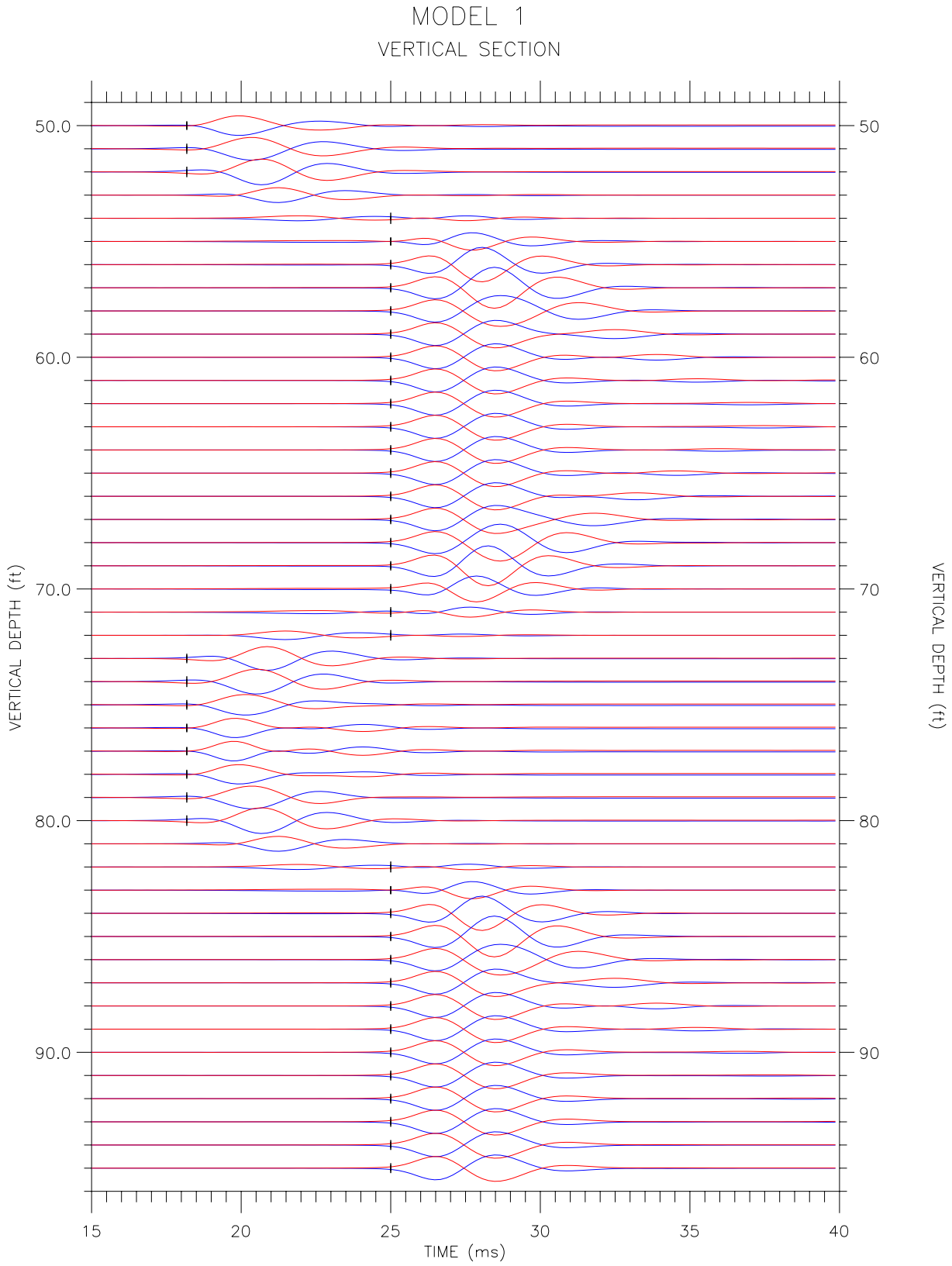

Figure C-2, continued.

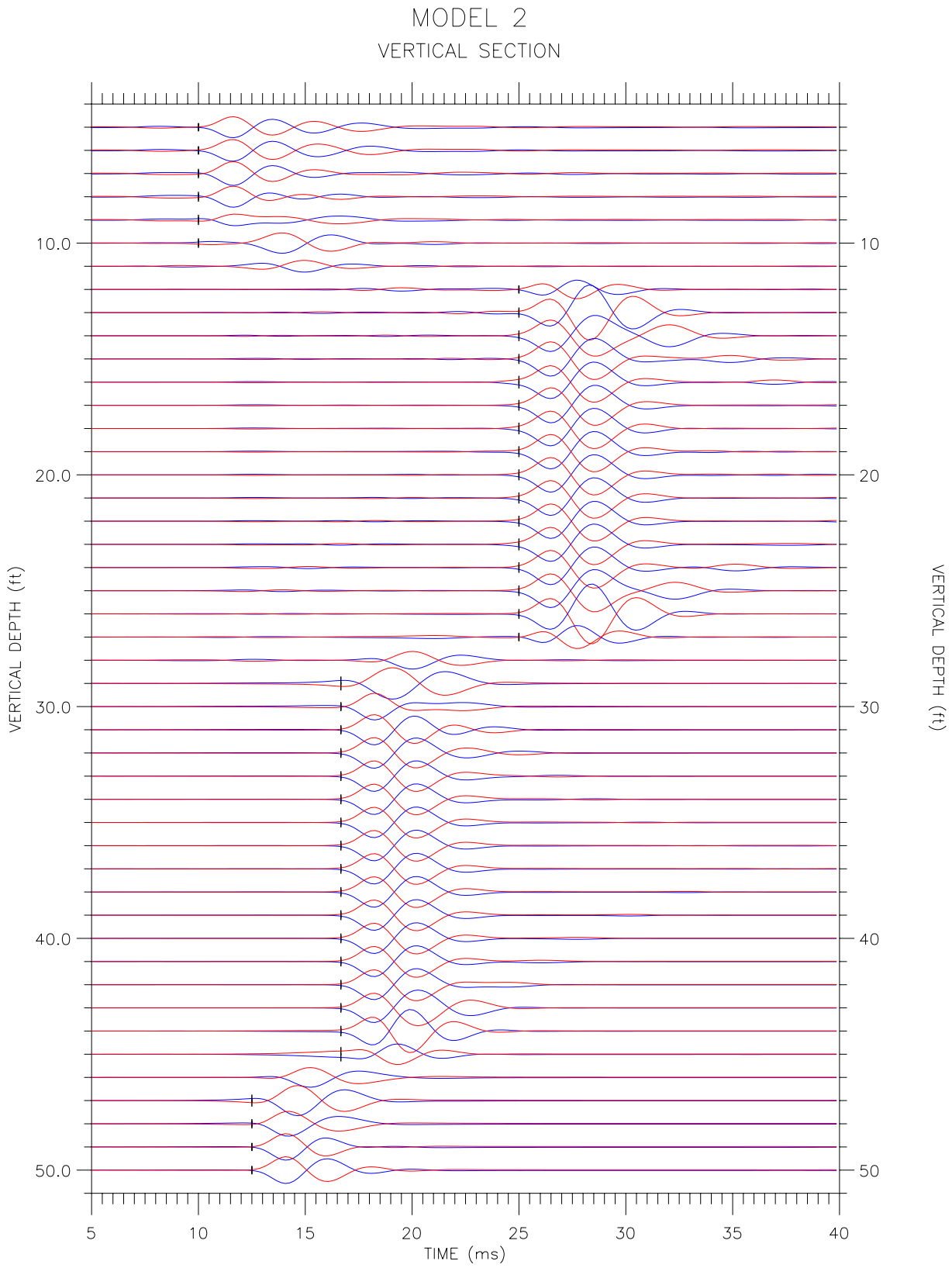

Figure C-3: Synthetic crosshole waveforms for model 2, near receiver.

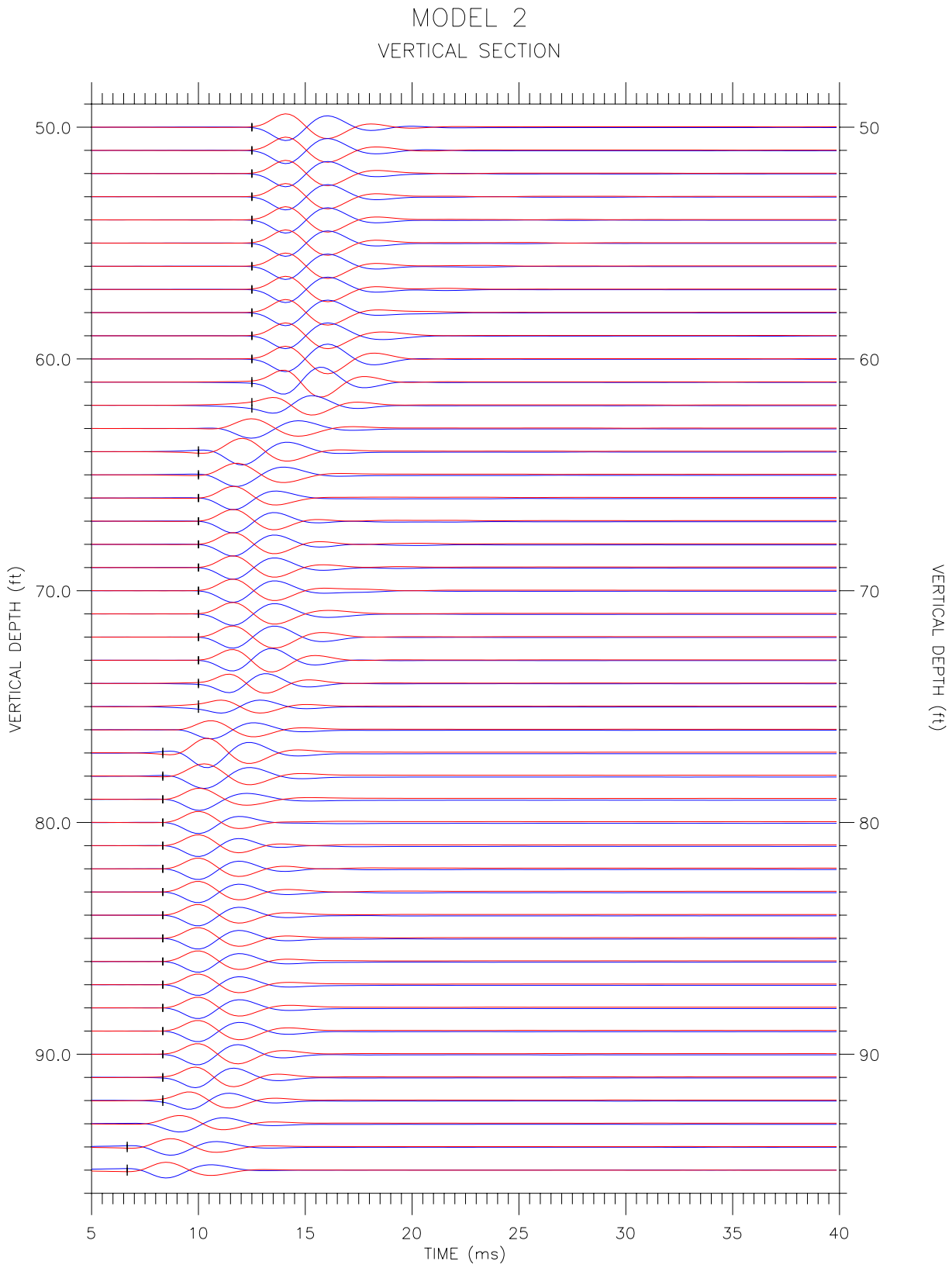

Figure C-3, continued.

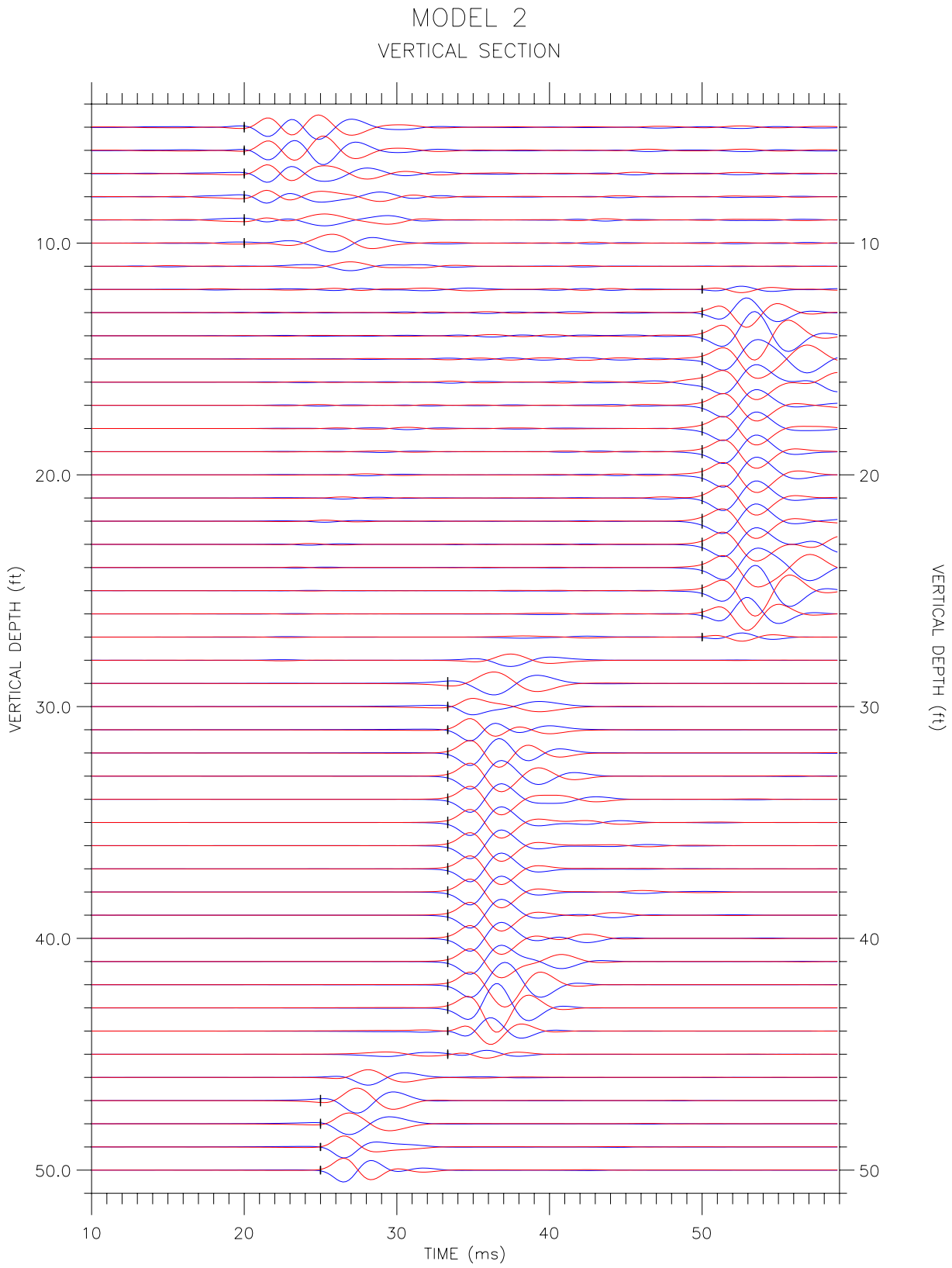

Figure C-4: Synthetic crosshole waveforms for model 2, far receiver.

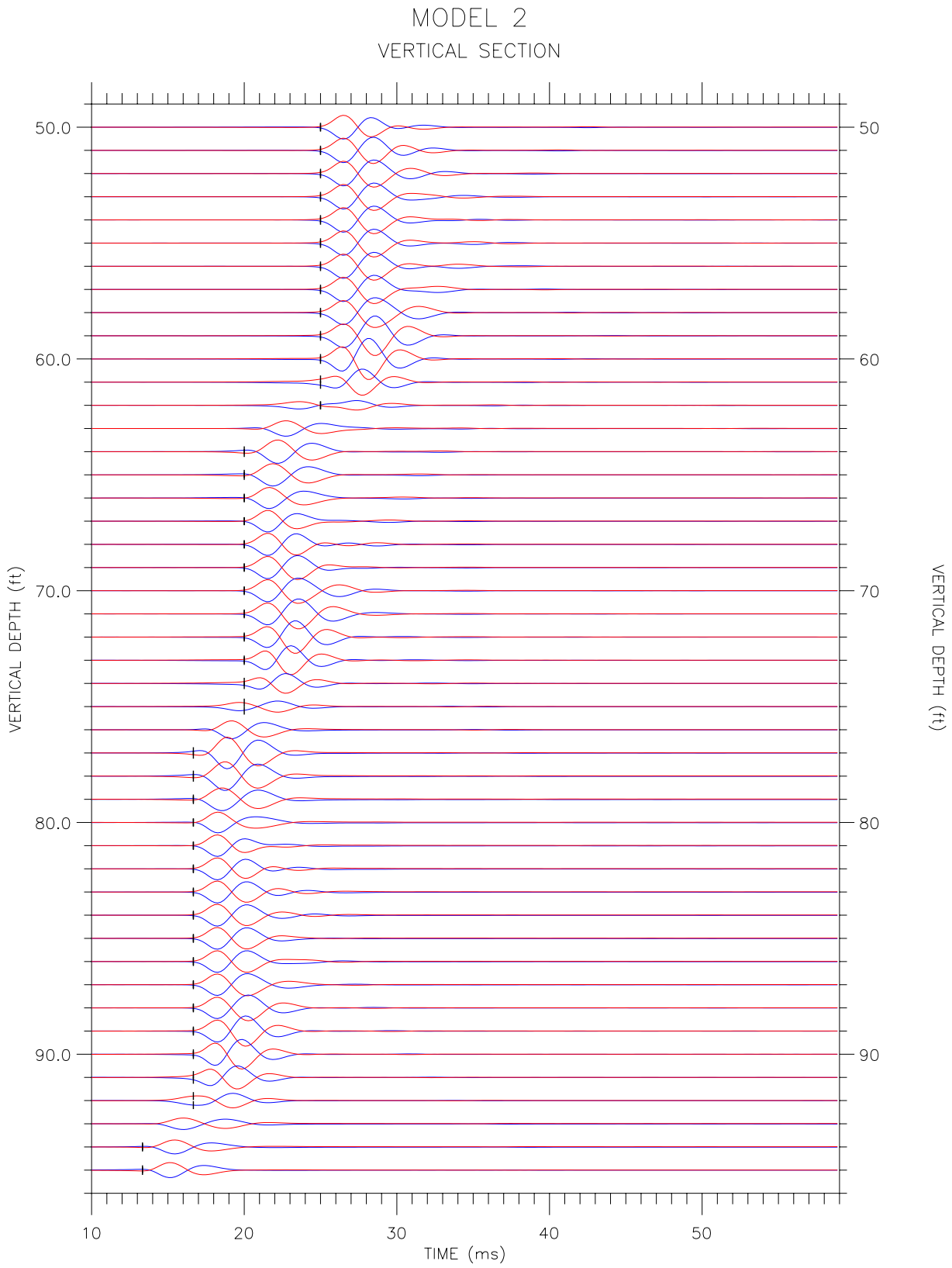

Figure C-4, continued.

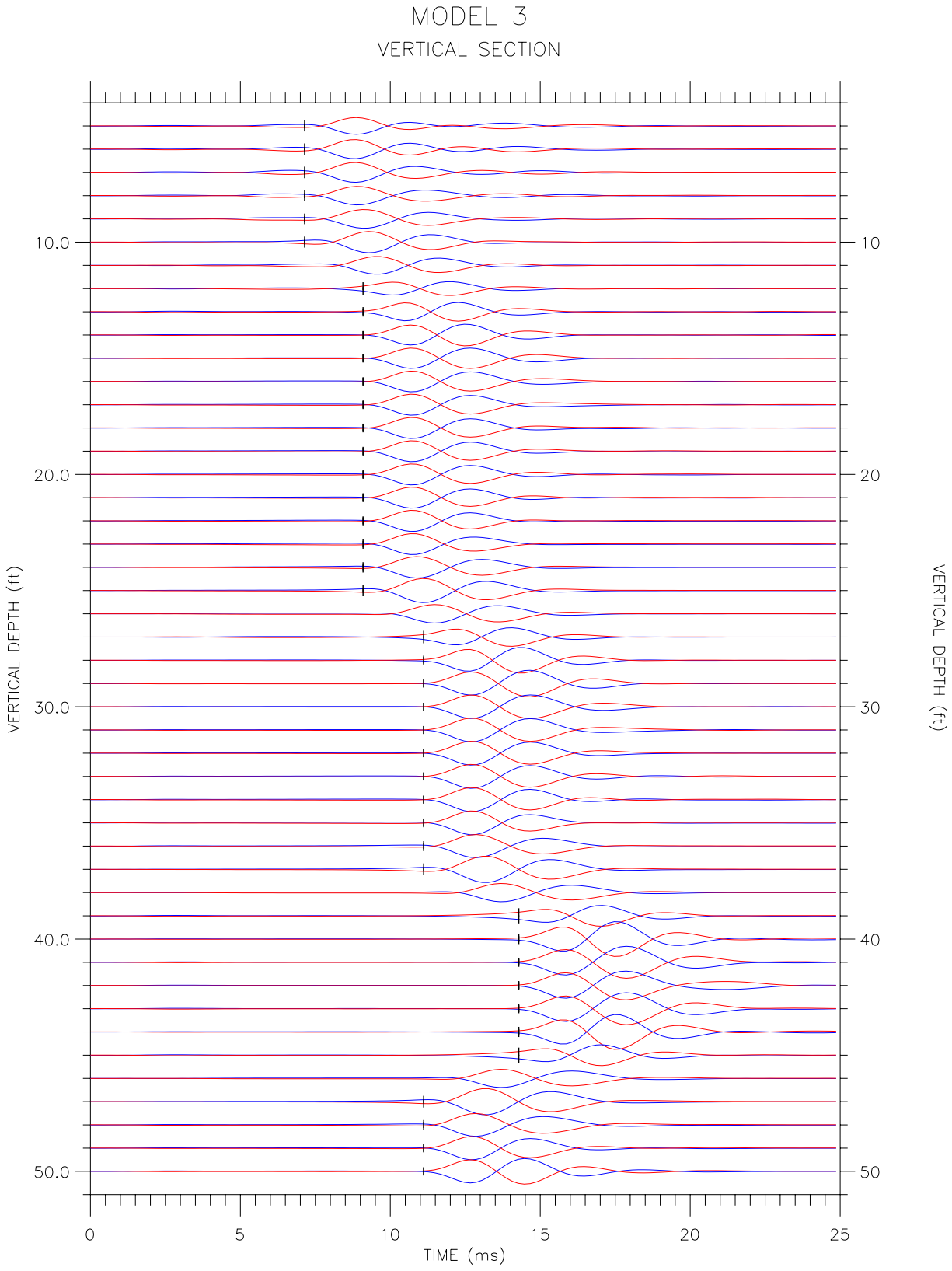

Figure C-5: Synthetic crosshole waveforms for model 3, near receiver.

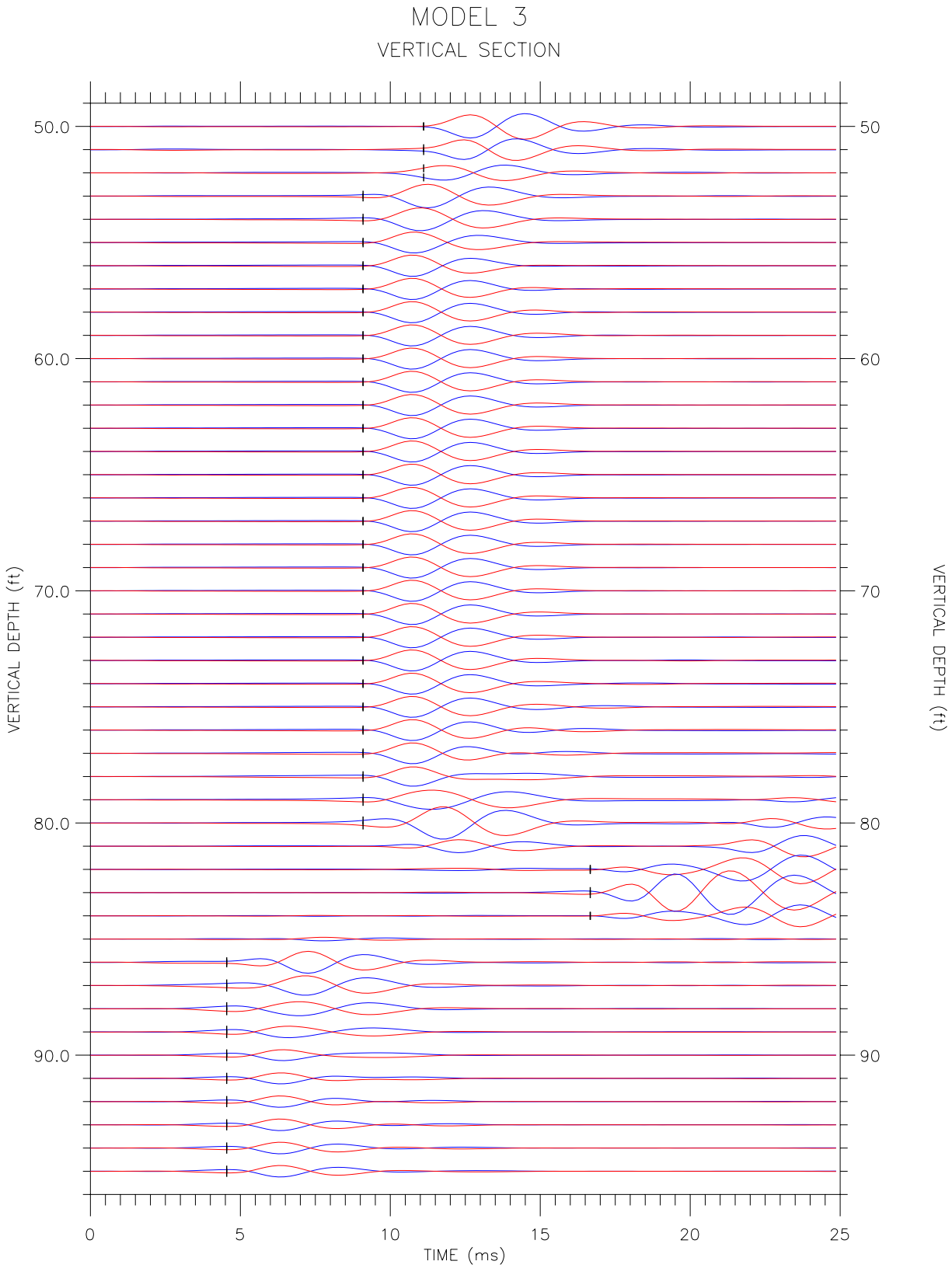

Figure C-5, continued.

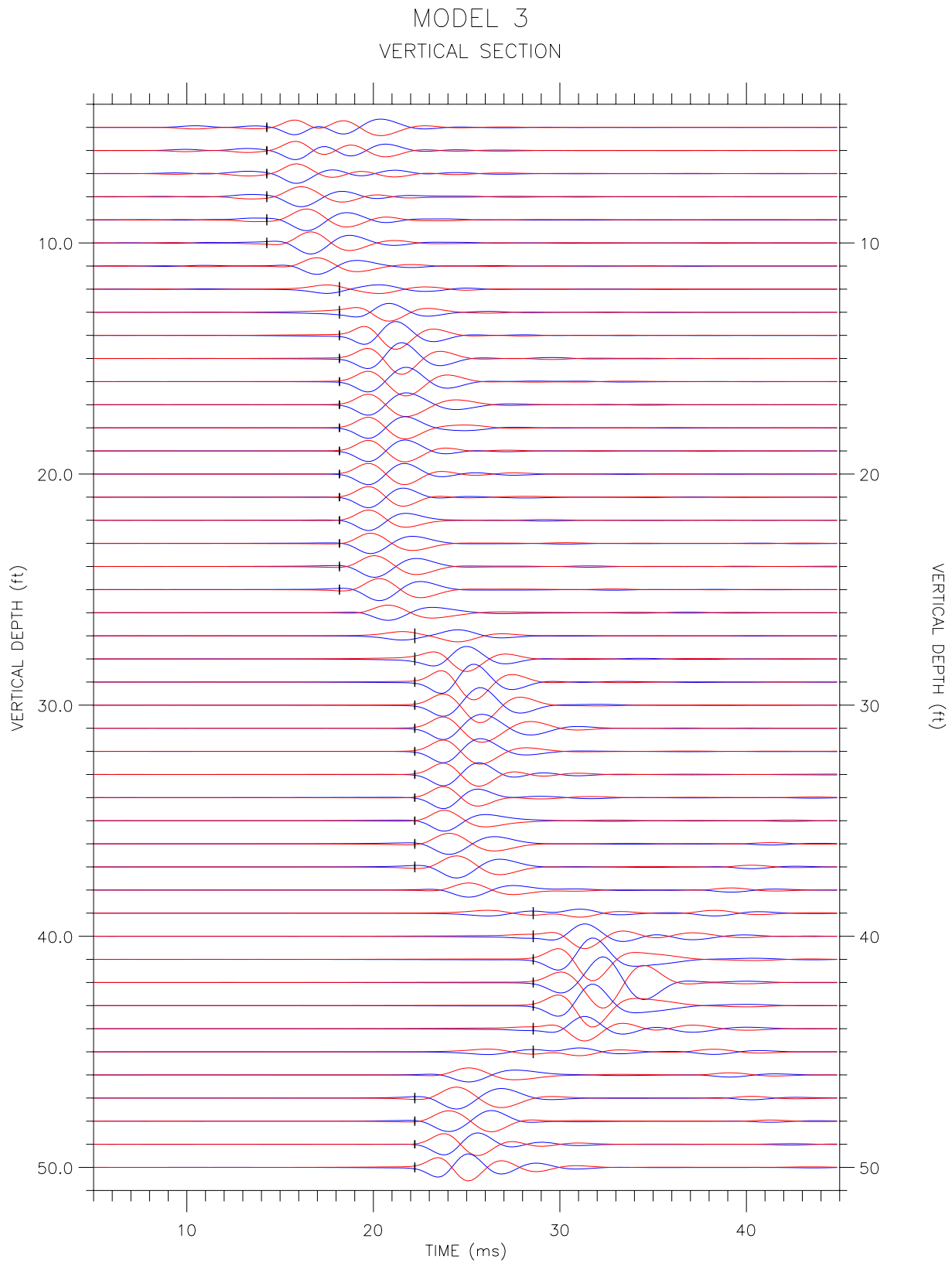

Figure C-6: Synthetic crosshole waveforms for model 3, far receiver.

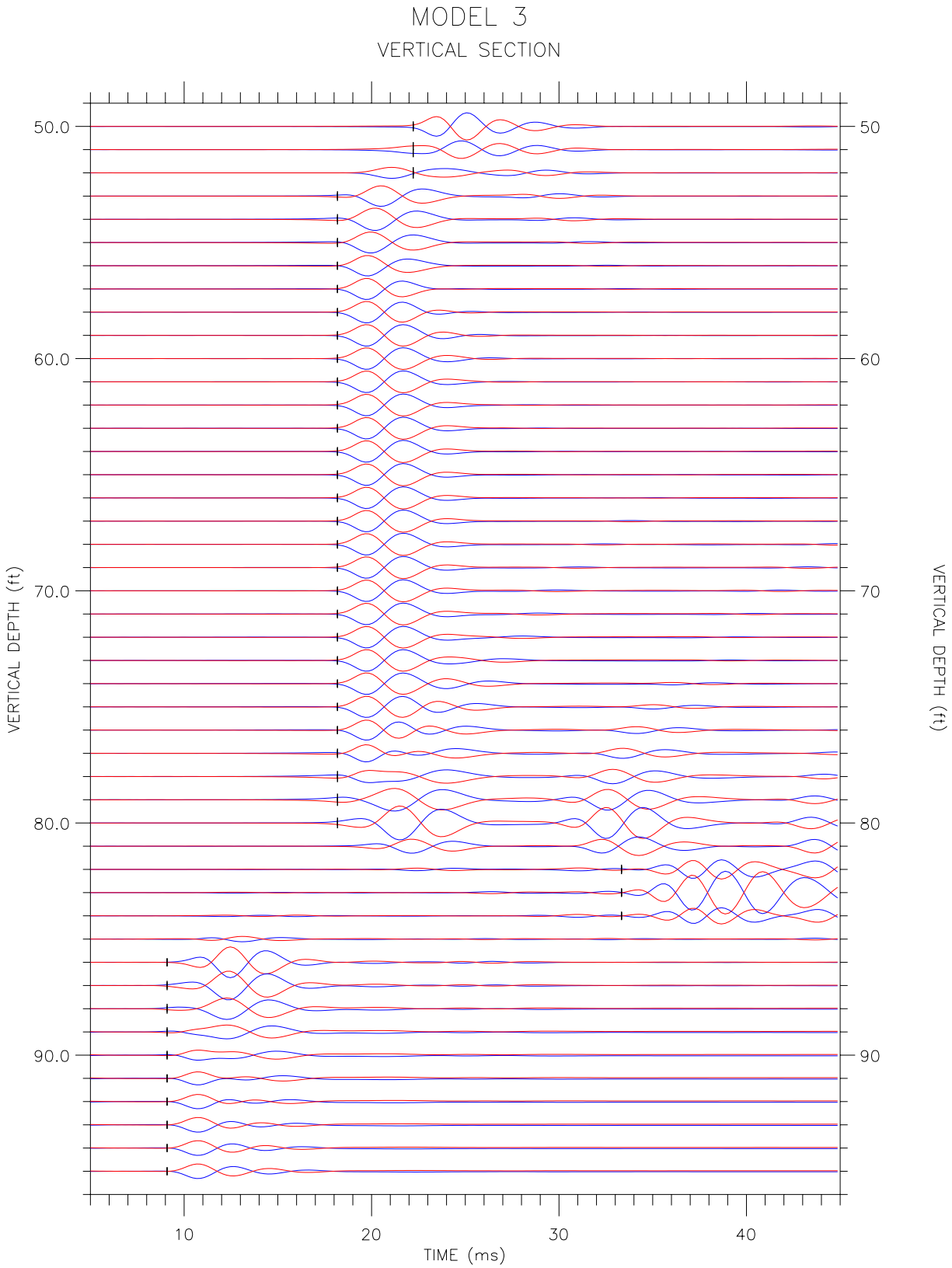

Figure C-6, continued.

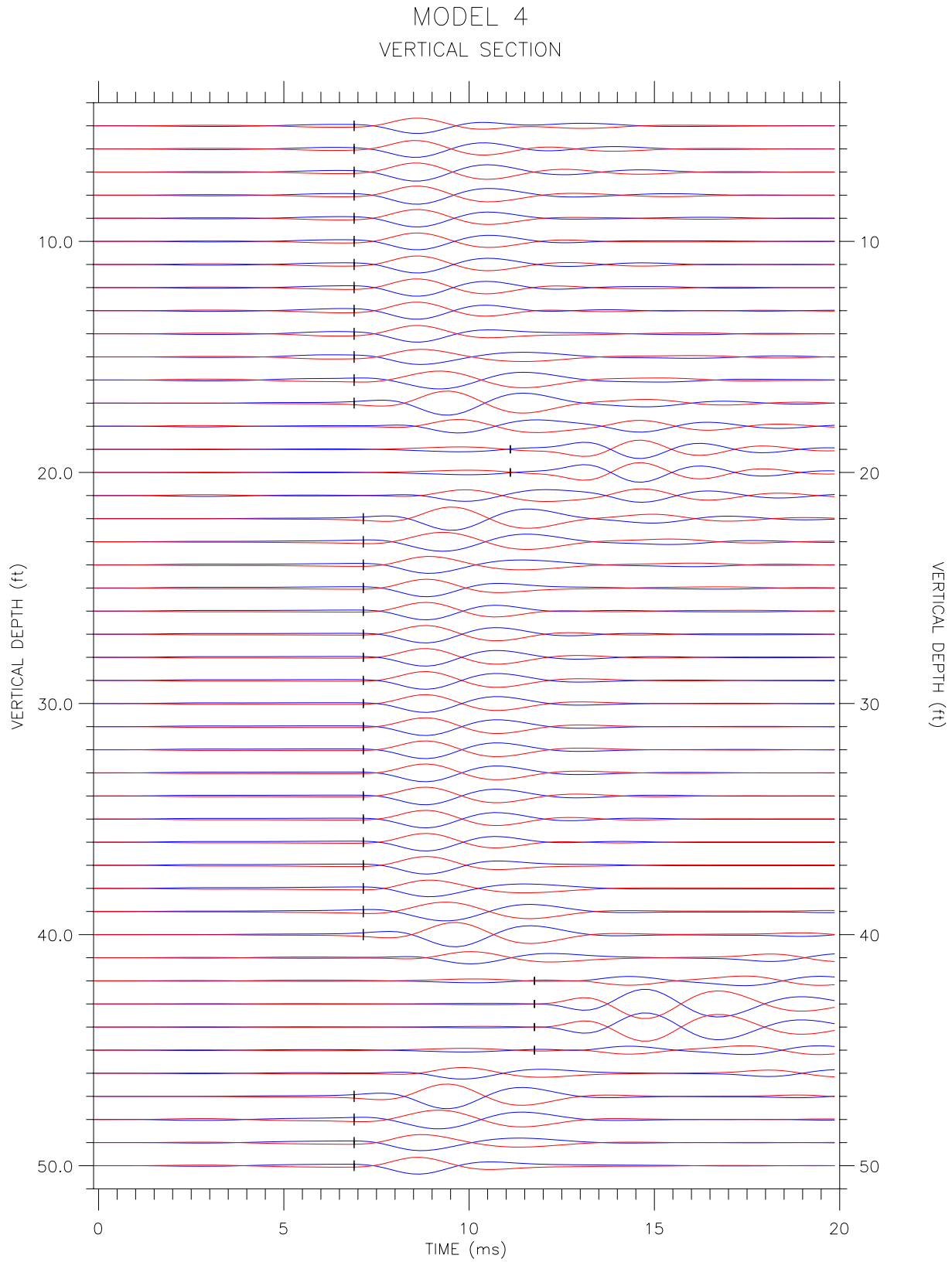

Figure C-7: Synthetic crosshole waveforms for model 4, near receiver.

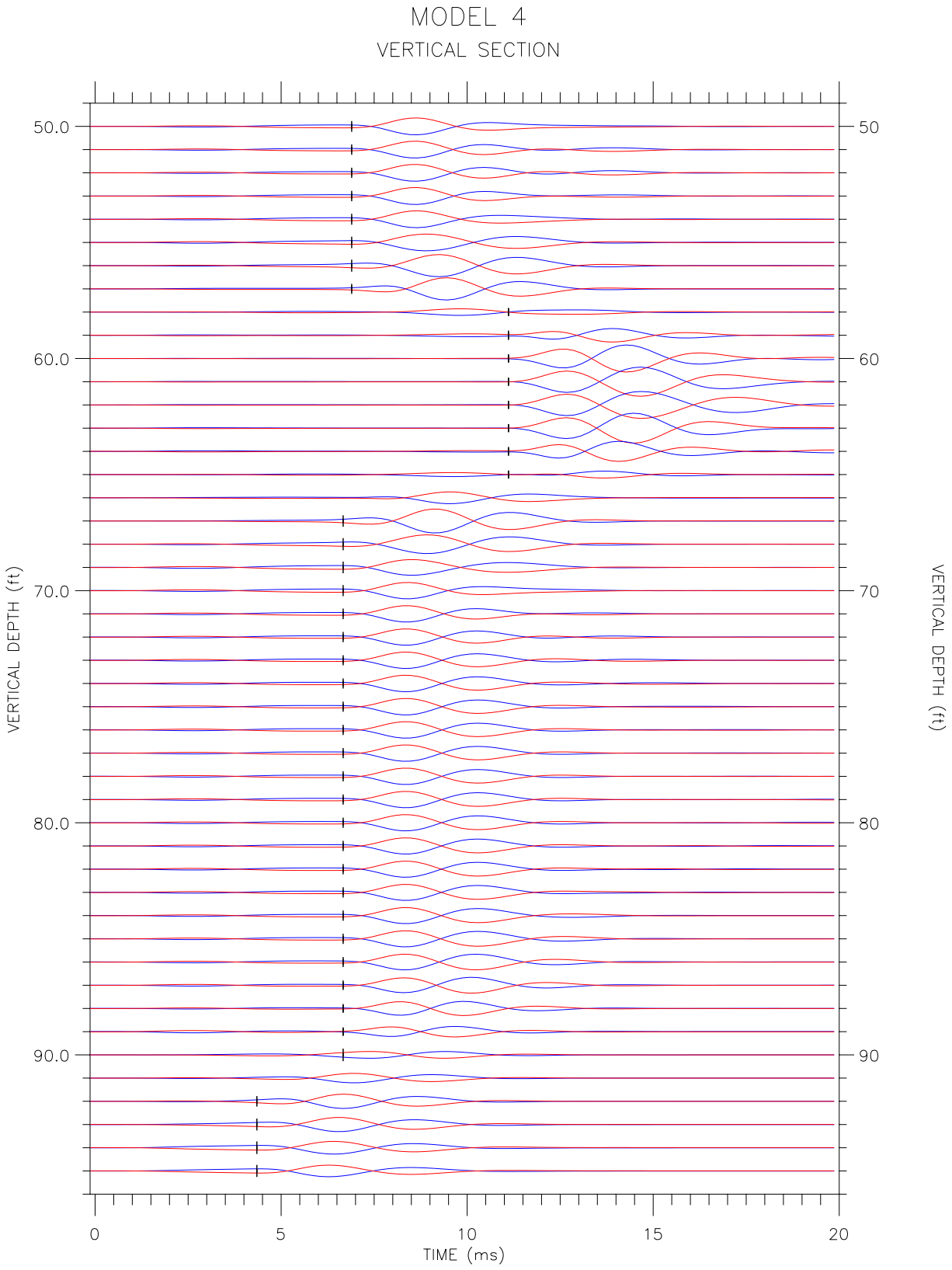

Figure C-7, continued.

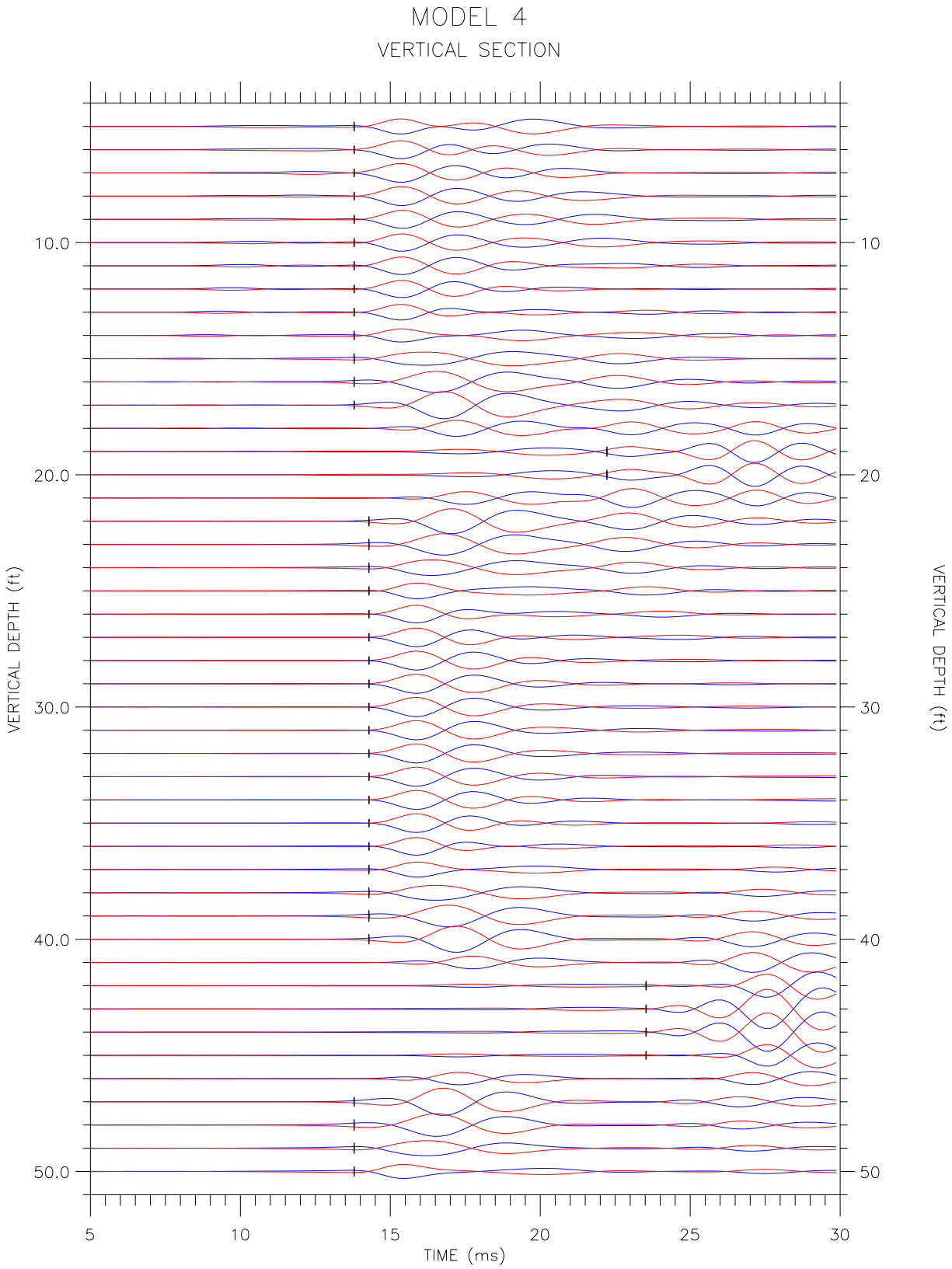

Figure C-8: Synthetic crosshole waveforms for model 4, far receiver.

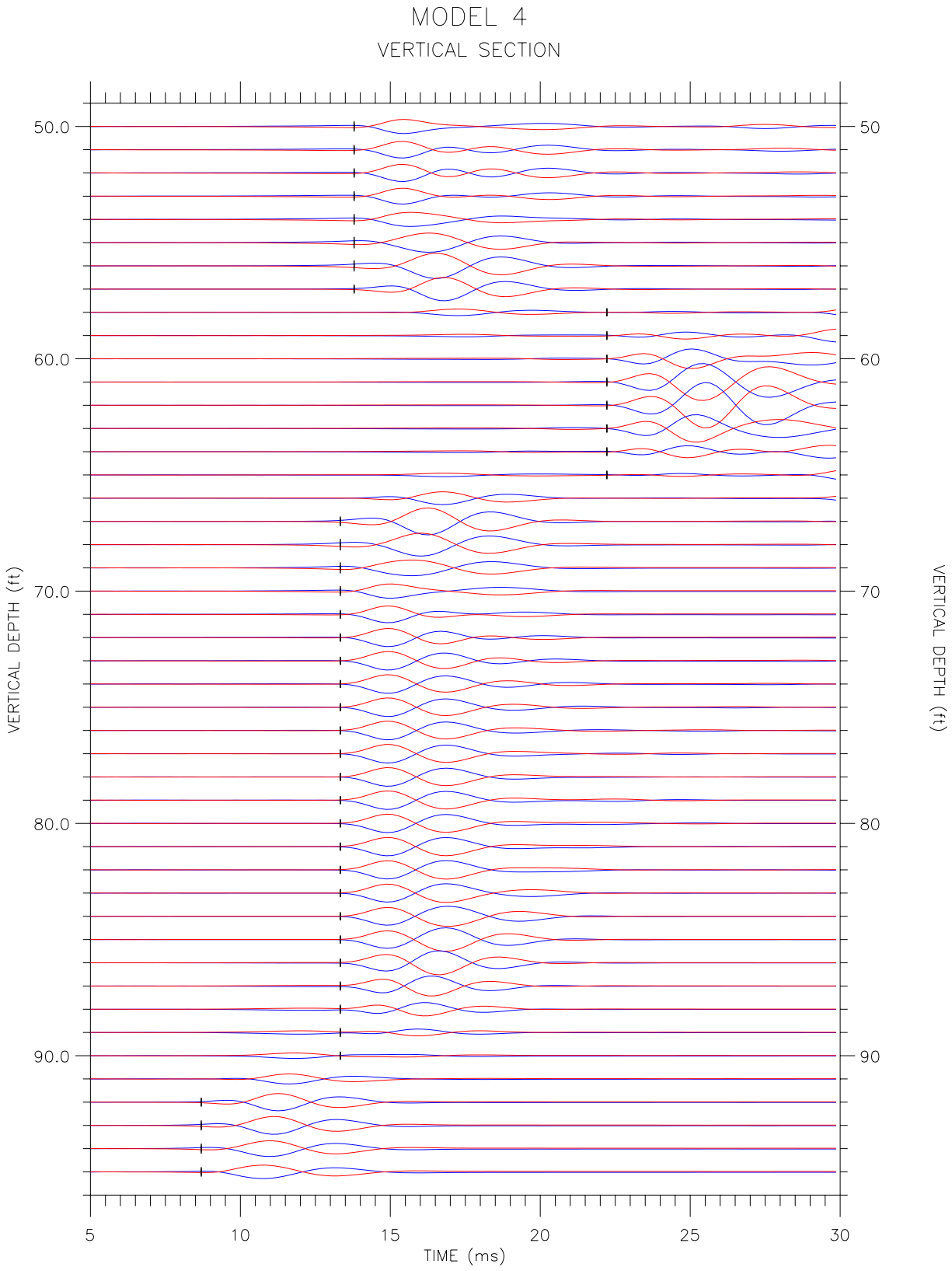

Figure C-8, continued.

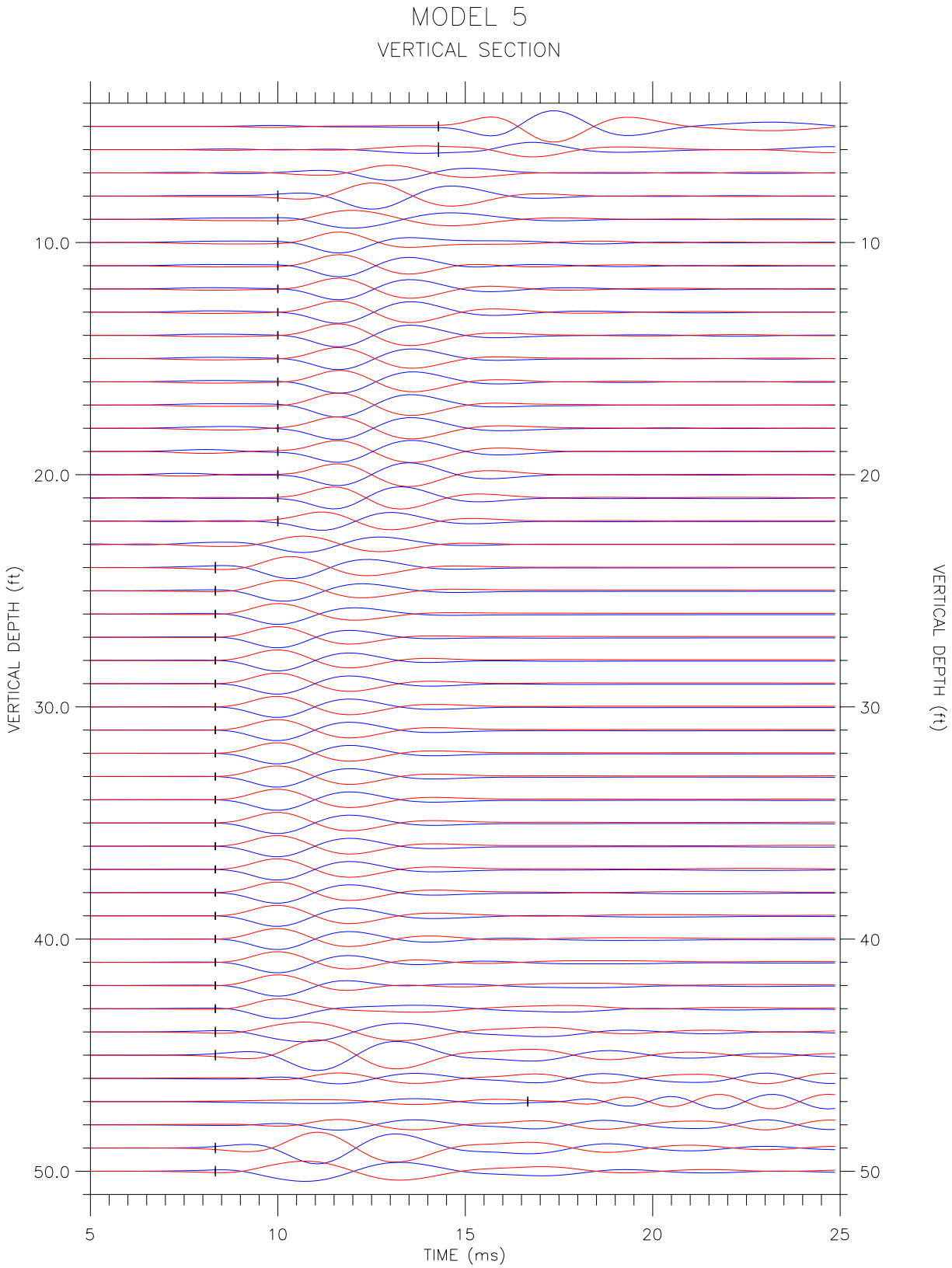

Figure C-9: Synthetic crosshole waveforms for model 5, near receiver.

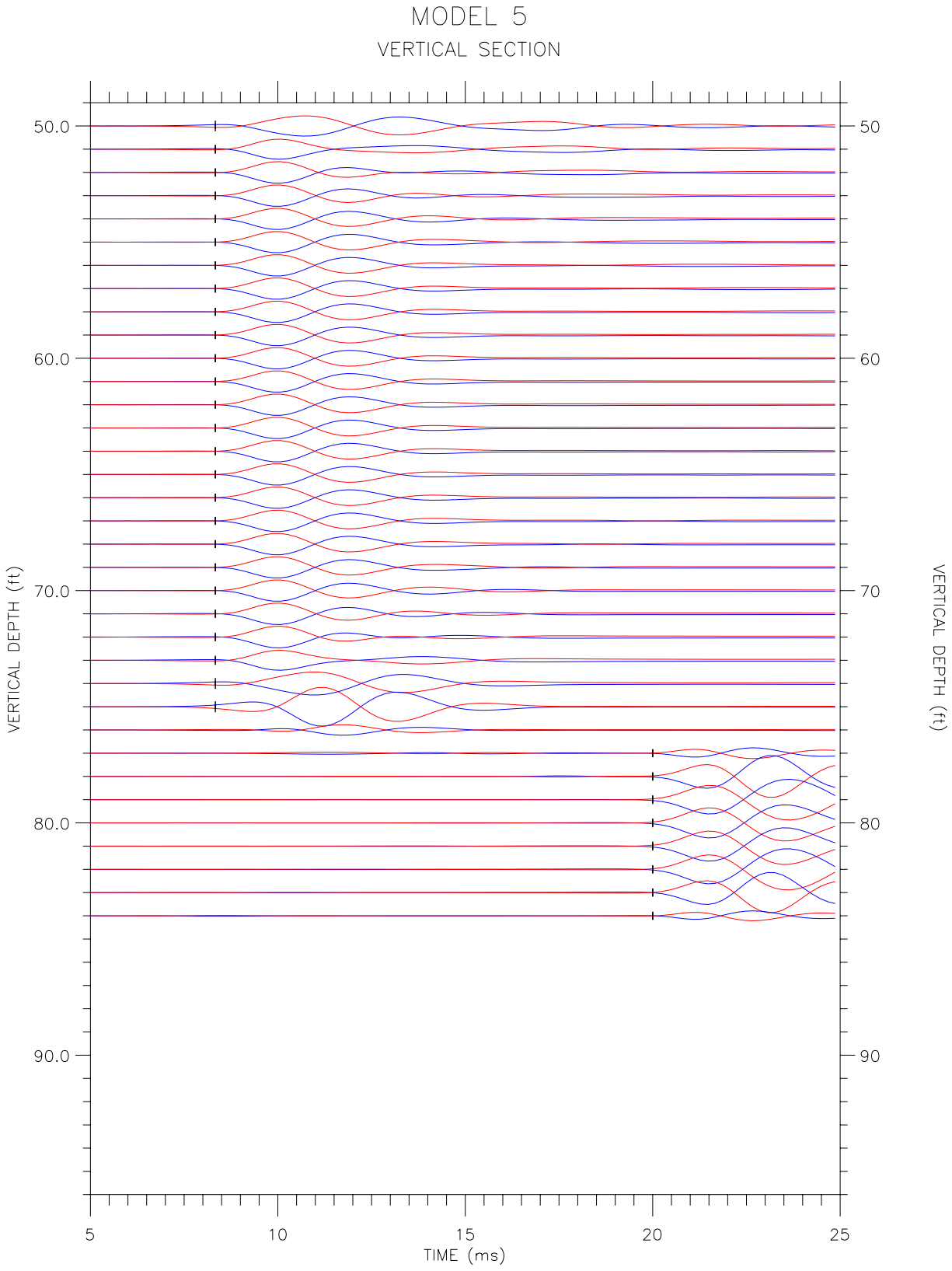

Figure C-9, continued.

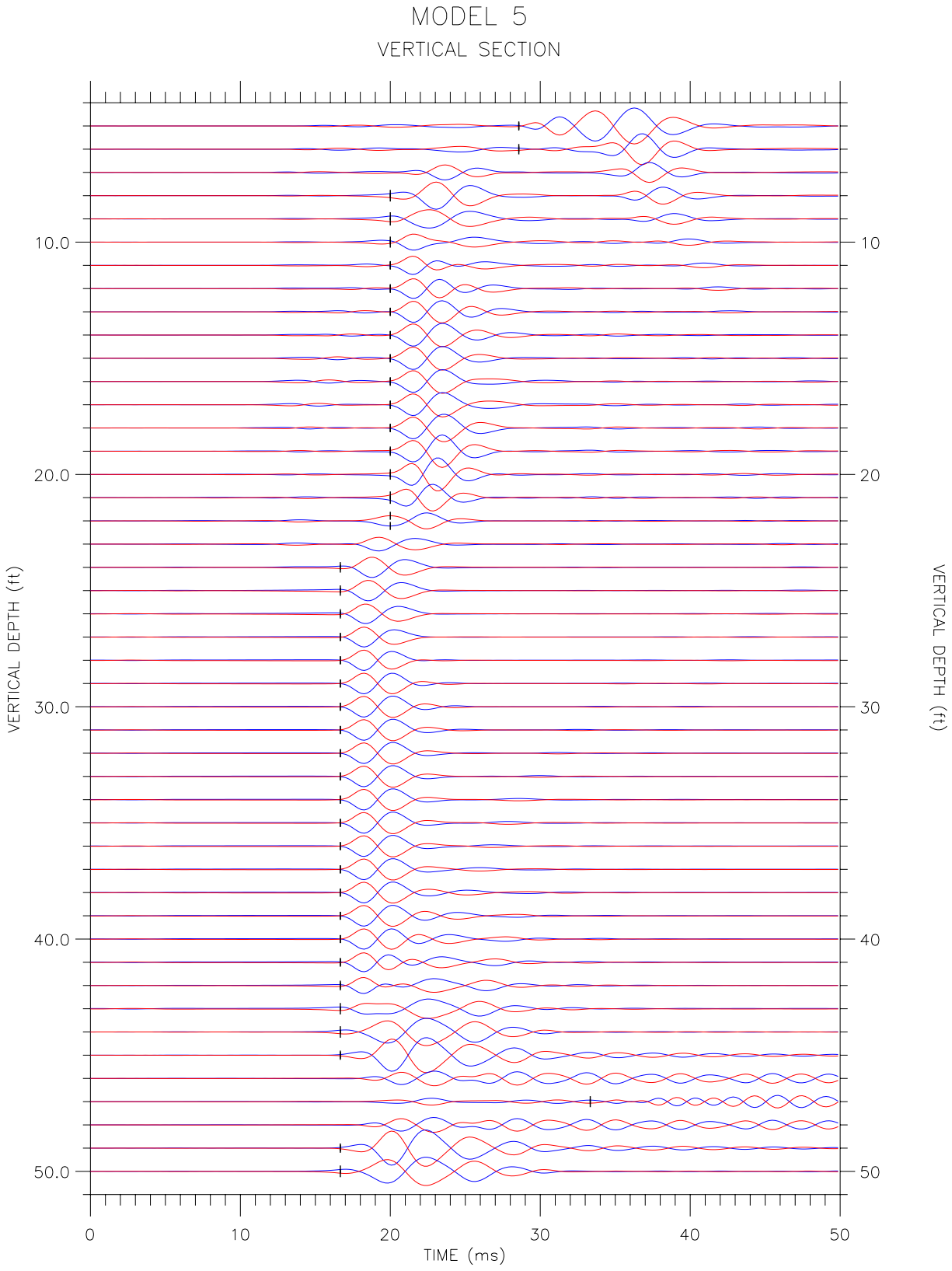

Figure C-10: Synthetic crosshole waveforms for model 5, far receiver.

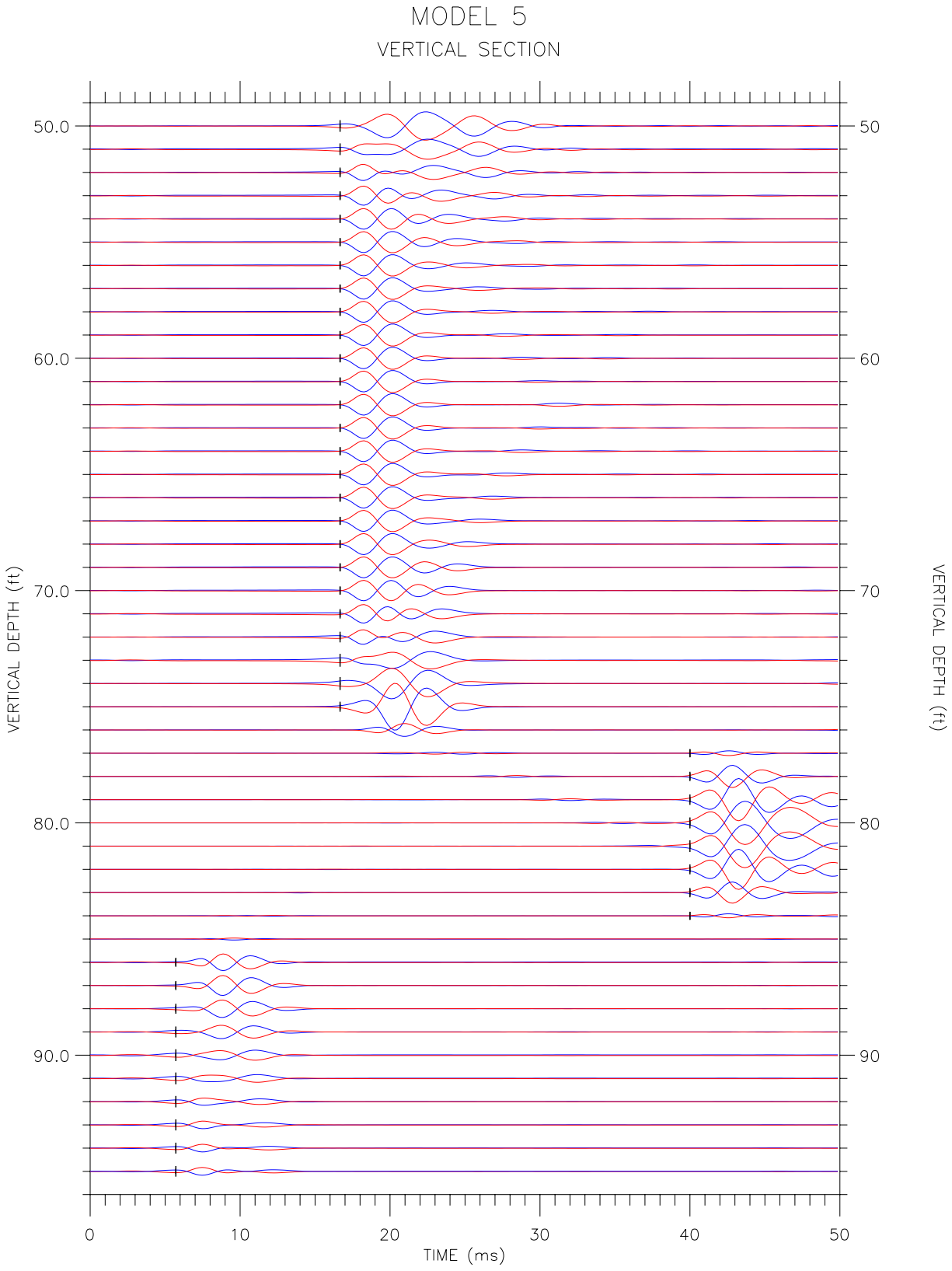

Figure C-10, continued.

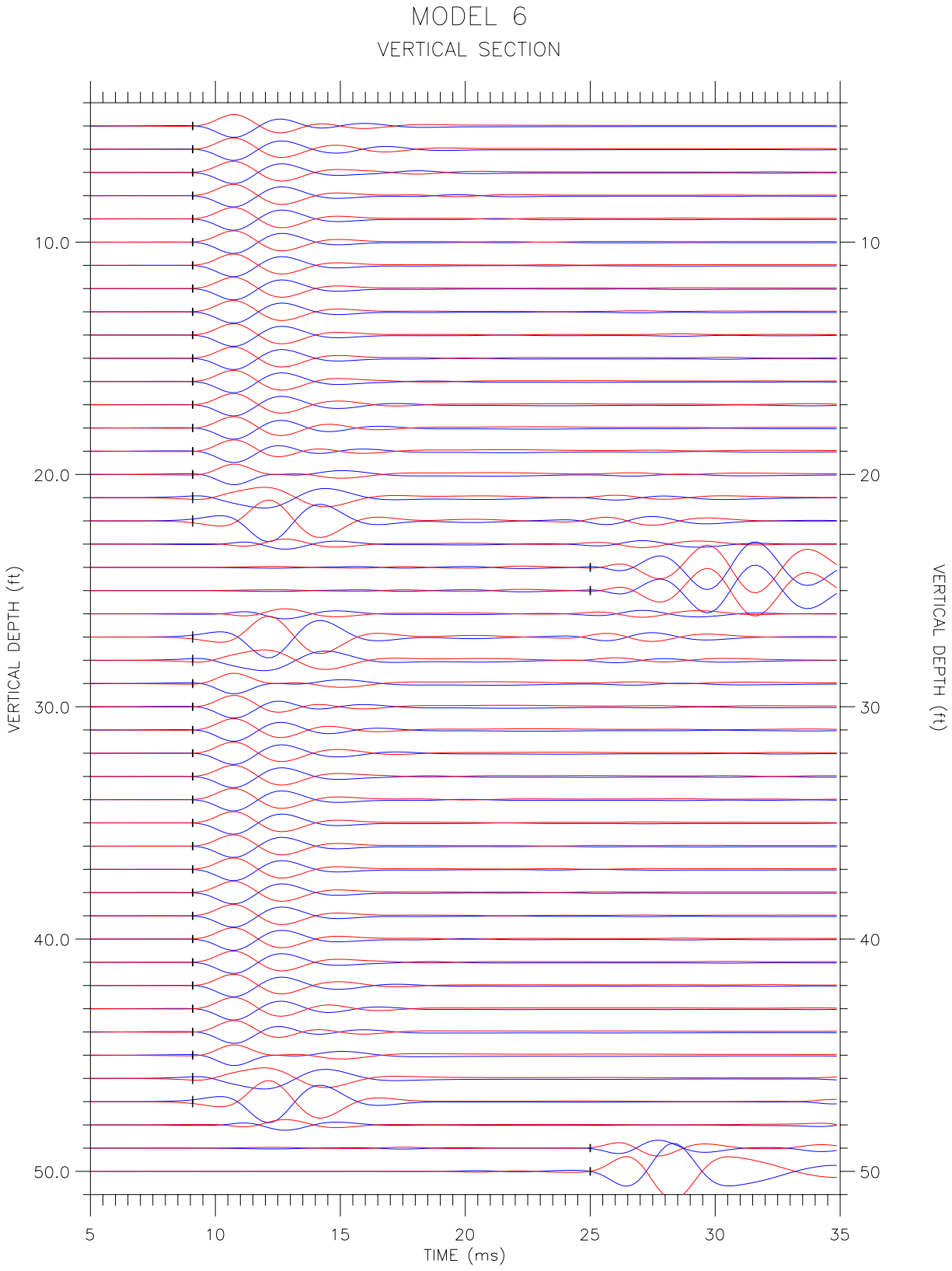

Figure C-11: Synthetic crosshole waveforms for model 6, near receiver.

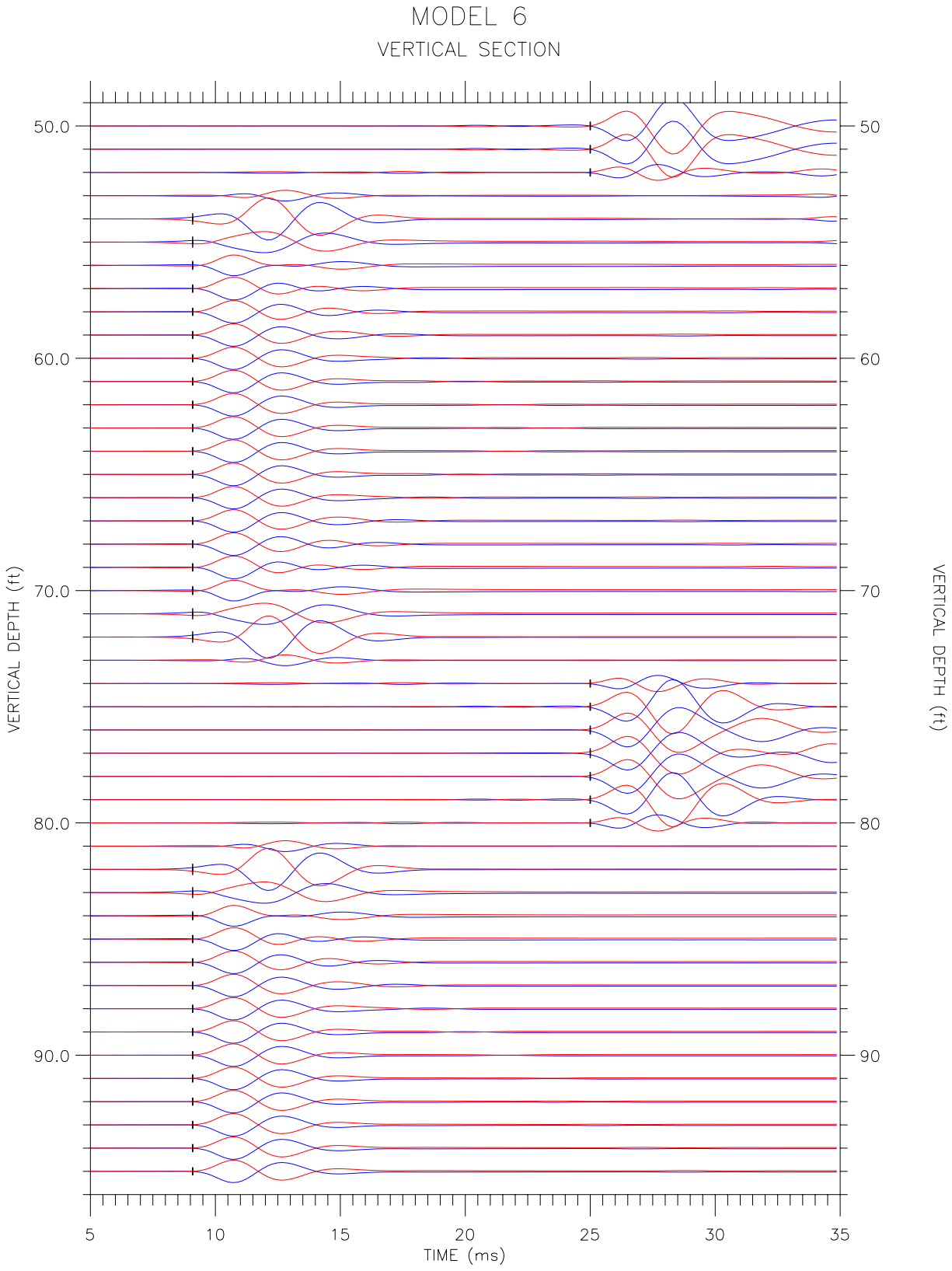

Figure C-11, continued.

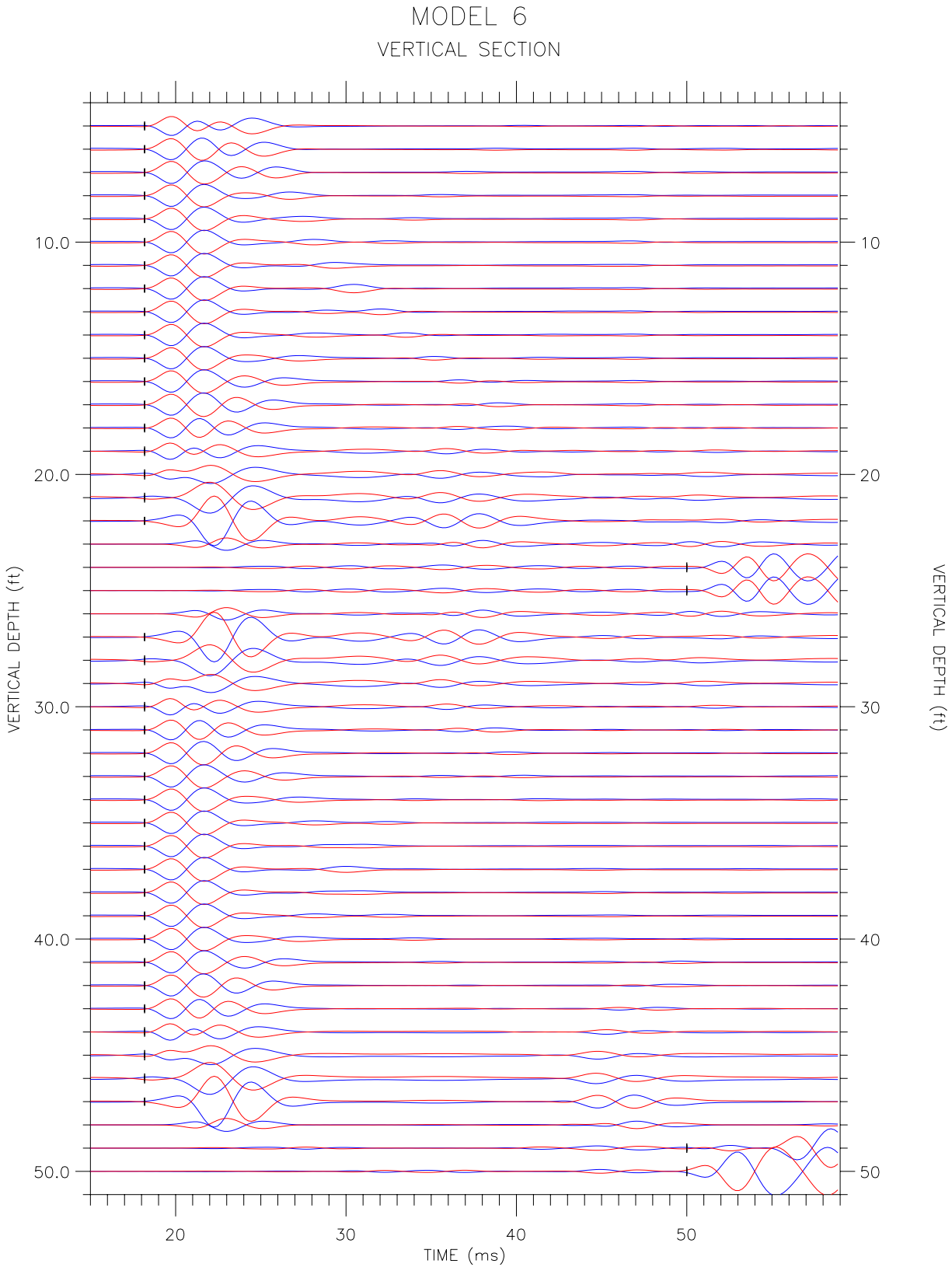

Figure C-12: Synthetic crosshole waveforms for model 6, far receiver.

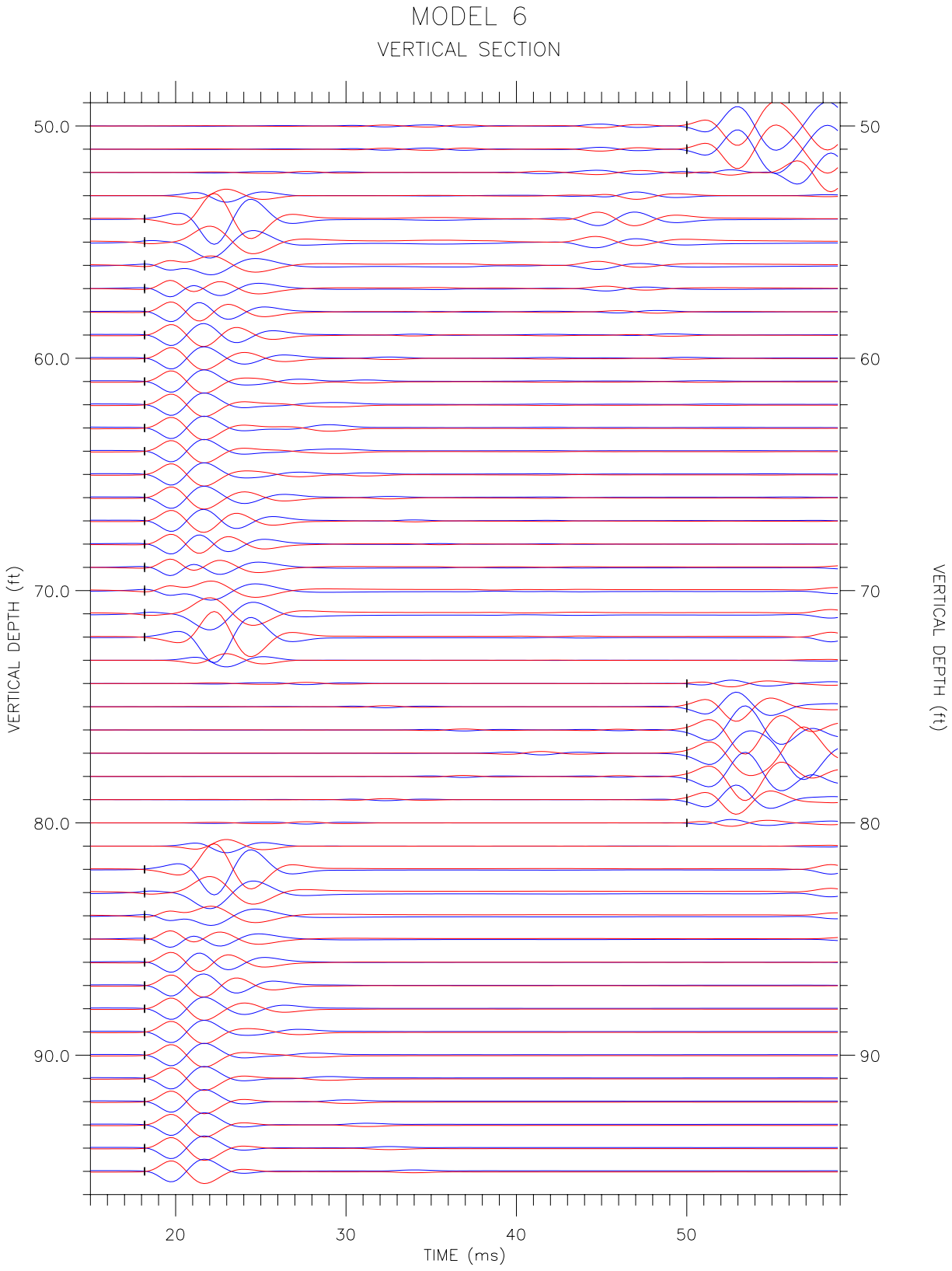

Figure C-12, continued.

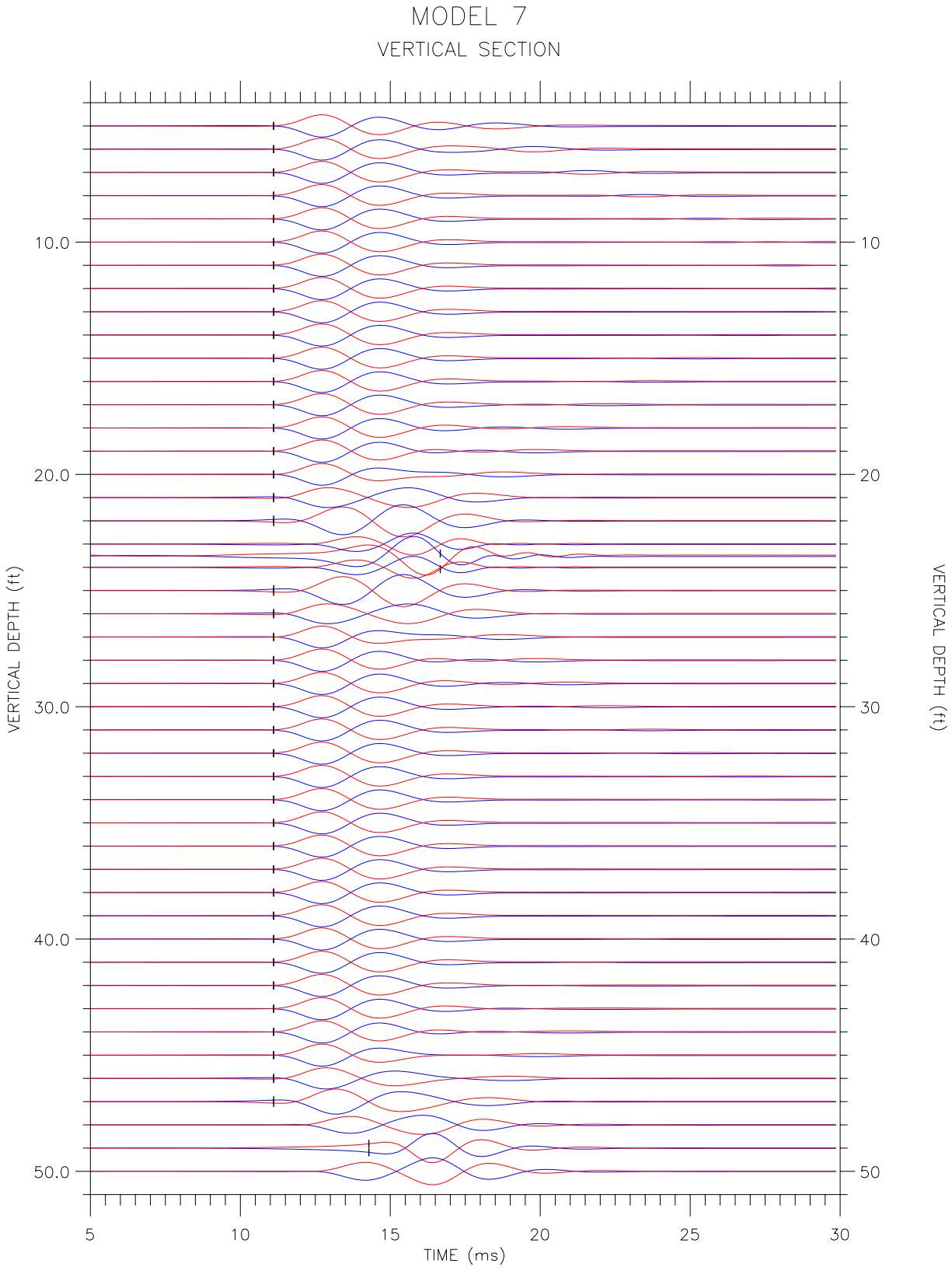

Figure C-13: Synthetic crosshole waveforms for model 7, near receiver.

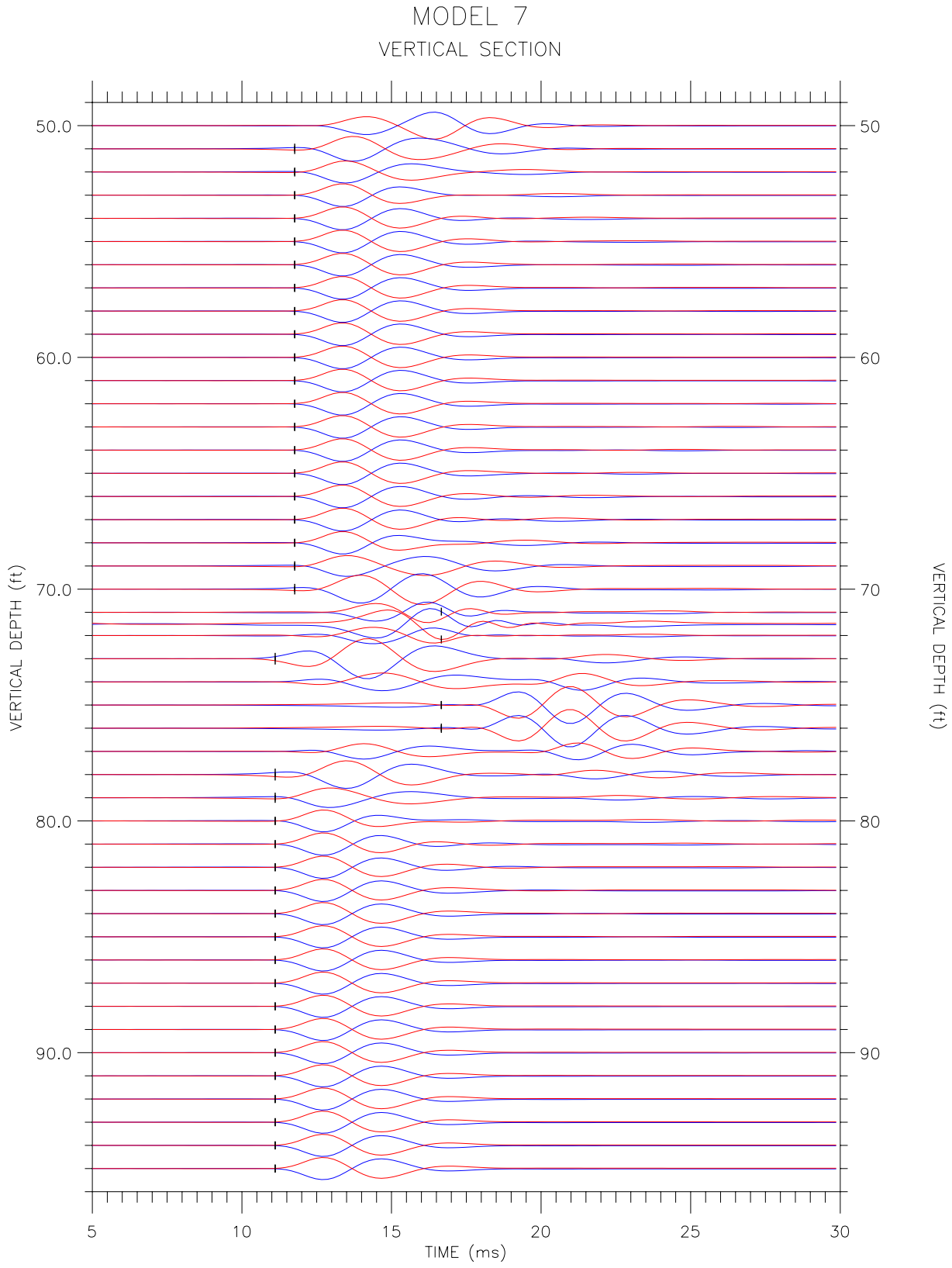

Figure C-13, continued.

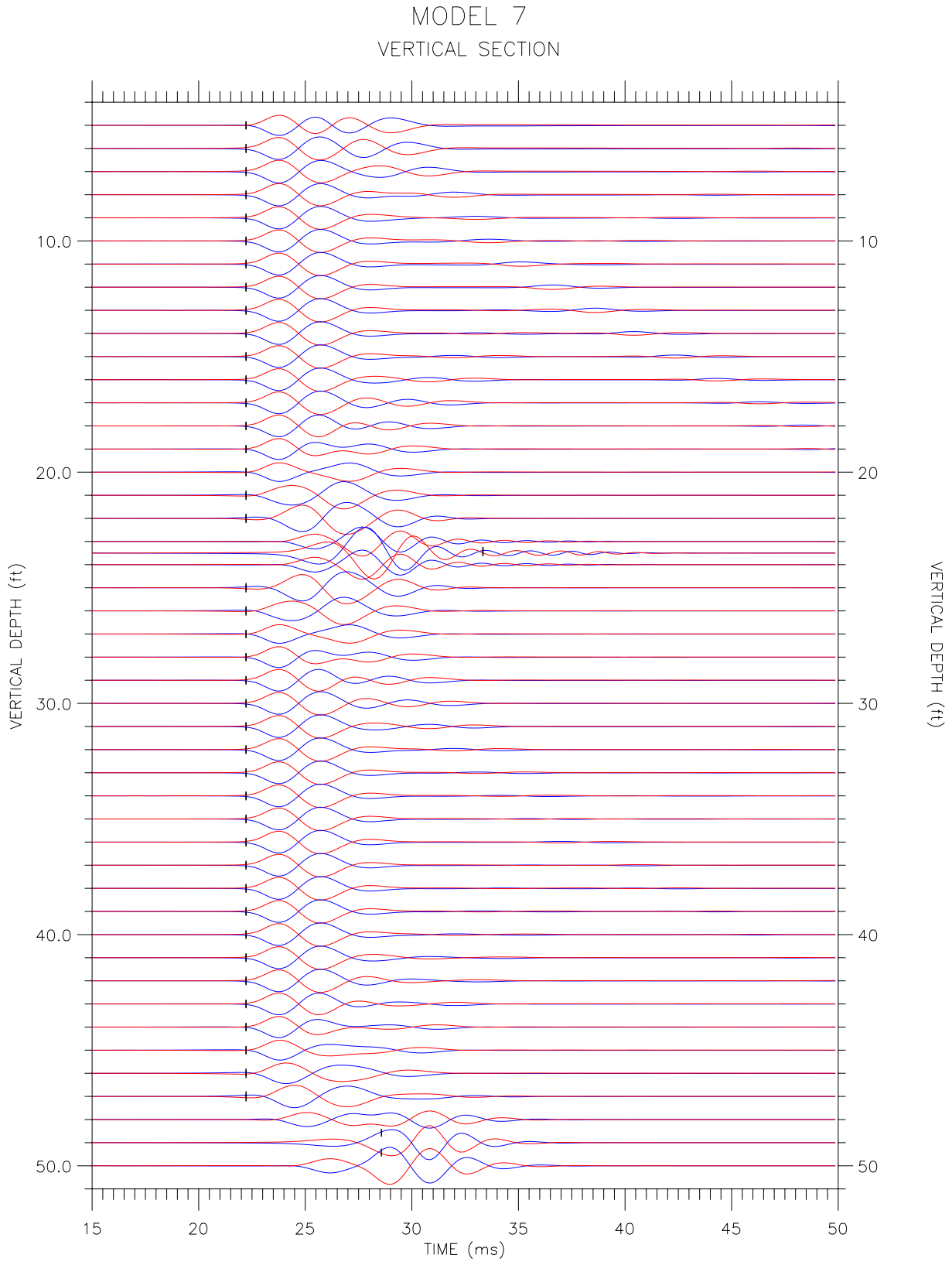

Figure C-14: Synthetic crosshole waveforms for model 7, far receiver.

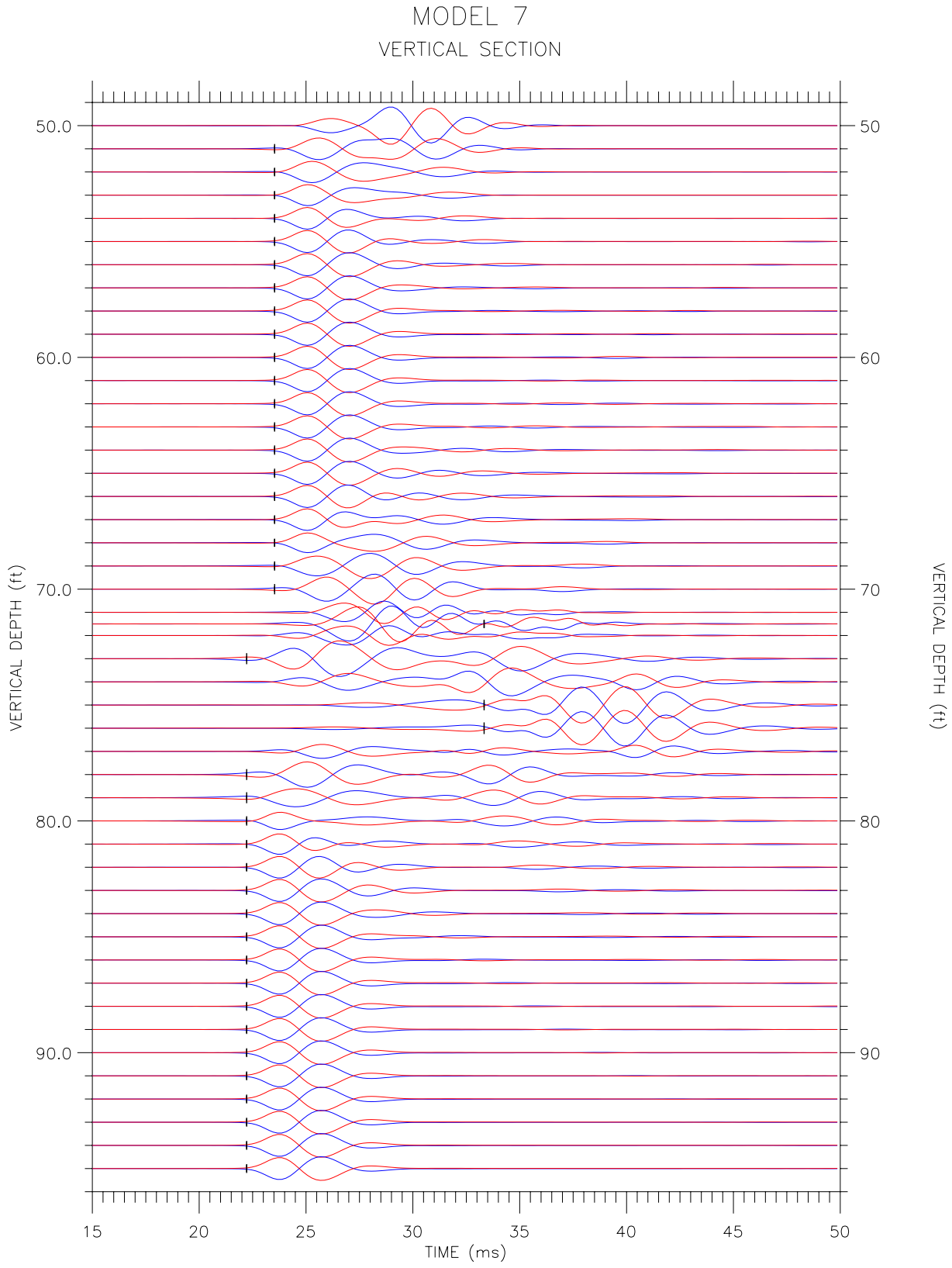

Figure C-14, continued.

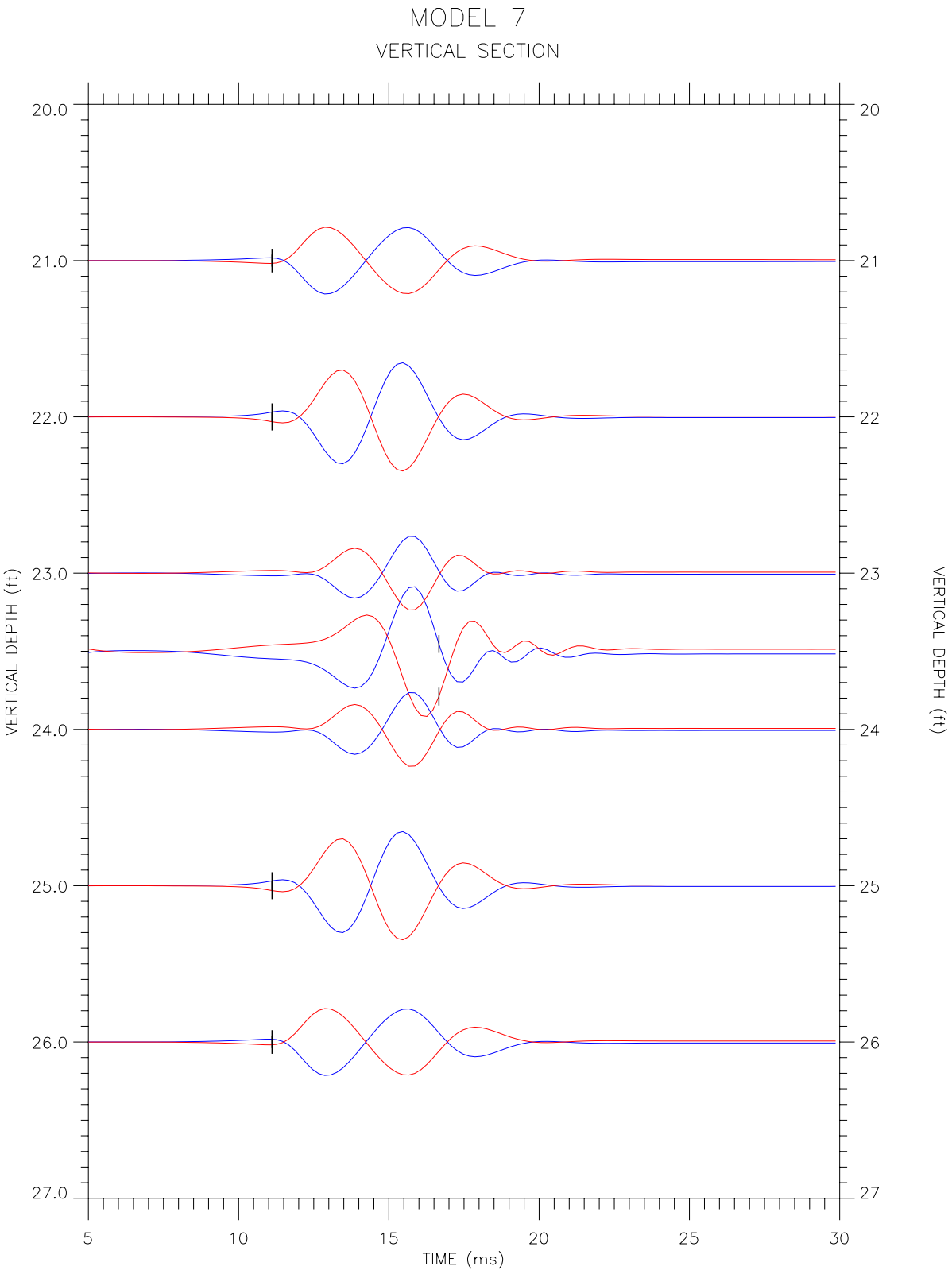

Figure C-15: Near-receiver synthetic waveforms across the upper 1-ft-thick layer (23-24 ft depth) in model 7.

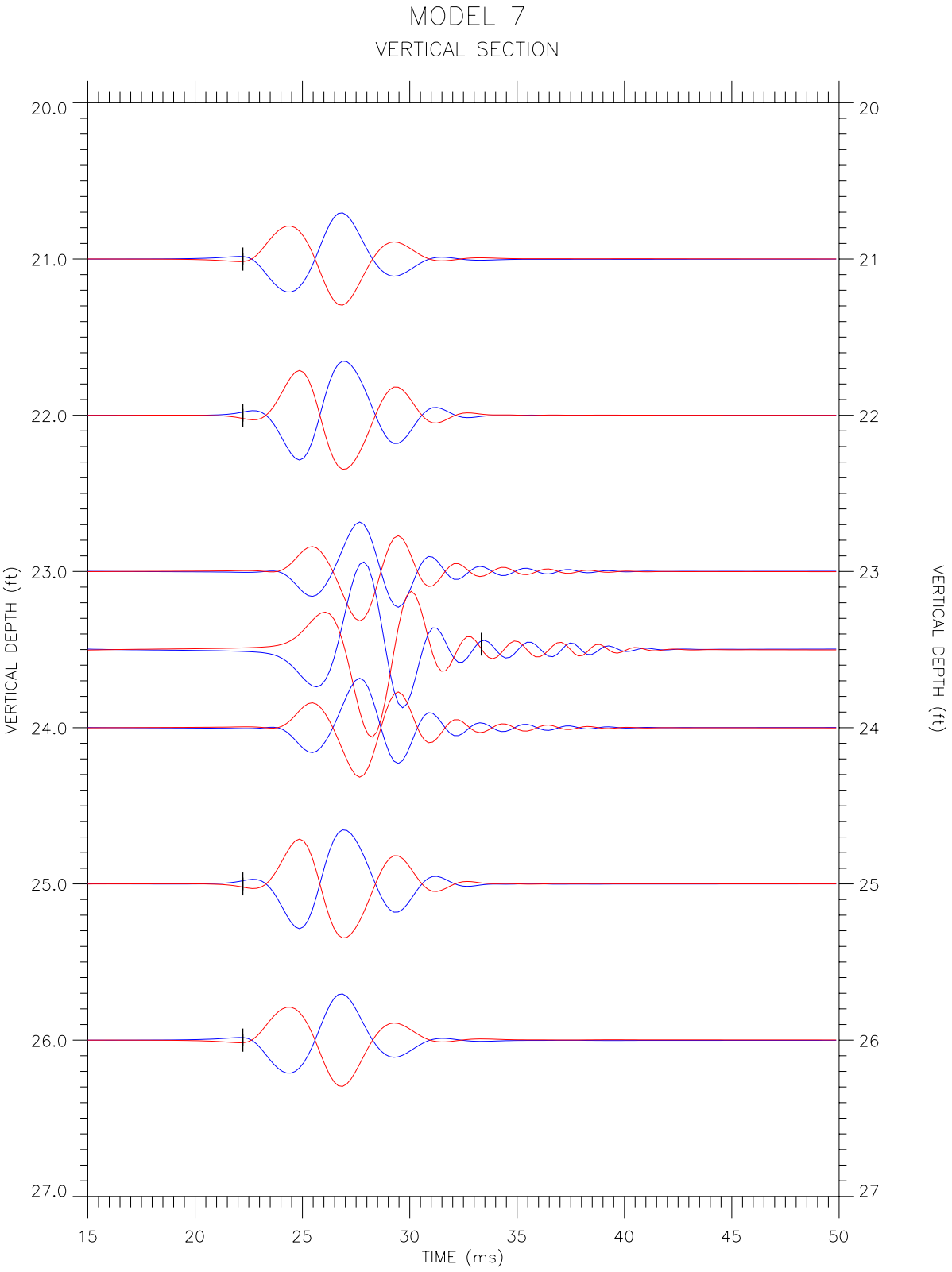

Figure C-16: Far-receiver synthetic waveforms across the upper 1-ft-thick layer (23-24 ft depth) in model 7.

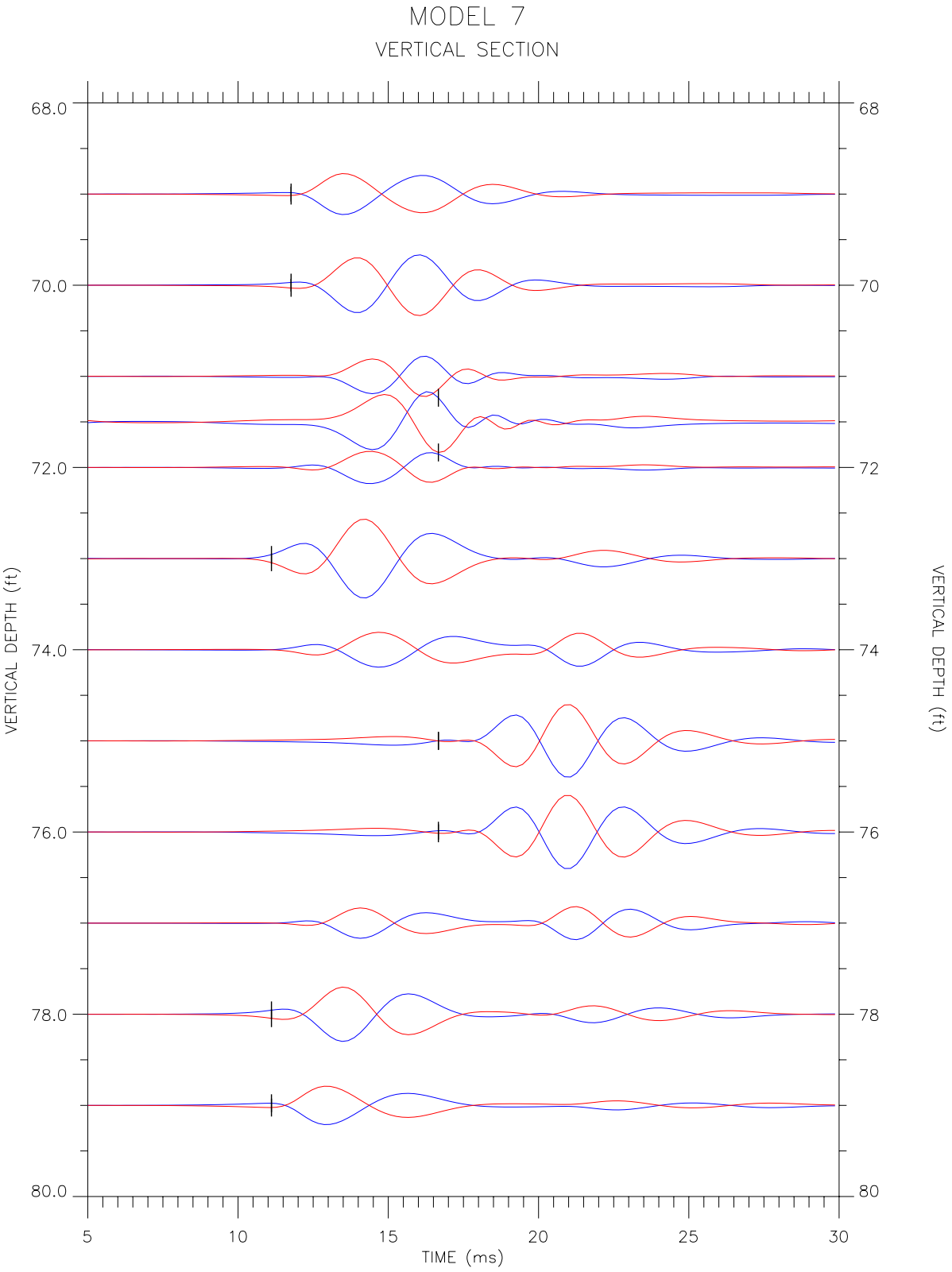

Figure C-17: Near-receiver synthetic waveforms across the lower 1-ft-thick layer (71-72 ft depth) in model 7.

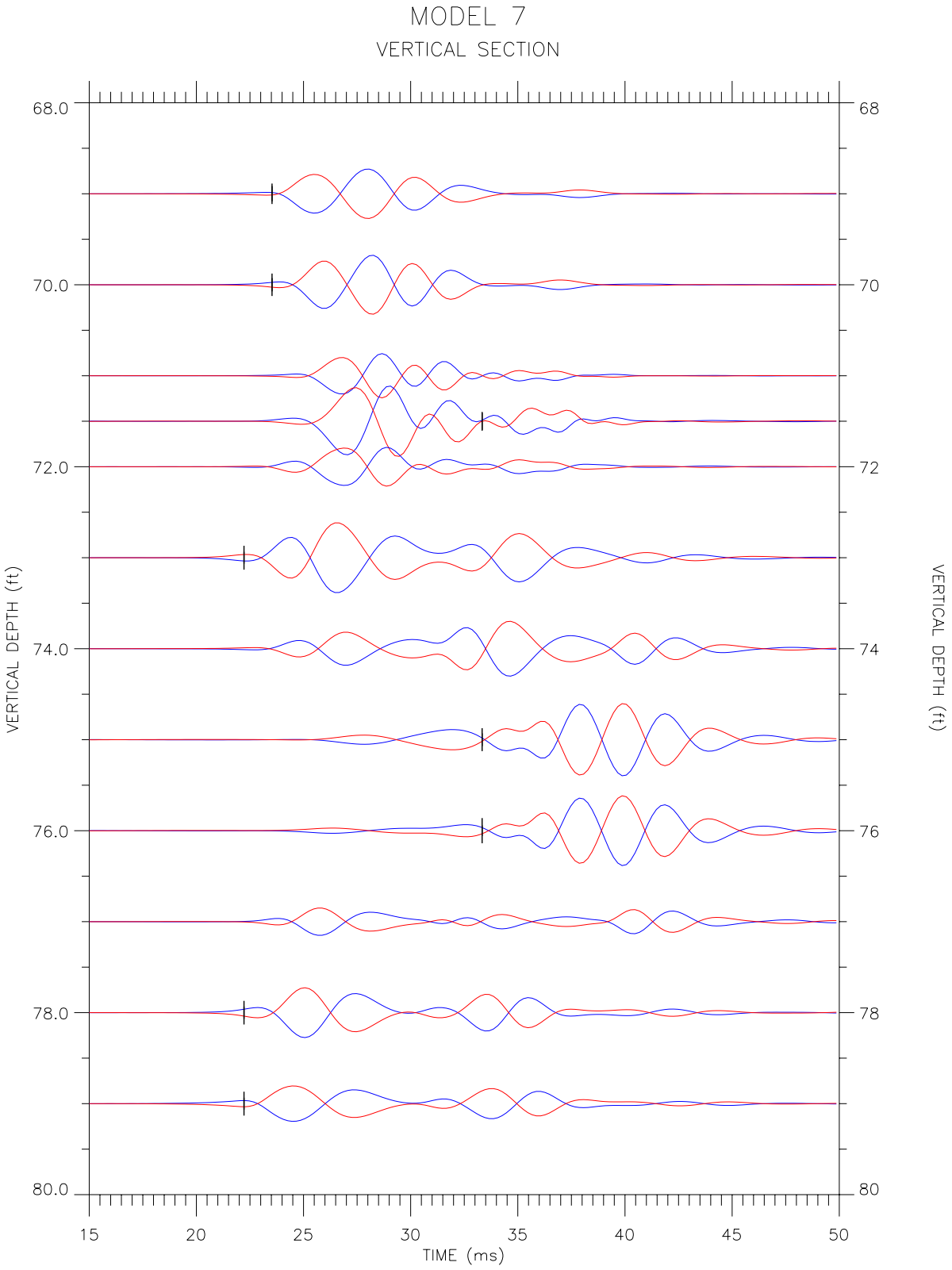

Figure C-18: Far-receiver synthetic waveforms across the lower 1-ft-thick layer (71-72 ft depth) in model 7.

APPENDIX D
FREQUENCY SPECTRA OF SYNTHETIC AND FIELD DATA

Magnitude frequency spectra were computed from representative synthetic and field crosshole waveforms. Waveforms from six source gathers of field and synthetic data were analyzed. Data from both the near and far receivers were included in each case. The field data were acquired at five dams in four states, at depths ranging from 20 to 105 feet. The synthetic waveforms were taken from five models, at depths ranging from 7 to 80 feet. Source-to-receiver distances range from 9.7 to 23.6 feet for the field data and 10 to 20 feet for the synthetic data. Each frequency spectrum was computed by performing a fast Fourier transform (FFT) on a window of seismic waveform data following the interpreted shear-wave direct arrival time. The window length was adjusted to include only the packet of direct shear-wave energy (1 to 1 1/2 cycles) and ranged from 5 to 11 ms. The data were extracted from the waveforms using a Hanning window (a tapered windowing function that reduces oscillations in the corresponding frequency spectrum).

The frequency spectra computed from the field and synthetic data are compared in figure D-1. The dashed black lines are magnitude spectra computed from field crosshole waveforms, while the solid magenta lines are magnitude spectra computed from synthetic data. (For simplicity, the near- and far-receiver data are not differentiated in the plot.) As can be seen, the magnitude frequency spectra computed from the synthetic waveforms are similar in shape and frequency range as those computed from the field data. On average, the maximum frequency is about 500 Hz. For typical shear-wave soil velocities, ranging from about 500 to 1500 ft/s, this maximum frequency corresponds to wavelengths of 1 to 3 ft. The peak frequency is about 200 Hz, corresponding to wavelengths of 2.5 to 7.5 ft.

LIST OF FIGURES

Page

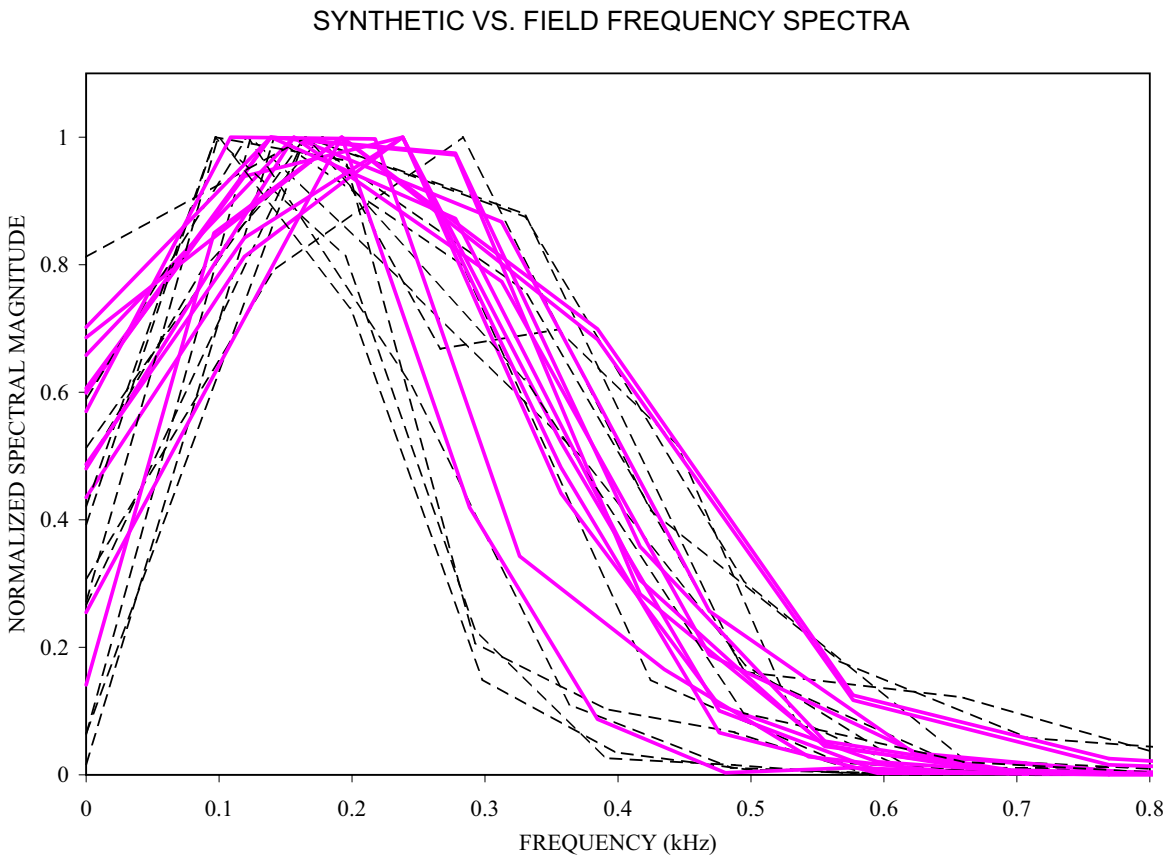

Figure D-1: Comparison of magnitude frequency spectra computed from field (black dashed lines) and synthetic (magenta solid lines) crosshole waveforms.

APPENDIX E
TABLES OF COMPUTED SHEAR-WAVE VELOCITIES

The following tables list the shear-wave velocities computed from the near- and far-receiver arrival times determined independently by geophysicists from the Bureau of Reclamation, U. S. Geological Survey, and the U. S. Army Corps. of Engineers. The median computed velocity is also listed for each depth, as well as the correct model velocity. The percent error, based on the median computed velocity, is listed in the last column. Errors are not listed for depths corresponding to layer interfaces.

LIST OF TABLES

Page

DEPTH (ft)	MODEL VELOCITY (ft/s)	COMPUTED SHEAR-WAVE VELOCITY (ft/s)							ERROR OF MEDIAN RESULT (%)
		BUREAU OF RECLAMATION		U. S. GEOLOGICAL SURVEY		CORPS. OF ENGINEERS		MEDIAN RESULT	
		NEAR RECEIVER	FAR RECEIVER	NEAR RECEIVER	FAR RECEIVER	NEAR RECEIVER	FAR RECEIVER		
5	800	794	798	787	786	801	818	796	-0.52
6	800	794	798	787	794	799	807	796	-0.52
7	800	794	798	783	803	794	814	796	-0.52
8	800	794	798	783	798	799	812	798	-0.23
9	800	794	798	787	798	799	817	798	-0.23
10	800	794	798	787	796	801	812	797	-0.38
11	800	794	798	787	796	801	814	797	-0.38
12	800	794	798	787	801	794	813	796	-0.47
13	800	794	798	791	801	792	814	796	-0.48
14	800	794	798	800	794	810	799	798	-0.19
15	800			869	786	892	1005	880	10.05
16	800	973	1032	1059	1181	971	1036	1034	
16	1100	973	1032	1059	1181	971	1036	1034	
17	1100	1025	1060	1109	1181	1027	1057	1059	-3.76
18	1100	1081	1079	1136	1186	1077	1075	1080	-1.84
19	1100	1080	1079	1140	1186	1080	1080	1080	-1.78
20	1100	1057	1057	1152	1161	1052	1059	1058	-3.81
21	1100	998	1030	1109	1109	992	1032	1031	
21	800	998	1030	1109	1109	992	1032	1031	
22	800			800	791	917	1032	858	7.31
23	800	799	803	791	806	813	800	802	0.22
24	800	799	803	791	808	796	807	801	0.10
25	800	799	803	791	811	796	802	800	0.02
26	800	799	803	791	808	796	803	801	0.09
27	800	799	803	791	808	808	802	802	0.30
28	800	799	803	791	808	801	804	802	0.24
29	800	799	803	791	806	808	804	804	0.45
30	800	797	803	796	806	804	807	804	0.48
31	800	797	803	796	804	807	805	803	0.43
32	800	797	803	793	802	801	805	801	0.15
33	800	797	803	796	799	804	805	801	0.15
34	800	797	803	796	799	804	807	801	0.15
35	800	797	803	796	797	805	803	800	0.02
36	800	797	803	793	799	804	804	801	0.15
37	800	797	803	796	799	805	804	801	0.15
38	800	797	803	798	799	801	804	800	0.01

Table E-1: Computed shear-wave velocities for model 1.

DEPTH (ft)	MODEL VELOCITY (ft/s)	COMPUTED SHEAR-WAVE VELOCITY (ft/s)							ERROR OF MEDIAN RESULT (%)
		BUREAU OF RECLAMATION		U. S. GEOLOGICAL SURVEY		CORPS. OF ENGINEERS		MEDIAN RESULT	
		NEAR RECEIVER	FAR RECEIVER	NEAR RECEIVER	FAR RECEIVER	NEAR RECEIVER	FAR RECEIVER		
39	800	798	803	798	802	795	800	799	-0.07
40	800	798	803	798	797	804	802	800	0.00
41	800	798	803	801	802	801	804	801	0.18
42	800		1034	969	1028	1000	1052	1028	28.50
42.5	800								
42.5	1100								
43	1100	1033	1053	981	1042	1022	1050	1038	-5.67
44	1100	1087	1085	1017	1061	1062	1084	1073	-2.48
45	1100	1113	1100	1061	1064	1093	1106	1096	-0.33
46	1100	1113	1106	1087	1095	1100	1117	1103	0.27
47	1100	1113	1106	1080	1087	1102	1119	1104	0.37
48	1100	1113	1106	1080	1104	1102	1119	1105	0.44
49	1100	1113	1106	1075	1096	1097	1111	1102	0.15
50	1100	1113	1106	1053	1084	1099	1111	1102	0.22
51	1100	1113	1097	1069	1073	1099	1094	1095	-0.43
52	1100	1058	1071	1011	1050	1047	1070	1054	-4.17
53	1100	1005	1033	977	1036	995	1032	1018	
53	800	1005	1033	977	1036	995	1032	1018	
54	800			797	787	987	1040	892	11.50
55	800	800	806	797	792	807		800	-0.02
56	800	800	806	791	806	807	808	806	0.76
57	800	800	806	788	806	808	803	804	0.55
58	800	800	806	791	802	804	807	803	0.38
59	800	801	806	788	804	805	810	805	0.60
60	800	801	806	794	804	808	808	805	0.63
61	800	801	806	797	806	805	809	806	0.73
62	800	801	806	791	806	804	809	805	0.64
63	800	801	806	795	804	805	813	804	0.54
64	800	801	806	795	809	805	809	805	0.67
65	800	801	806	788	805	805	809	805	0.57
66	800	801	806	788	805	801	808	803	0.37
67	800	801	806	785	797	800	808	800	0.06
68	800	801	806	785	800	805	804	803	0.32
69	800	801	806	785	800	807	803	802	0.25
70	800	801	806	785	795	805	803	802	0.25
71	800	801	806	791	790	799		799	-0.11
72	800		1037	987	1034	993		1014	26.72

Table E-1: Computed shear-wave velocities for model 1.

DEPTH (ft)	MODEL VELOCITY (ft/s)	COMPUTED SHEAR-WAVE VELOCITY (ft/s)							ERROR OF MEDIAN RESULT (%)
		BUREAU OF RECLAMATION		U. S. GEOLOGICAL SURVEY		CORPS. OF ENGINEERS		MEDIAN RESULT	
		NEAR RECEIVER	FAR RECEIVER	NEAR RECEIVER	FAR RECEIVER	NEAR RECEIVER	FAR RECEIVER		
72.5	800								
72.5	1100								
73	1100	1030	1053	987	1047	1027	1051	1038	-5.61
74	1100	1080	1082	1002	1059	1085	1084	1081	-1.71
75	1100	1101	1102	1059	1081	1097	1100	1098	-0.18
76	1100	1101	1102	1081	1094	1097	1114	1099	-0.10
77	1100	1101	1102	1090	1094	1100	1108	1101	0.05
78	1100	1101	1102	1076	1091	1091	1108	1096	-0.34
79	1100	1101	1102	1050	1079	1079	1096	1088	-1.14
80	1100	1051	1067	995	1054	1039	1066	1052	-4.33
81	1100	1005	1032	978	1019	995	1032	1012	
81	800	1005	1032	978	1019	995	1032	1012	
82	800			796	801	969	1006	885	10.64
83	800	799	803	796	794	801		799	-0.16
84	800	799	803	792	801	799	806	800	0.03
85	800	799	803	792	804	805	797	801	0.10
86	800	799	803	803	808	804	802	803	0.38
87	800	799	803	799	804	805	804	803	0.41
88	800	799	803	796	797	803	805	801	0.10
89	800	798	803	792	806	799	807	801	0.13
90	800	798	803	799	806	801	806	802	0.23
91	800	798	803	799	811	799	807	801	0.15
92	800	798	803	807	811	797	809	805	0.62
93	800	798	803	807	811	797	807	805	0.62
94	800	798	803	807	808	799	807	805	0.62
95	800	798	803	803	811	801	808	803	0.38

Table E-1: Computed shear-wave velocities for model 1.

DEPTH (ft)	MODEL VELOCITY (ft/s)	COMPUTED SHEAR-WAVE VELOCITY (ft/s)							ERROR OF MEDIAN RESULT (%)
		BUREAU OF RECLAMATION		U. S. GEOLOGICAL SURVEY		CORPS. OF ENGINEERS		MEDIAN RESULT	
		NEAR RECEIVER	FAR RECEIVER	NEAR RECEIVER	FAR RECEIVER	NEAR RECEIVER	FAR RECEIVER		
5	1000	989	1003	1011	994	989	1008	998	-0.16
6	1000	989	1003	1011	994	1003	1011	1003	0.28
7	1000	989	1003	1011	998	1007	1008	1005	0.50
8	1000	989	1003	985	986	1007	1011	996	-0.41
9	1000	989	1003	989	974	983	998	989	-1.10
10	1000	846	869	951	952	908	875	892	-10.80
11	1000	771	828	891	941	771	826	827	
11	400	771	828	891	941	771	826	827	
12	400	402	403	415	404	406	403	404	0.88
13	400	402	403	409	403	400	403	403	0.66
14	400	402	403	410	403	404	403	403	0.81
15	400	401	403	407	403	404	402	403	0.84
16	400	401	403	413	404	403	401	403	0.77
17	400	401	403	406	404	401	401	402	0.59
18	400	401	403	405	404	400	403	403	0.83
19	400	401	403	404	405	398	404	404	0.88
20	400	401	403	404	405	401	403	403	0.83
21	400	401	403	402	403	402	404	403	0.70
22	400	401	403	402	406	403	407	403	0.77
23	400	401	403	405	406	403	406	404	1.05
24	400	401	403	405	406	403	407	404	1.05
25	400	401	403	405	404	403	407	404	0.96
26	400	401	403	402	405	401	407	403	0.67
27	400	401	403	403	403	401	574	403	0.81
28	400	550	569	589	588	551	568	569	
28	600	550	569	589	588	551	568	569	
29	600	595	594	592	598	583	596	595	-0.87
30	600	601	603	601	604	600	609	602	0.38
31	600	601	603	610	604	599	607	604	0.59
32	600	602	603	607	605	599	605	604	0.66
33	600	602	603	610	604	604	606	604	0.65
34	600	602	603	607	603	600	605	603	0.53
35	600	602	603	610	603	601	609	603	0.53
36	600	602	603	610	603	601	608	603	0.53
37	600	602	603	610	607	596	607	605	0.85
38	600	602	603	616	605	597	608	604	0.64

Table E-2: Computed shear-wave velocities for model 2.

DEPTH (ft)	MODEL VELOCITY (ft/s)	COMPUTED SHEAR-WAVE VELOCITY (ft/s)							ERROR OF MEDIAN RESULT (%)
		BUREAU OF RECLAMATION		U. S. GEOLOGICAL SURVEY		CORPS. OF ENGINEERS		MEDIAN RESULT	
		NEAR RECEIVER	FAR RECEIVER	NEAR RECEIVER	FAR RECEIVER	NEAR RECEIVER	FAR RECEIVER		
39	600	602	603	611	602	597	608	603	0.44
40	600	602	603	613	602	601	607	603	0.44
41	600	602	603	618	604	596	607	603	0.54
42	600	602	603	611	602	597	607	603	0.45
43	600	602	603	601	604	597	606	602	0.42
44	600	602	603	604	598	596	602	602	0.32
45	600			686	599	690	766	688	14.63
46	600	750	769	743	764	738	767	757	
46	800	750	769	743	764	738	767	757	
47	800	791	794	775	780	772	789	785	-1.91
48	800	800	800	783	795	793	802	797	-0.33
49	800	800	800	790	802	797	808	800	-0.02
50	800	800	800	798	802	795	808	800	-0.02
51	800	800	800	799	802	793	808	800	-0.02
52	800	799	800	796	804	790	810	799	-0.07
53	800	800	800	796	803	797	810	800	-0.02
54	800	799	800	792	802	806	813	801	0.13
55	800	799	800	792	803	803	813	801	0.18
56	800	799	800	796	801	806	815	800	0.06
57	800	799	800	792	802	803	815	801	0.12
58	800	799	800	796	803	803	817	801	0.18
59	800	799	800	796	801	795	812	800	-0.04
60	800	799	800	792	801	795	805	800	-0.04
61	800	799	800	802	827	797	842	801	0.12
62	800	800	800	860	934	807	958	834	4.21
63	800	948	961	912	947	930	958	947	
63	1000	948	961	912	947	930	958	947	
64	1000	981	983	947	972	964	985	977	-2.32
65	1000	998	999	970	983	973	1001	991	-0.93
66	1000	998	999	1005	997	973	1010	999	-0.14
67	1000	998	999	1000	1004	980	1004	999	-0.07
68	1000	998	999	995	1004	985	1006	999	-0.14
69	1000	998	999	990	999	977	1004	999	-0.14
70	1000	998	999	1000	999	978	1006	999	-0.09
71	1000	998	999	1010	1001	982	1008	1000	0.02
72	1000	998	999	1005	1011	980	1010	1002	0.18
73	1000	998	999	987	1008	980	1006	999	-0.14

Table E-2: Computed shear-wave velocities for model 2.

DEPTH (ft)	MODEL VELOCITY (ft/s)	COMPUTED SHEAR-WAVE VELOCITY (ft/s)							ERROR OF MEDIAN RESULT (%)
		BUREAU OF RECLAMATION		U. S. GEOLOGICAL SURVEY		CORPS. OF ENGINEERS		MEDIAN RESULT	
		NEAR RECEIVER	FAR RECEIVER	NEAR RECEIVER	FAR RECEIVER	NEAR RECEIVER	FAR RECEIVER		
74	1000	998	1000	994	1034	970	1030	999	-0.08
75	1000			1068	1129	1003	1147	1098	9.80
76	1000	1104	1148	1104	1135	1084	1144	1120	
76	1200	1104	1148	1104	1135	1084	1144	1120	
77	1200	1139	1170	1113	1154	1111	1160	1147	-4.45
78	1200	1189	1196	1133	1164	1133	1180	1172	-2.32
79	1200	1194	1196	1153	1174	1167	1190	1182	-1.51
80	1200	1194	1195	1168	1195	1156	1195	1194	-0.50
81	1200	1194	1195	1158	1198	1171	1199	1194	-0.47
82	1200	1194	1195	1168	1193	1156	1204	1193	-0.55
83	1200	1194	1195	1168	1183	1163	1199	1188	-0.97
84	1200	1194	1195	1179	1180	1166	1202	1187	-1.12
85	1200	1194	1195	1183	1190	1184	1199	1192	-0.69
86	1200	1194	1195	1177	1187	1167	1202	1190	-0.83
87	1200	1194	1195	1171	1190	1159	1197	1192	-0.69
88	1200	1194	1195	1177	1193	1156	1199	1193	-0.55
89	1200	1194	1195	1183	1190	1166	1195	1192	-0.69
90	1200	1194	1194	1189	1193	1163	1195	1193	-0.55
91	1200	1194	1194	1207	1255	1149	1242	1201	0.05
92	1200			1259	1381	1215	1362	1310	9.20
93	1200	1371	1410	1323	1405	1294	1441	1388	
93	1500	1371	1410	1323	1405	1294	1441	1388	
94	1500	1453	1481	1361	1439	1388	1462	1446	-3.59
95	1500	1498	1498	1402	1475	1418	1473	1474	-1.73

Table E-2: Computed shear-wave velocities for model 2.

DEPTH (ft)	MODEL VELOCITY (ft/s)	COMPUTED SHEAR-WAVE VELOCITY (ft/s)							ERROR OF MEDIAN RESULT (%)
		BUREAU OF RECLAMATION		U. S. GEOLOGICAL SURVEY		CORPS. OF ENGINEERS		MEDIAN RESULT	
		NEAR RECEIVER	FAR RECEIVER	NEAR RECEIVER	FAR RECEIVER	NEAR RECEIVER	FAR RECEIVER		
5	1400	1411	1413	1354	1364	1396	1442	1404	0.27
6	1400	1411	1413	1335	1395	1431	1485	1412	0.87
7	1400	1411	1413	1335	1372	1435	1485	1412	0.87
8	1400	1411	1415	1325	1350	1414	1471	1412	0.88
9	1400	1363	1382	1306	1328	1350	1407	1357	-3.10
10	1400	1318	1347	1236	1315	1319	1355	1319	-5.81
11	1400	1280	1310	1212	1281	1264	1316	1281	
11	1100	1280	1310	1212	1281	1264	1316	1281	
12	1100	1178	1255	1158	1262	1171	1297	1217	10.61
13	1100	1092		1096	1117	1095	1163	1096	-0.36
14	1100	1092	1096	1077	1088	1081	1101	1090	-0.91
15	1100	1092	1096	1064	1083	1085	1101	1089	-1.04
16	1100	1092	1096	1052	1074	1089	1104	1090	-0.87
17	1100	1092	1096	1058	1083	1091	1108	1092	-0.75
18	1100	1091	1096	1058	1083	1093	1110	1092	-0.70
19	1100	1091	1096	1064	1083	1090	1114	1091	-0.85
20	1100	1091	1096	1052	1083	1089	1105	1090	-0.89
21	1100	1091	1096	1058	1093	1081	1104	1092	-0.72
22	1100	1091	1096	1058	1097	1083	1107	1094	-0.56
23	1100	1091	1096	1058	1079	1075	1103	1085	-1.36
24	1100	1092	1096	1034	1070	1068	1095	1081	-1.75
25	1100	1068	1081	1017	1056	1051	1076	1062	-3.43
26	1100	1037	1058	990	1052	1002	1054	1044	
26	900	1037	1058	990	1052	1002	1054	1044	
27	900			944	1039	940	1021	982	9.15
28	900	903	922	898	921	897	942	912	1.32
29	900	903	907	893	892	892	909	898	-0.27
30	900	903	907	884	889	891	910	897	-0.37
31	900	903	907	884	889	889	909	896	-0.46
32	900	903	907	884	892	891	909	897	-0.29
33	900	903	907	884	895	892	908	899	-0.12
34	900	903	907	884	892	881	905	897	-0.32
35	900	903	906	880	889	886	906	896	-0.46
36	900	903	906	868	881	889	902	895	-0.51
37	900	881	893	848	864	869	889	875	-2.77
38	900	845	863	812	843	832	866	844	

Table E-3: Computed shear-wave velocities for model 3.

DEPTH (ft)	MODEL VELOCITY (ft/s)	COMPUTED SHEAR-WAVE VELOCITY (ft/s)							ERROR OF MEDIAN RESULT (%)
		BUREAU OF RECLAMATION		U. S. GEOLOGICAL SURVEY		CORPS. OF ENGINEERS		MEDIAN RESULT	
		NEAR RECEIVER	FAR RECEIVER	NEAR RECEIVER	FAR RECEIVER	NEAR RECEIVER	FAR RECEIVER		
38	700	845	863	812	843	832	866	844	
39	700			741	669	747	831	744	6.33
40	700	707	701	695	666	709	752	704	0.59
41	700	707	701	695	661	701	717	701	0.12
42	700	707	701	692	660	701	722	701	0.12
43	700	707	701	692	659	704	718	703	0.38
44	700	707	701	695	667	696	754	698	-0.25
45	700			735	825	738	866	781	11.62
46	700	845	865	819	850	835	864	847	
46	900	845	865	819	850	835	864	847	
47	900	878	891	848	869	864	889	873	-2.95
48	900	890	905	872	876	874	902	883	-1.90
49	900	897	905	875	894	884	904	896	-0.47
50	900	899	905	875	907	882	917	902	0.23
51	900	910	952	904	946	897	977	928	3.11
52	900	988	1037	982	1032	972	1055	1010	12.24
52.5	900								
52.5	1100								
53	1100	1052	1077	1013	1050	1024	1068	1051	-4.46
54	1100	1082	1092	1035	1064	1059	1090	1073	-2.45
55	1100	1092	1101	1058	1076	1073	1101	1084	-1.48
56	1100	1092	1101	1064	1083	1077	1108	1087	-1.14
57	1100	1092	1101	1088	1083	1086	1108	1090	-0.92
58	1100	1092	1101	1064	1076	1090	1112	1091	-0.83
59	1100	1092	1101	1076	1087	1090	1113	1091	-0.83
60	1100	1092	1100	1076	1083	1090	1111	1091	-0.83
61	1100	1092	1100	1064	1095	1085	1108	1093	-0.61
62	1100	1092	1100	1070	1089	1086	1107	1090	-0.89
63	1100	1092	1100	1064	1086	1073	1111	1089	-1.03
64	1100	1092	1100	1070	1095	1085	1106	1093	-0.61
65	1100	1093	1101	1064	1095	1086	1109	1094	-0.54
66	1100	1093	1101	1064	1092	1092	1113	1093	-0.68
67	1100	1093	1101	1064	1092	1080	1113	1093	-0.68
68	1100	1093	1101	1080	1092	1084	1112	1093	-0.68
69	1100	1093	1101	1071	1098	1084	1110	1096	-0.40
70	1100	1093	1101	1071	1083	1082	1113	1088	-1.09
71	1100	1093	1101	1061	1092	1081	1113	1093	-0.68

Table E-3: Computed shear-wave velocities for model 3.

DEPTH (ft)	MODEL VELOCITY (ft/s)	COMPUTED SHEAR-WAVE VELOCITY (ft/s)							ERROR OF MEDIAN RESULT (%)
		BUREAU OF RECLAMATION		U. S. GEOLOGICAL SURVEY		CORPS. OF ENGINEERS		MEDIAN RESULT	
		NEAR RECEIVER	FAR RECEIVER	NEAR RECEIVER	FAR RECEIVER	NEAR RECEIVER	FAR RECEIVER		
72	1100	1093	1101	1071	1095	1086	1112	1094	-0.54
73	1100	1094	1101	1071	1095	1106	1111	1098	-0.20
74	1100	1094	1101	1071	1086	1080	1112	1090	-0.93
75	1100	1094	1101	1071	1092	1078	1111	1093	-0.65
76	1100	1094	1101	1071	1086	1080	1110	1090	-0.93
77	1100	1093	1101	1071	1077	1099	1107	1096	-0.37
78	1100	1093	1102	1052	1072	1088	1099	1090	-0.89
79	1100	1074	1080	1066	1073	1068	1080	1073	-2.42
80	1100	1016	1031	1071	1055	1001	1025	1028	-6.54
81	1100	941	987	1001	1036	932	989	988	
81	600	941	987	1001	1036	932	989	988	
82	600	606	607	547	576	511	560	568	-5.28
83	600	606	607	543	576	511	562	569	-5.11
84	600	606	607	548	576	511	559	568	-5.39
85	600	1603	1740	1808	1922	1605	1740	1740	
85	2200	1603	1740	1808	1922	1605	1740	1740	
86	2200	1759	1836	2010	2019	1770	1858	1847	-16.04
87	2200	1950	1917	2475	2094	1884	1906	1934	-12.09
88	2200	2080	1917	2845	2175	2042	2029	2061	-6.32
89	2200	2108	1917	2972	2245	2086	2127	2117	-3.76
90	2200	2176	2197	2985	2264	2057	2169	2186	-0.62
91	2200	2186	2197	3114	2124	2086	2201	2191	-0.39
92	2200	2186	2197	3027	2124	2086	2265	2191	-0.39
93	2200	2186	2197	3255	2124	2132	2244	2191	-0.39
94	2200	2186	2197	3114	2158	2116	2244	2191	-0.39
95	2200	2186	2197	3027	2158	2132	2235	2191	-0.39

Table E-3: Computed shear-wave velocities for model 3.

DEPTH (ft)	MODEL VELOCITY (ft/s)	COMPUTED SHEAR-WAVE VELOCITY (ft/s)							ERROR OF MEDIAN RESULT (%)
		BUREAU OF RECLAMATION		U. S. GEOLOGICAL SURVEY		CORPS. OF ENGINEERS		MEDIAN RESULT	
		NEAR RECEIVER	FAR RECEIVER	NEAR RECEIVER	FAR RECEIVER	NEAR RECEIVER	FAR RECEIVER		
5	1450	1444	1438	1422	1425	1485	1458	1441	-0.62
6	1450	1444	1439	1440	1457	1485	1486	1450	0.02
7	1450	1444	1439	1428	1457	1441	1482	1442	-0.53
8	1450	1444	1441	1405	1441	1466	1451	1442	-0.53
9	1450	1444	1444	1393	1441	1466	1458	1444	-0.43
10	1450	1444	1445	1393	1425	1479	1454	1444	-0.38
11	1450	1444	1446	1371	1430	1429	1448	1437	-0.90
12	1450	1444	1447	1371	1430	1435	1448	1439	-0.74
13	1450	1444	1447	1371	1435	1447	1444	1444	-0.41
14	1450	1444	1447	1360	1420	1485	1451	1445	-0.32
15	1450	1444	1447	1371	1384	1435	1438	1436	-0.95
16	1450	1375	1404	1298	1346	1354	1396	1365	-5.88
17	1450	1295	1334	1242	1301	1292	1339	1298	-10.47
18	1450	1234	1294	1190	1263	1223	1286	1248	
18	900	1234	1294	1190	1263	1223	1286	1248	
19	900	865	850	846	820	757	981	848	-5.79
20	900	865	848	846	823	755	976	847	-5.87
21	900	1206	1265	1191	1244	1207	1263	1225	
21	1400	1206	1265	1191	1244	1207	1263	1225	
22	1400	1280	1315	1262	1295	1280	1315	1287	-8.05
23	1400	1351	1358	1342	1336	1333	1363	1347	-3.81
24	1400	1387	1388	1381	1365	1384	1386	1385	-1.07
25	1400	1387	1386	1381	1395	1377	1395	1386	-0.97
26	1400	1387	1388	1358	1380	1371	1410	1383	-1.19
27	1400	1387	1388	1341	1395	1380	1419	1387	-0.91
28	1400	1387	1388	1366	1395	1380	1405	1387	-0.91
29	1400	1387	1389	1374	1403	1362	1424	1388	-0.84
30	1400	1387	1391	1358	1395	1366	1420	1389	-0.79
31	1400	1387	1392	1358	1391	1362	1404	1389	-0.79
32	1400	1387	1392	1358	1391	1362	1404	1389	-0.79
33	1400	1387	1391	1358	1391	1369	1399	1389	-0.79
34	1400	1387	1394	1358	1387	1362	1406	1387	-0.94
35	1400	1387	1392	1349	1387	1361	1404	1387	-0.94
36	1400	1387	1394	1341	1383	1366	1406	1385	-1.08
37	1400	1387	1394	1341	1382	1361	1401	1385	-1.11
38	1400	1387	1395	1333	1379	1375	1385	1382	-1.28

Table E-4: Computed shear-wave velocities for model 4.

DEPTH (ft)	MODEL VELOCITY (ft/s)	COMPUTED SHEAR-WAVE VELOCITY (ft/s)							ERROR OF MEDIAN RESULT (%)
		BUREAU OF RECLAMATION		U. S. GEOLOGICAL SURVEY		CORPS. OF ENGINEERS		MEDIAN RESULT	
		NEAR RECEIVER	FAR RECEIVER	NEAR RECEIVER	FAR RECEIVER	NEAR RECEIVER	FAR RECEIVER		
39	1400	1353	1356	1280	1348	1380	1359	1354	-3.26
40	1400	1279	1309	1213	1281	1265	1312	1280	-8.56
41	1400	1201	1255	1152	1221	1192	1254	1211	
41	850	1201	1255	1152	1221	1192	1254	1211	
42	850	827	845	842	767	777	770	802	-5.63
43	850	839	845	812	763		770	812	-4.47
44	850	843	845	806	763	831		831	-2.20
45	850	836	845	803	758	770	770	786	-7.53
46	850	1225	1285	1206	1279	1231	1292	1255	
46	1450	1225	1285	1206	1279	1231	1292	1255	
47	1450	1307	1340	1250	1312	1301	1349	1310	-9.67
48	1450	1389	1395	1348	1357	1389	1398	1389	-4.22
49	1450	1443	1431	1393	1418	1460	1436	1433	-1.14
50	1450	1450	1434	1393	1431	1432	1446	1433	-1.15
51	1450	1450	1436	1412	1422	1422	1472	1429	-1.43
52	1450	1450	1438	1395	1397	1427	1477	1432	-1.21
53	1450	1450	1436	1387	1414	1431	1451	1434	-1.12
54	1450	1450	1440	1387	1414	1427	1446	1433	-1.15
55	1450	1443	1422	1369	1393	1391	1431	1407	-2.95
56	1450	1371	1377	1305	1393	1354	1371	1371	-5.45
57	1450	1289	1329	1283	1355	1280	1327	1308	-9.79
57.5	1450								
57.5	900								
58	900	1293	1325	1254	1299	1241	1315	1296	43.99
59	900	890	901	888	895	889	916	893	-0.83
60	900	890	900	892	895	891	907	894	-0.71
61	900	890	900	878	892	891	904	892	-0.93
62	900	890	900	874	889	889	899	889	-1.18
63	900	890	900	881	892	890	912	891	-1.01
64	900	890	900	864	886	885	904	888	-1.36
65	900	886	901	871	886	1296	1377	893	-0.74
66	900	1277	1332	1226	1370	1262	1337	1305	
66	1500	1277	1332	1226	1370	1262	1337	1305	
67	1500	1346	1384	1290	1416	1342	1404	1365	-9.00
68	1500	1446	1446	1337	1449	1426	1447	1446	-3.60
69	1500	1488	1480	1413	1433	1444	1483	1462	-2.53
70	1500	1489	1498	1415	1458	1457	1504	1473	-1.78

Table E-4: Computed shear-wave velocities for model 4.

DEPTH (ft)	MODEL VELOCITY (ft/s)	COMPUTED SHEAR-WAVE VELOCITY (ft/s)							ERROR OF MEDIAN RESULT (%)
		BUREAU OF RECLAMATION		U. S. GEOLOGICAL SURVEY		CORPS. OF ENGINEERS		MEDIAN RESULT	
		NEAR RECEIVER	FAR RECEIVER	NEAR RECEIVER	FAR RECEIVER	NEAR RECEIVER	FAR RECEIVER		
71	1500	1489	1502	1401	1458	1445	1509	1473	-1.79
72	1500	1493	1501	1401	1466	1452	1505	1479	-1.37
73	1500	1496	1501	1422	1484	1452	1505	1490	-0.67
74	1500	1500	1504	1408	1492	1452	1508	1496	-0.25
75	1500	1503	1504	1408	1475	1452	1503	1489	-0.74
76	1500	1496	1501	1408	1481	1458	1503	1489	-0.76
77	1500	1496	1501	1408	1475	1465	1498	1486	-0.96
78	1500	1499	1501	1422	1481	1458	1493	1487	-0.88
79	1500	1499	1501	1415	1481	1458	1495	1488	-0.80
80	1500	1499	1501	1408	1481	1452	1498	1489	-0.71
81	1500	1499	1501	1408	1481	1445	1495	1488	-0.80
82	1500	1499	1501	1417	1487	1452	1495	1491	-0.60
83	1500	1499	1501	1393	1487	1427	1493	1490	-0.68
84	1500	1499	1501	1393	1463	1427	1498	1480	-1.30
85	1500	1500	1501	1403	1475	1419	1490	1483	-1.16
86	1500	1500	1499	1412	1475	1472	1495	1485	-0.99
87	1500	1500	1499	1412	1481	1480	1499	1490	-0.69
88	1500	1503	1494	1462	1487	1484	1491	1489	-0.74
89	1500	1518		1537	1513	1720	1484	1518	1.20
90	1500	1989		1757	1930	1888	2065	1930	28.70
91	1500	1965	2021	1787	1942	1879	2030	1953	
91	2300	1965	2021	1787	1942	1879	2030	1953	
92	2300	2016	2090	1850	1987	1945	2101	2001	-12.98
93	2300	2119	2160	1972	2060	2069	2146	2094	-8.95
94	2300	2235	2221	1936	2092	2176	2218	2197	-4.49
95	2300	2263	2266	1945	2118	2202	2268	2232	-2.95

Table E-4: Computed shear-wave velocities for model 4.

DEPTH (ft)	MODEL VELOCITY (ft/s)	COMPUTED SHEAR-WAVE VELOCITY (ft/s)						MEDIAN RESULT	ERROR OF MEDIAN RESULT (%)
		BUREAU OF RECLAMATION		U. S. GEOLOGICAL SURVEY		CORPS. OF ENGINEERS			
		NEAR RECEIVER	FAR RECEIVER	NEAR RECEIVER	FAR RECEIVER	NEAR RECEIVER	FAR RECEIVER		
5	700	693	712	685	667	692	707	693	-1.02
6	700			812	841	851	921	846	20.86
7	700	900	918	864	895	885	921	898	
7	1000	900	918	864	895	885	921	898	
8	1000	945	955	901	925	925	961	935	-6.49
9	1000	988	992	941	970	981	995	984	-1.55
10	1000	1016	1000	965	1000	1002	1017	1001	0.06
11	1000	1016	1000	959	1005	998	1034	1002	0.23
12	1000	1013	1000	959	990	989	998	994	-0.63
13	1000	1013	1000	972	995	1029	998	999	-0.13
14	1000	1015	1000	972	990	1029	1006	1003	0.28
15	1000	1015	1000	959	980	1014	1006	1003	0.28
16	1000	1015	1000	959	985	1009	1006	1003	0.28
17	1000	1016	1000	972	990	1017	1009	1004	0.42
18	1000	1015	1000	965	985	1021	1003	1001	0.14
19	1000	1015	1001	965	990	998	1000	999	-0.09
20	1000	1015	1001	959	990	979	1002	995	-0.45
21	1000	1016	1022	965	1026	1000	1030	1019	1.91
22	1000	1084	1100	1032	1088	1059	1125	1086	8.63
23	1000	1126	1154	1054	1113	1118	1152	1122	
23	1200	1126	1154	1054	1113	1118	1152	1122	
24	1200	1160	1178	1093	1152	1142	1176	1156	-3.68
25	1200	1186	1203	1144	1180	1164	1200	1183	-1.44
26	1200	1188	1203	1162	1187	1171	1216	1187	-1.05
27	1200	1188	1204	1162	1201	1171	1219	1195	-0.45
28	1200	1188	1203	1168	1201	1171	1216	1195	-0.45
29	1200	1188	1203	1150	1201	1174	1206	1195	-0.45
30	1200	1188	1202	1174	1201	1182	1205	1195	-0.45
31	1200	1189	1201	1168	1201	1182	1206	1195	-0.39
32	1200	1189	1201	1162	1184	1179	1201	1186	-1.13
33	1200	1189	1201	1168	1180	1176	1205	1185	-1.27
34	1200	1189	1200	1156	1180	1174	1203	1185	-1.27
35	1200	1189	1200	1162	1177	1173	1203	1183	-1.40
36	1200	1189	1200	1156	1180	1176	1206	1185	-1.27
37	1200	1189	1200	1150	1184	1176	1201	1186	-1.13
38	1200	1189	1202	1162	1177	1179	1200	1184	-1.34

Table E-5: Computed shear-wave velocities for model 5.

DEPTH (ft)	MODEL VELOCITY (ft/s)	COMPUTED SHEAR-WAVE VELOCITY (ft/s)							ERROR OF MEDIAN RESULT (%)
		BUREAU OF RECLAMATION		U. S. GEOLOGICAL SURVEY		CORPS. OF ENGINEERS		MEDIAN RESULT	
		NEAR RECEIVER	FAR RECEIVER	NEAR RECEIVER	FAR RECEIVER	NEAR RECEIVER	FAR RECEIVER		
39	1200	1189	1201	1162	1170	1176	1200	1182	-1.47
40	1200	1189	1202	1162	1174	1181	1203	1185	-1.24
41	1200	1189	1202	1145	1167	1173	1207	1181	-1.59
42	1200	1191	1203	1162	1170	1174	1207	1183	-1.43
43	1200	1190	1203	1156	1157	1174	1195	1182	-1.49
44	1200	1170	1176	1108	1135	1147	1170	1159	-3.45
45	1200	1085	1105	1026	1156	1070	1098	1091	-9.05
46	1200	631	782	578	538	986	1044	707	
46	600	631	782	578	538	986	1044	707	
47	600	596	554	575	539	549	1116	565	-5.87
48	600	631	782	579	536	982	1060	707	
48	1200	631	782	579	536	982	1060	707	
49	1200	1087	1103	1033	1170	1068	1105	1095	-8.76
50	1200	1177	1172	1108	1149	1156	1166	1161	-3.24
51	1200	1203	1197	1154	1154	1178	1203	1187	-1.05
52	1200	1203	1202	1146	1174	1172	1199	1186	-1.15
53	1200	1203	1202	1162	1174	1180	1203	1191	-0.73
54	1200	1203	1202	1162	1174	1175	1212	1189	-0.95
55	1200	1203	1202	1146	1174	1169	1200	1187	-1.09
56	1200	1203	1202	1162	1177	1167	1204	1190	-0.87
57	1200	1205	1202	1162	1180	1185	1198	1192	-0.68
58	1200	1205	1202	1154	1184	1172	1198	1191	-0.76
59	1200	1205	1202	1154	1187	1175	1198	1193	-0.62
60	1200	1205	1203	1154	1190	1180	1196	1193	-0.56
61	1200	1203	1203	1154	1191	1180	1200	1196	-0.35
62	1200	1203	1203	1170	1191	1188	1196	1194	-0.52
63	1200	1203	1203	1172	1191	1172	1196	1194	-0.52
64	1200	1203	1203	1149	1173	1181	1198	1190	-0.86
65	1200	1203	1203	1195	1173	1171	1198	1197	-0.26
66	1200	1203	1203	1160	1191	1174	1202	1197	-0.27
67	1200	1203	1203	1138	1191	1174	1202	1197	-0.27
68	1200	1203	1203	1138	1182	1189	1202	1196	-0.35
69	1200	1203	1203	1160	1182	1182	1215	1193	-0.62
70	1200	1203	1203	1172	1182	1189	1212	1196	-0.33
71	1200	1205	1203	1160	1182	1178	1212	1193	-0.62
72	1200	1204	1203	1160	1182	1189	1212	1196	-0.33
73	1200	1204	1195	1127	1156	1194	1192	1193	-0.56

Table E-5: Computed shear-wave velocities for model 5.

DEPTH (ft)	MODEL VELOCITY (ft/s)	COMPUTED SHEAR-WAVE VELOCITY (ft/s)							ERROR OF MEDIAN RESULT (%)
		BUREAU OF RECLAMATION		U. S. GEOLOGICAL SURVEY		CORPS. OF ENGINEERS		MEDIAN RESULT	
		NEAR RECEIVER	FAR RECEIVER	NEAR RECEIVER	FAR RECEIVER	NEAR RECEIVER	FAR RECEIVER		
74	1200	1163	1159	1086	1147	1165	1140	1153	-3.91
75	1200	1072	1088	1047	1139	1076	1087	1082	-9.87
76	1200	988	1041	970	1106	988	1041	1014	
76	500	988	1041	970	1106	988	1041	1014	
77	500	506	506	499	503	510	510	506	1.17
78	500	506	506	499	502	502	511	504	0.73
79	500	506	506	501	502	509	511	506	1.17
80	500	506	506	506	502	507	511	506	1.18
81	500	506	506	497	504	508	507	506	1.17
82	500	506	506	491	502	505	508	505	1.06
83	500	506	506	489	501	502	510	504	0.72
84	500	506	506	489	503	501	512	504	0.83
85	500		2498		3386		2511	2511	
85	3500		2498		3386		2511	2511	
86	3500		2713		3239		2681	2713	-22.49
87	3500		2750		3275		2731	2750	-21.44
88	3500		2846		3647		2894	2894	-17.32
89	3500		3221		4569		3144	3221	-7.96
90	3500		3457		4878		3286	3457	-1.21
91	3500		3457		4961		3388	3457	-1.21
92	3500		3457		5048		3414	3457	-1.21
93	3500		3461		5048		3414	3461	-1.12
94	3500		3461		5137		3441	3461	-1.11
95	3500		3464		5230		3496	3496	-0.12

Table E-5: Computed shear-wave velocities for model 5.

DEPTH (ft)	MODEL VELOCITY (ft/s)	COMPUTED SHEAR-WAVE VELOCITY (ft/s)							ERROR OF MEDIAN RESULT (%)
		BUREAU OF RECLAMATION		U. S. GEOLOGICAL SURVEY		CORPS. OF ENGINEERS		MEDIAN RESULT	
		NEAR RECEIVER	FAR RECEIVER	NEAR RECEIVER	FAR RECEIVER	NEAR RECEIVER	FAR RECEIVER		
5	1100	1092	1091	1089	1080	1091	1103	1091	-0.82
6	1100	1092	1091	1064	1084	1086	1106	1088	-1.05
7	1100	1092	1091	1064	1093	1083	1106	1091	-0.78
8	1100	1092	1091	1053	1088	1091	1109	1091	-0.84
9	1100	1092	1091	1053	1088	1094	1112	1091	-0.78
10	1100	1092	1091	1041	1088	1081	1112	1090	-0.94
11	1100	1093	1091	1053	1088	1081	1106	1090	-0.94
12	1100	1093	1092	1053	1084	1083	1112	1088	-1.10
13	1100	1093	1092	1064	1084	1091	1109	1091	-0.80
14	1100	1093	1092	1064	1084	1081	1106	1088	-1.10
15	1100	1093	1092	1064	1084	1091	1109	1091	-0.78
16	1100	1093	1092	1041	1084	1091	1103	1091	-0.78
17	1100	1093	1092	1041	1088	1088	1109	1090	-0.90
18	1100	1093	1092	1041	1084	1095	1103	1092	-0.69
19	1100	1092	1092	1030	1080	1102	1103	1092	-0.73
20	1100		981	1041	1058	1109	1095	1058	-3.79
21	1100		981	1030	1028	1069	1013	1028	-6.50
22	1100	978	981	1030	1007	976	985	983	-10.61
23	1100	894	943	384	396	898	947	896	
23	400	894	943	384	396	898	947	896	
24	400	397	384	378	390	359	385	385	-3.83
25	400	397	384	366	391	359	385	385	-3.84
26	400	897	943	384	391	898	947	897	
26	1100	897	943	384	391	898	947	897	
27	1100	980	980	1019	1066	973	991	986	-10.38
28	1100		980	1030	1058	1078	1035	1035	-5.92
29	1100		980	1064	1058	1094	1089	1064	-3.24
30	1100	1101	1102	1053	1076	1106	1103	1102	0.14
31	1100	1101	1102	1041	1084	1093	1109	1097	-0.24
32	1100	1101	1102	1053	1084	1085	1109	1093	-0.61
33	1100	1101	1102	1053	1088	1083	1114	1095	-0.47
34	1100	1103	1101	1053	1088	1093	1107	1097	-0.26
35	1100	1103	1101	1053	1088	1104	1114	1102	0.18
36	1100	1103	1101	1041	1093	1088	1114	1097	-0.29
37	1100	1103	1101	1053	1097	1088	1110	1099	-0.08
38	1100	1103	1101	1060	1097	1081	1110	1099	-0.08

Table E-6: Computed shear-wave velocities for model 6.

DEPTH (ft)	MODEL VELOCITY (ft/s)	COMPUTED SHEAR-WAVE VELOCITY (ft/s)							ERROR OF MEDIAN RESULT (%)
		BUREAU OF RECLAMATION		U. S. GEOLOGICAL SURVEY		CORPS. OF ENGINEERS		MEDIAN RESULT	
		NEAR RECEIVER	FAR RECEIVER	NEAR RECEIVER	FAR RECEIVER	NEAR RECEIVER	FAR RECEIVER		
39	1100	1103	1100	1082	1093	1077	1112	1097	-0.29
40	1100	1103	1100	1071	1093	1084	1110	1097	-0.29
41	1100	1102	1100	1049	1089	1081	1112	1095	-0.47
42	1100	1102	1100	1060	1089	1088	1110	1095	-0.47
43	1100	1102	1100	1082	1085	1073	1105	1093	-0.66
44	1100	1102	1100	1082	1081	1100	1105	1100	0.02
45	1100		992	1082	1089	1084	1094	1084	-1.41
46	1100		992	1082	1089	1076	1008	1076	-2.18
47	1100	976	992	1039	1065	965	984	988	-10.15
48	1100	895	945	989	1019	891	948	946	
48	400	895	945	989	1019	891	948	946	
49	400	402		402	399	404	992	402	0.59
50	400	402	402	399	399	400	378	400	-0.03
51	400	402	402	398	396	402	378	400	-0.09
52	400	402		399	394	403	1006	402	0.53
53	400	893	945	944	1026	903	944	944	
53	1100	893	945	944	1026	903	944	944	
54	1100	980	989	980	1041	985	992	987	-10.31
55	1100		986	1018	1065	1076	1072	1065	-3.21
56	1100		981	1060	1073	1082	1088	1073	-2.48
57	1100	1097	1096	1049	1073	1091	1104	1094	-0.57
58	1100	1096	1096	1060	1089	1088	1100	1093	-0.67
59	1100	1096	1096	1071	1089	1081	1106	1093	-0.67
60	1100	1096	1096	1071	1097	1086	1106	1096	-0.34
61	1100	1096	1096	1082	1089	1088	1106	1093	-0.67
62	1100	1096	1096	1093	1093	1076	1104	1094	-0.50
63	1100	1094	1096	1082	1106	1080	1102	1095	-0.44
64	1100	1094	1096	1071	1090	1074	1104	1092	-0.69
65	1100	1094	1096	1058	1090	1073	1102	1092	-0.69
66	1100	1094	1096	1058	1090	1084	1104	1092	-0.69
67	1100	1094	1096	1058	1085	1070	1106	1090	-0.93
68	1100	1094	1096	1058	1085	1091	1104	1093	-0.64
69	1100	1093	1096	1058	1080	1088	1096	1090	-0.87
70	1100		990	1058	1059	1079	1090	1059	-3.68
71	1100		990	1058	1050	1076	1070	1058	-3.86
72	1100	978	990	1022	1050	974	994	992	-9.85
73	1100	896	944	979	1013	900	950	947	

Table E-6: Computed shear-wave velocities for model 6.

DEPTH (ft)	MODEL VELOCITY (ft/s)	COMPUTED SHEAR-WAVE VELOCITY (ft/s)							ERROR OF MEDIAN RESULT (%)
		BUREAU OF RECLAMATION		U. S. GEOLOGICAL SURVEY		CORPS. OF ENGINEERS		MEDIAN RESULT	
		NEAR RECEIVER	FAR RECEIVER	NEAR RECEIVER	FAR RECEIVER	NEAR RECEIVER	FAR RECEIVER		
73	400	896	944	979	1013	900	950	947	
74	400	403	404	398	402	406	407	404	0.95
75	400	403	404	399	405	406	410	405	1.21
76	400	403	404	399	404	406	408	404	1.06
77	400	403	404	399	404	405	409	404	1.06
78	400	403	404	399	403	402	410	403	0.77
79	400	403	404	399	404	404	411	404	0.98
80	400	403	404	398	404	404	406	404	0.98
81	400	896	945	969	1028	901	947	946	
81	1100	896	945	969	1028	901	947	946	
82	1100	982	991	990	1050	982	994	990	-9.97
83	1100		991	1022	1050	1086	1041	1041	-5.38
84	1100		991	1058	1059	1099	1098	1059	-3.68
85	1100	1102	1104	1070	1075	1081	1102	1092	-0.76
86	1100	1102	1104	1058	1080	1092	1111	1097	-0.27
87	1100	1102	1104	1058	1090	1086	1098	1094	-0.54
88	1100	1102	1104	1082	1090	1089	1106	1096	-0.34
89	1100	1101	1104	1070	1090	1094	1111	1098	-0.22
90	1100	1101	1104	1070	1096	1094	1106	1098	-0.15
91	1100	1101	1104	1070	1108	1093	1106	1102	0.22
92	1100	1101	1104	1070	1108	1090	1111	1102	0.22
93	1100	1101	1104	1070	1108	1082	1124	1102	0.22
94	1100	1101	1104	1058	1100	1082	1120	1101	0.06
95	1100	1101	1104	1058	1108	1089	1106	1102	0.22

Table E-6: Computed shear-wave velocities for model 6.

DEPTH (ft)	MODEL VELOCITY (ft/s)	COMPUTED SHEAR-WAVE VELOCITY (ft/s)							ERROR OF MEDIAN RESULT (%)
		BUREAU OF RECLAMATION		U. S. GEOLOGICAL SURVEY		CORPS. OF ENGINEERS		MEDIAN RESULT	
		NEAR RECEIVER	FAR RECEIVER	NEAR RECEIVER	FAR RECEIVER	NEAR RECEIVER	FAR RECEIVER		
5	900	898.89	899.181	887.859	897.253			898	-0.21
6	900	898.89	899.181	882.809	903.435			899	-0.11
7	900	898.89	899.181	882.809	905.515			899	-0.11
8	900	898.14	899.181	887.859	901.365			899	-0.15
9	900	898.14	899.181	887.859	903.435			899	-0.15
10	900	898.14	899.181	887.859	903.435			899	-0.15
11	900	898.14	899.181	892.968	905.515			899	-0.15
12	900	898.14	899.157	892.968	903.435			899	-0.15
13	900	898.14	899.133	892.968	905.515			899	-0.15
14	900	898.14	899.133	882.809	905.515			899	-0.15
15	900	898.14	899.133	892.968	906.729			899	-0.15
16	900	898.975	899.133	887.859	904.693			899	-0.11
17	900	898.975	899.133	882.809	906.729			899	-0.11
18	900	898.975	899.133	892.968	902.665			899	-0.11
19	900	898.975	899.133	892.968	906.729			899	-0.11
20	900	898.975	899.133	875.455	898.637			899	-0.13
21	900	893.656	891.618	870.857	892.661			892	-0.87
22	900	863.016	866.272	844.256	863.938			863	-4.06
23	900	808.65	829.566	811.218	826.697			819	
23	600								
23.5	600	799	817	803.358	828.398			810	35.03
24	600	808.65	831.033	807.269	831.82			820	
24	900								
25	900	868.88	863.061	848.576	873.305			866	-3.78
26	900	893.563	884.578	875.455	886.223			885	-1.62
27	900	893.563	890.852	875.455	894.565			892	-0.87
28	900	893.563	897.216	884.796	900.926			895	-0.51
29	900	893.563	897.216	880.101	900.926			895	-0.51
30	900	893.563	897.216	880.101	900.926			895	-0.51
31	900	893.563	897.207	894.34	898.796			896	-0.47
32	900	893.563	897.216	894.34	903.066			896	-0.47
33	900	893.563	897.216	889.543	900.926			895	-0.51
34	900	893.563	897.216	894.34	903.066			896	-0.47
35	900	893.48	897.216	884.796	905.217			895	-0.52
36	900	893.48	897.216	889.543	898.796			895	-0.52
37	900	893.48	897.162	889.246	898.796			895	-0.52

Table E-7: Computed shear-wave velocities for model 7.

DEPTH (ft)	MODEL VELOCITY (ft/s)	COMPUTED SHEAR-WAVE VELOCITY (ft/s)							ERROR OF MEDIAN RESULT (%)
		BUREAU OF RECLAMATION		U. S. GEOLOGICAL SURVEY		CORPS. OF ENGINEERS		MEDIAN RESULT	
		NEAR RECEIVER	FAR RECEIVER	NEAR RECEIVER	FAR RECEIVER	NEAR RECEIVER	FAR RECEIVER		
38	900	893.48	897.162	885.893	898.418			895	-0.52
39	900	893.48	897.162	885.893	903.409			895	-0.52
40	900	893.48	897.162	885.893	903.409			895	-0.52
41	900	893.421	897.162	885.893	903.409			895	-0.52
42	900	893.421	897.162	885.893	900.906			895	-0.52
43	900	893.421	897.162	889.246	905.924			895	-0.52
44	900	894.231	897.162	889.246	900.906			896	-0.48
45	900	894.231	897.162	892.625	895.944			895	-0.55
46	900	894.231	897.162	872.729	891.035			893	-0.82
47	900	880.27	888.099	847.541	893.483			884	-1.76
48	900	841.459	859.334	812.373	878.997			850	
48	700								
49	700	740.293		738.334	809.039			740	5.76
50	700	801.482	810.748	790.505	809.039			805	
50	850								
51	850	838.068	843.872	818.03	831.149			835	-1.81
52	850	852.256	848.727	832.524	846.285			848	-0.29
53	850	851.955	848.507	842.998	846.285			847	-0.31
54	850	851.955	848.507	847.136	857.439			850	0.03
55	850	851.955	848.507	842.998	857.439			850	0.03
56	850	851.955	848.507	838.901	861.983			850	0.03
57	850	851.955	848.507	834.843	857.439			850	0.03
58	850	851.955	848.507	842.998	864.273			850	0.03
59	850	852.537	848.72	838.901	861.983			851	0.07
60	850	852.537	848.72	838.901	864.273			851	0.07
61	850	852.537	848.72	842.998	864.273			851	0.07
62	850	851.454	848.72	842.998	866.576			850	0.01
63	850	851.454	848.72	838.901	868.891			850	0.01
64	850	851.454	848.72	838.901	866.576			850	0.01
65	850	851.454	848.561	838.901	863.652			850	0.00
66	850	851.454	848.561	838.901	853.972			850	0.00
67	850	851.757	848.561	838.901	844.507			847	-0.41
68	850	852.06	848.666	834.843	841.399			845	-0.58
69	850	852.06	848.666	830.825	835.25			842	-0.95
70	850	825.101	833.255	813.091	835.25			829	-2.45
71	850	789.114	803.668	768.782	838.313			796	
71	600								

Table E-7: Computed shear-wave velocities for model 7.

DEPTH (ft)	MODEL VELOCITY (ft/s)	COMPUTED SHEAR-WAVE VELOCITY (ft/s)						MEDIAN RESULT	ERROR OF MEDIAN RESULT (%)
		BUREAU OF RECLAMATION		U. S. GEOLOGICAL SURVEY		CORPS. OF ENGINEERS			
		NEAR RECEIVER	FAR RECEIVER	NEAR RECEIVER	FAR RECEIVER	NEAR RECEIVER	FAR RECEIVER		
71.5	600	768	775	772.61	841.399			774	28.97
72	600	799.781	808.219	834.965	853.972			822	
72	900								
73	900	818.92	819.434	935.649	870.228			845	-6.13
74	900	795.507	806.276	872.521	853.972			830	
74	600								
75	600	589.397	569.238	554.513	567.668			568	-5.26
76	600	596.267	569.238	552.539	569.082			569	-5.14
77	600	808.944	840.371	796.4	860.401			825	
77	900								
78	900	863.26	873.313	867.643	876.905			870	-3.28
79	900	898.578	900.503	882.444	883.685			891	-0.99
80	900	898.126	899.402	882.444	897.564			898	-0.24
81	900	898.126	899.637	897.759	899.363			899	-0.14
82	900	898.126	899.637	892.595	908.736			899	-0.12
83	900	898.126	899.637	887.491	906.375			899	-0.12
84	900	897.191	899.637	892.595	901.688			898	-0.18
85	900	897.191	899.637	902.983	897.05			898	-0.18
86	900	897.191	899.637	887.938	899.363			898	-0.19
87	900	897.191	899.24	896.313	901.688			898	-0.20
88	900	897.191	899.24	887.938	901.688			898	-0.20
89	900	897.191	899.24	896.313	901.688			898	-0.20
90	900	897.336	899.24	892.106	906.375			898	-0.19
91	900	897.336	899.24	883.809	908.736			898	-0.19
92	900	897.336	899.24	887.938	904.025			898	-0.19
93	900	897.336	899.24	892.106	906.375			898	-0.19
94	900	897.336	899.24	892.106	906.375			898	-0.19
95	900	897.392	899.24	896.313	906.375			898	-0.19

Table E-7: Computed shear-wave velocities for model 7.

MISSION STATEMENTS

The mission of the Department of the Interior is to protect and provide access to our Nation's natural and cultural heritage and honor our trust responsibilities to Indian tribes and our commitments to island communities.

The mission of the Bureau of Reclamation is to manage, develop, and protect water and related resources in an environmentally and economically sound manner in the interest of the American public.